NASA TECHNICAL NOTE

NASA TN D-8309

NASA TN D-8309

WIND-TUNNEL INVESTIGATION OF INTERNALLY BLOWN JET-FLAP STOL AIRPLANE MODEL

Raymond D. Vogler
Langley Research Center
Hampton, Va. 23665

NATIONAL AERONAUTICS AND SPACE ADMINISTRATION • WASHINGTON, D. C. • NOVEMBER 1976

1. Report No. NASA TN D-8309	2. Government Accession No.	3. Recipient's Catalog No.
4. Title and Subtitle WIND-TUNNEL INVESTIGATION OF INTERNALLY BLOWN JET-FLAP STOL AIRPLANE MODEL		5. Report Date November 1976 6. Performing Organization Code
7. Author(s) Raymond D. Vogler		8. Performing Organization Report No. L-10887
9. Performing Organization Name and Address NASA Langley Research Center Hampton, VA 23665		10. Work Unit No. 505-10-41-03 11. Contract or Grant No.
12. Sponsoring Agency Name and Address National Aeronautics and Space Administration Washington, DC 20546		13. Type of Report and Period Covered Technical Note 14. Sponsoring Agency Code
15. Supplementary Notes		

16. Abstract

An investigation was made to determine the low-speed longitudinal characteristics of the jet-flap STOL model. The 17-percent-thick supercritical swept wing had leading-edge slats and a full-span 0.30-chord plain flap with flaperons divided into six equal spanwise segments. The angle-of-attack range was -4° to 24°, and the blowing momentum range was from 0 to 2.3. Flap deflections were from 0° to 70°. Most flap deflections were full span although there were some tests of partial-span deflections and partial-span blowing.

17. Key Words (Suggested by Author(s)) STOL transport Internally blown jet flap Partial-span blowing	18. Distribution Statement Unclassified - Unlimited Subject Category 02		
19. Security Classif. (of this report) Unclassified	20. Security Classif. (of this page) Unclassified	21. No. of Pages 86	22. Price* $4.75

* For sale by the National Technical Information Service, Springfield, Virginia 22161

WIND-TUNNEL INVESTIGATION OF INTERNALLY BLOWN JET-FLAP STOL AIRPLANE MODEL

Raymond D. Vogler
Langley Research Center

SUMMARY

An investigation was made to determine the low-speed longitudinal aerodynamic characteristics of a model of an internally blown jet-flap STOL airplane. Jet momentum was obtained with compressed air. The supercritical swept wing had leading-edge slats and a full-span 0.30-chord plain flap divided into six equal spanwise segments. The flaps had 0.15-chord trailing-edge flaperons. Data were obtained through an angle-of-attack range for momentum coefficients from 0 to 2.3 and for flap deflections from 0° to 70°.

The wing leading-edge slats delayed the wing stall to higher angles of attack and higher lift coefficients. The 0.25-chord slat was more effective than the 0.15-chord slat at the higher flap deflections. The 0.15-chord flaperons suffered flow separation at much lower deflections and produced lower maximum lift than did the 0.30-chord flaps. For a given momentum coefficient, higher lift coefficients are obtained by blowing over the entire wing than can be obtained by blowing over partial spans.

INTRODUCTION

Recent activity concerned with developing short takeoff and landing (STOL) transport airplanes using propulsive lift has received considerable attention. In response to this interest, a comparison of several configurations which use different propulsive methods to produce high lift was undertaken in the Langley V/STOL tunnel. Except for wing thickness, all the configurations studied had the same wing-body-tail combination for cruise. The propulsive-lift methods studied include externally blown flaps (ref. 1), upper surface blown flaps (ref. 2), and deflected thrust with mechanical flaps (ref. 3). All these configurations use a 9.3-percent-thick supercritical airfoil for the wing. An augmented flap and the internally blown jet flap used in this study were tested with the use of a 17-percent-thick supercritical airfoil for the wing. An initial comparison of the aerodynamic characteristics of these configurations at low speeds is presented in reference 4.

The present investigation dealt with the internally blown jet-flap configuration. The model combined a swept wing (nominally 30° at the quarter chord) with leading-edge slats and 0.30-chord blown flaps with 0.15-chord flaperons. The slat was configured to delay stall to high angles of attack at all conditions. The flap plus flaperon combination was designed to improve flow turning with powered lift and to provide some high lift without

power. In addition, the wing had a 17-percent-thick supercritical airfoil which provided sufficient volume for the internal ducts required on this airplane concept. The model had no engine nacelles as would be required on the full-scale airplane.

The purpose of this investigation was to determine the low-speed longitudinal characteristics of the internally blown jet-flap configuration. Data were obtained through an angle-of-attack range for several flap and flaperon deflections at low and at high levels of blowing as well as with no blowing. Effects of wing leading-edge slats and partial-span flap blowing were also determined. Some runs were made to determine the effect of horizontal-tail incidence and tail flap deflections.

SYMBOLS

Force and moment data are presented about stability axes and include jet momentum effects. Measurements and calculations were made in U.S. Customary Units and are presented in International System of Units (SI) (ref. 5).

b' exposed wing span, m

b_f flap span, m

C_D drag coefficient, $\frac{\text{Drag}}{q_\infty S}$

C_L lift coefficient, $\frac{\text{Lift}}{q_\infty S}$

C_m pitching-moment coefficient about $0.40\bar{c}$, $\frac{\text{Pitching moment}}{q_\infty S\bar{c}}$

C_μ momentum coefficient, $\frac{\sqrt{F_A^2 + F_N^2}}{q_\infty S}$

c wing local chord, m

$\bar{c}$ wing mean aerodynamic chord, m

F_A balance measured static axial force with flaps removed, N

F_N balance measured static normal force with flaps removed, N

i_t tail incidence; positive when trailing edge is down, deg

q_∞ free-stream dynamic pressure, N/m^2

S wing area, m^2

α angle of attack of wing or fuselage, deg

δ_{f1} flap deflection, measured with respect to wing; positive when trailing edge is down, deg

δ_{f2} flaperon deflection, measured with respect to flap; positive when trailing edge is down, deg

δ_s wing slat deflection; positive when leading edge is down, deg

δ_{tf} tail flap deflection; positive when trailing edge is down, deg

δ_{ts} tail slat deflection; positive when leading edge is down, deg

MODEL AND APPARATUS

A three-view drawing of the model is shown in figure 1, and flap and slat details are shown in figure 2. The wing ordinates are given in figure 3, and photographs of the model are given in figure 4. The wing was a 17-percent-thick supercritical airfoil, and the tail surfaces were 11-percent-thick symmetrical supercritical airfoils. The full-span 0.30-chord plain flaps were equipped with 0.15-chord trailing-edge flaperons which could be deflected positively and negatively. The full-span flaps and flaperons were divided into six equal spanwise segments that could be deflected independently of each other. These segments were numbered 1 to 6 from left to right wing tips. Deflection angle was varied by means of fixed angle plates. The removable leading-edge slats had a St Cyr 178 airfoil section of 15- and 25-percent wing chord. The horizontal tail also had a 0.15-chord slat and a flap with a constant chord that was 20 percent of the tail mean aerodynamic chord. A transition strip of No. 60 carborundum grains was applied to the wing 3.2 cm behind the leading edge.

Compressed air for blowing over the nose of the wing flaps was brought through a tube (3.17 cm in diameter) in the center of the sting to a manifold in the fuselage. Air from the manifold was carried through wing ducts (1.27 cm square) to six individual plenums in the rear of the wing just ahead of the flap nose. Air from these plenums flowed over the upper surface of the flap nose through holes drilled into the plenums parallel to the wing chord plane and normal to the flap hinge line. There were 500 exit holes for each wing semispan; these exit holes varied in diameter from 0.244 cm at the fuselage to 0.051 cm at the wing tip. This reduction in hole diameter was necessary because of taper in wing thickness and was useful in attaining nearly constant wing-section momentum coefficient. The mass flow through the group of exit holes for any flap segment could be controlled by a valve in the wing duct near the fuselage manifold.

The model was attached to a six-component strain-gage balance inside the fuselage on the end of the mounting sting in the Langley V/STOL tunnel. The air supply line coming through the sting was also attached to the model

inside the fuselage. Tunnel variables and model forces, moments, and pressures were recorded on magnetic tape.

TESTS AND CORRECTIONS

Tests were made at a tunnel dynamic pressure of 814 N/m^2 at a Reynolds number of 720 000 based on the wing mean aerodynamic chord of 28.99 cm. The angle-of-attack range varied from -4° to 24°, and the blowing-momentum coefficient range varied from 0 to 2.3. Data were obtained with wing slats on and off, with wing slats of different chords and deflections, with various flap and flaperon deflections, with combinations of flap and flaperon deflections, with various horizontal-tail incidences, with tail off, and with tail flap on and off. Most flap deflections involved the full span, although there were some tests of partial-span deflections and partial-span blowing.

With the flaps removed, the balance-measured static jet force $\sqrt{F_A^2 + F_N^2}$ was determined for a range of wing duct pressures. From this calibration and the tunnel dynamic pressure, the momentum coefficient C_μ was determined. The adjustable duct pressure for each flap segment in conjunction with the different jet hole sizes provided a rather uniform momentum coefficient for each spanwise wing element. The static jet force was essentially the axial force because the normal force was very small, and the side force was negligible since one wing panel nullified the side force of the other. It is well to note that the momentum coefficient determined from axial force on a swept-wing model is not a true indication of the quantity of blowing air, and comparisons between complete models on the basis of momentum coefficient may be misleading if the wing sweep angles are significantly different. The momentum coefficients presented are about 5 percent less than those for a wing with zero sweep of the jet thrust line.

Attachment of the air supply line to the model affects the sensitivity of the strain-gage balance, and variations in air-line pressure produce forces and moments on the balance. Calibrations were made to determine these nonaerodynamic effects, and corrections to the data were made. Wind-tunnel wall corrections to the data were made by the method of reference 6.

RESULTS AND DISCUSSION

The early exploratory part of this investigation (figs. 5 to 9) determined the overall aerodynamic characteristics. Model longitudinal aerodynamic characteristics were obtained for several flap deflections and a few combinations of flap and flaperon deflections to establish a useful flap deflection range for further testing. Several runs were made to determine the wing-slat chord and slat deflection most desirable for this wing and its range of flap deflections. Since attention was focused on developing the high lift characteristics of the wing, much of the data was obtained with the horizontal tail removed. The early part of the investigation showed that the 0.25-chord wing slat was more effective than the 0.15-chord slat;

therefore, the longer chord slat only was used in the latter part of the investigation (figs. 10 to 29). Some attention was also given to increasing the lift effectiveness of the horizontal tail since blown flaps are noted for large negative pitching moments.

Wing-Slat Effects

Figures 5 and 6 show the lift characteristics of the model with low flap deflections (0°,15°) without wing slats, and with high flap deflections with 0.15-chord wing slats. The 0.15-chord slats increase the stall angle of the wing with flaps deflected except for some flap deflections with no blowing, and the 50° slat deflection gives larger stall angles than the 40° deflection except at low (30°) flap deflections with no blowing.

The effect of the slats is more clearly shown in figure 7 with the flaps deflected 30°, in figure 8(a) with the flaps deflected 45°, and in figure 10 with the flaps undeflected. The 0.15-chord slat is satisfactory for a flap deflection of 30° without blowing (fig. 7(a)); the 0.25-chord slat is more effective with higher flap deflections with blowing (figs. 7 and 8). Figure 8 shows a direct comparison between the two slats and the improvement in lift characteristics of the wing with slats as compared with the wing without slats for flap deflections of 45° or more. The angle of attack at which the wing stalled varied with flap deflection and blowing momentum coefficient. With no slats and flaps deflected, the stall angle varied from about 6° to 15°; with the 0.15-chord slats, the stall angle varied from about 12° to 20° (figs. 7 and 8). The wing seldom stalled with the 0.25-chord slats up to angles of attack of 20° to 23°, the maximum angles of attack investigated (figs. 7 and 8).

With a flap deflection of 45° (fig. 8(a)), the 0.15-chord slats have little effect on the drag and pitching moment of the unstalled model with tail off, but the 0.25-chord slats reduce the nose-down pitching moments for all the higher (45° to 70°) flap deflections with blowing (fig. 8). Also the drag of the model with the 0.25-chord slats is less than the drag of the model with the 0.15-chord slats. There is a small difference in C_μ for the two slat configurations, but the difference in C_μ could produce only a small part of the drag difference shown. Elimination of the C_μ difference would result in even larger differences in pitching moments than shown.

Flap and Flaperon Characteristics

The flap characteristics of the model through a range of flap deflections are presented in figures 5 and 6 for the model with the 0.15-chord wing slats, and data for combined flap and flaperon deflections are presented in figure 9. As noted earlier, the wing stalled at a lower angle of attack with the 0.15-chord slats than with the 0.25-chord slats, and the following discussion relates to the data obtained with the 0.25-chord slats on the wing.

The lift characteristics of the model with the flaps and flaperons undeflected are shown in figure 10, and the effect of deflecting the flaperons only is shown in figure 11. Blowing with the flaperons deflected 30° increases the maximum lift coefficient from 2.0 to over 7.0 (figs. 11(a) and 11(c)). Flaperon deflections of 45° show some lift improvement over 30° with low blowing momentums but show a lift little greater than that at 0° deflection at high blowing momentums. This lift breakdown at high blowing would indicate complete separation over the flaperon. The blowing exits are 0.15 chord ahead of the flaperons, and this distance allows the jet to increase in thickness before it gets to the nose of the flaperons. This increase in thickness, the high jet velocity, and the small flaperon nose radius cause the separation.

Data for combined flap and flaperon deflections are presented in figures 12 to 16. The flap and flaperons are similar in that each is a plain trailing-edge flap when deflected alone. The flap and flaperons differ in chord length, nose radius, and flap nose location with respect to the jet exits. Blowing with the flap alone deflected 60° increases the maximum lift coefficient from 2.1 (fig. 15(a)) to 9.6 (fig. 15(c)). At a deflection of 70° (fig. 16), the flow is still attached to the flap; on the other hand, the flow over the flaperon was separated at a deflection of 45°. Separation on the flaperon results in a reduction of the magnitude of the negative pitching moments and usually results in an increase in drag at equivalent lift coefficients (fig. 11).

Cross plots of the lift data against combined deflections of the flap and flaperon taken from figures 11 to 16 are shown in figure 17. The data indicate that deflections of the flap alone ($\delta_{f2} = 0°$) give lift coefficients as high or higher than the combined deflections of the flap and flaperon, except at a flap deflection of 60° combined with a flaperon deflection of 15°. Higher flaperon deflections cause the flap system to lose effectiveness with blowing, especially at the higher combined deflections because of flow separation on the flaperon.

Partial-Span Flap Deflections

The longitudinal characteristics of the model with partial-span flap deflections compared with full-span deflections are shown in figures 18 to 23. In all cases, the plenum pressures were essentially the same for the three groups of flap segments for the low and for the high blowing. In other words, the pressure ratios across the jet exits did not vary with the number of flap segments deflected, but the total mass flow did, and the momentum coefficient varied because it was based on the total wing area and not on the area being blown. By varying the number and diameter of the exit holes, an attempt was made to make the total exit-hole area of any wing segment proportional to the blown (exposed) area of the segment. For such conditions, the mass flow rates and momentum coefficients would also be approximately proportional to the blown areas for equal flap plenum pressures, and constant C_μ for spanwise wing elements would be attained.

Figure 22 also shows the effect of deflecting the midspan flap segments without blowing and with blowing on the deflected inboard segments. This combination in comparison with the results of the blown inboard segments alone reduces the angle of attack and, consequently, the drag for a given lift coefficient. Deflecting the inboard and midspan flaps unequally (fig. 23) gives little more benefit than deflecting them equally (fig. 20). Deflections of $45^{\circ},45^{\circ}$ as opposed to unequal deflections of $30^{\circ},60^{\circ}$ show less drag at equivalent lift coefficients but larger negative pitching moments.

Cross plots of the lift data against flap deflection taken from figures 11 to 16 and 18 to 22 are presented in figure 24 for the three spanwise segments of the wing at zero angle of attack. The lift coefficients are for equal momentum coefficients and approximately equal total mass flows. The lift coefficients show the advantage of distributing a given mass flow over the entire wing area rather than over a part of the wing.

The lift variation with flap span is shown in figure 25 for four flap deflections for a range of momentum coefficients at a model angle of attack of zero. This figure was obtained by cross-plotting the lift (figs. 18 to 22) against momentum coefficient for the three flap spans and then by cross-plotting the lift for each span against the ratio of flap span to exposed wing span at constant momentum coefficients.

Horizontal-Tail Characteristics

Figures 26 to 29 show the effects of the horizontal tail on the aerodynamic characteristics of the model with various wing-flap deflections and wing blowing momentums. The negative moments produced by the wing flaps required a download on the tail to balance the model, which resulted in a considerable reduction in model lift for some conditions. The tail with leading-edge slats and a flap which increased the tail area was more than adequate to trim the model for all conditions except when the tail stalled. Large wing-flap deflections and high blowing momentums produce large downwash angles which, combined with a tail incidence of -15°, result in a stalled tail at low model angles of attack for some conditions (fig. 28). Otherwise, the tail-on model is stable in attitude until the wing stalls.

SUMMARY OF RESULTS

A wind-tunnel investigation was made to determine the longitudinal aerodynamic characteristics of a model of an internally blown jet-flap STOL airplane. Jet momentum coefficients as high as 2.3 were obtained with compressed air. The supercritical swept wing had leading-edge slats and a full-span 0.30-chord plain flap divided into six equal spanwise segments. The flaps had 0.15-chord trailing-edge flaperons which were deflected with respect to the flap. Data were obtained through an angle-of-attack range for various flap deflections and momentum coefficients.

Some of the results follow:

1. The leading-edge wing slats improved the lift characteristics of the wing by delaying wing stall to much higher angles of attack and higher lift coefficients. The 0.25-chord slat was more effective than the 0.15-chord slat at the higher flap deflections.

2. The shorter-chord flaperon suffered flow separation at much lower deflections and produced much lower maximum lift than did the longer chord flaps.

3. For a given momentum coefficient, higher lift coefficients are obtained by blowing over the entire wing than by blowing over partial spans.

Langley Research Center
National Aeronautics and Space Administration
Hampton, VA 23665
September 23, 1976

REFERENCES

1. Johnson, William G., Jr.: Aerodynamic Characteristics of a Powered, Externally Blown Flap STOL Transport Model With Two Engine Simulator Sizes. NASA TN D-8057, 1975.

2. Sleeman, William C., Jr.; and Hohlweg, William C.: Low-Speed Wind-Tunnel Investigation of a Four-Engine Upper Surface Blown Model Having a Swept Wing and Rectangular and D-Shaped Exhaust Nozzles. NASA TN D-8061, 1975.

3. Hoad, Danny R.: Longitudinal Aerodynamic Characteristics of a Deflected-Thrust Propulsive-Lift Transport Model. NASA TM X-3234, 1975.

4. Hoad, Danny R.: Comparison of Aerodynamic Characteristics of Several STOL Concepts. NASA SP-320, 1972, pp. 111-119.

5. Mechtly, E. A.: The International System of Units - Physical Constants and Conversion Factors (Second Revision). NASA SP-7012, 1973.

6. Heyson, Harry H.: Linearized Theory of Wind-Tunnel Jet-Boundary Corrections and Ground Effect for VTOL-STOL Aircraft. NASA TR R-124, 1962.

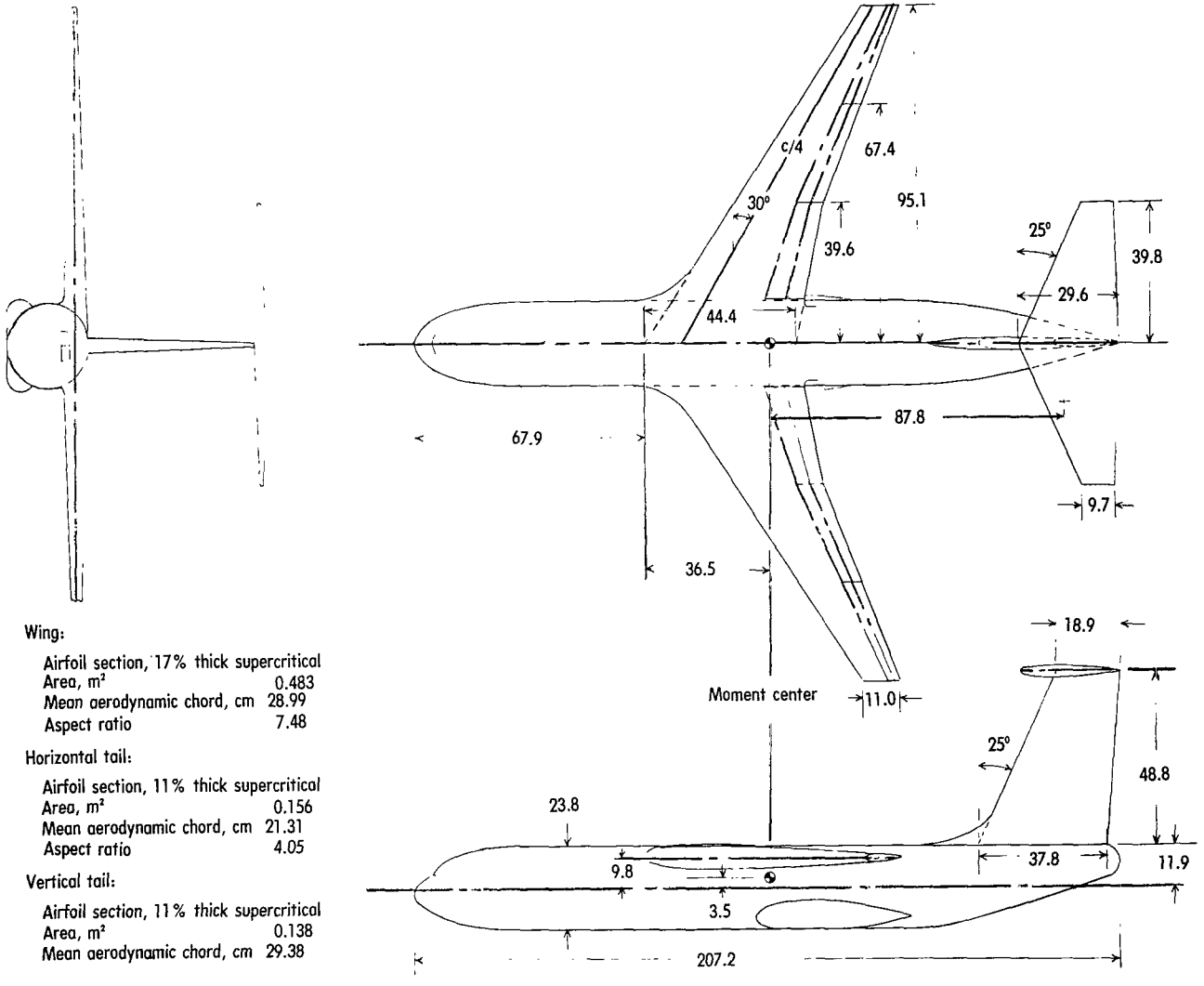

Wing:

Airfoil section, 17% thick supercritical	
Area, m^2	0.483
Mean aerodynamic chord, cm	28.99
Aspect ratio	7.48

Horizontal tail:

Airfoil section, 11% thick supercritical	
Area, m^2	0.156
Mean aerodynamic chord, cm	21.31
Aspect ratio	4.05

Vertical tail:

Airfoil section, 11% thick supercritical	
Area, m^2	0.138
Mean aerodynamic chord, cm	29.38

Figure 1.- Three-view drawing of model. All dimensions are in centimeters.

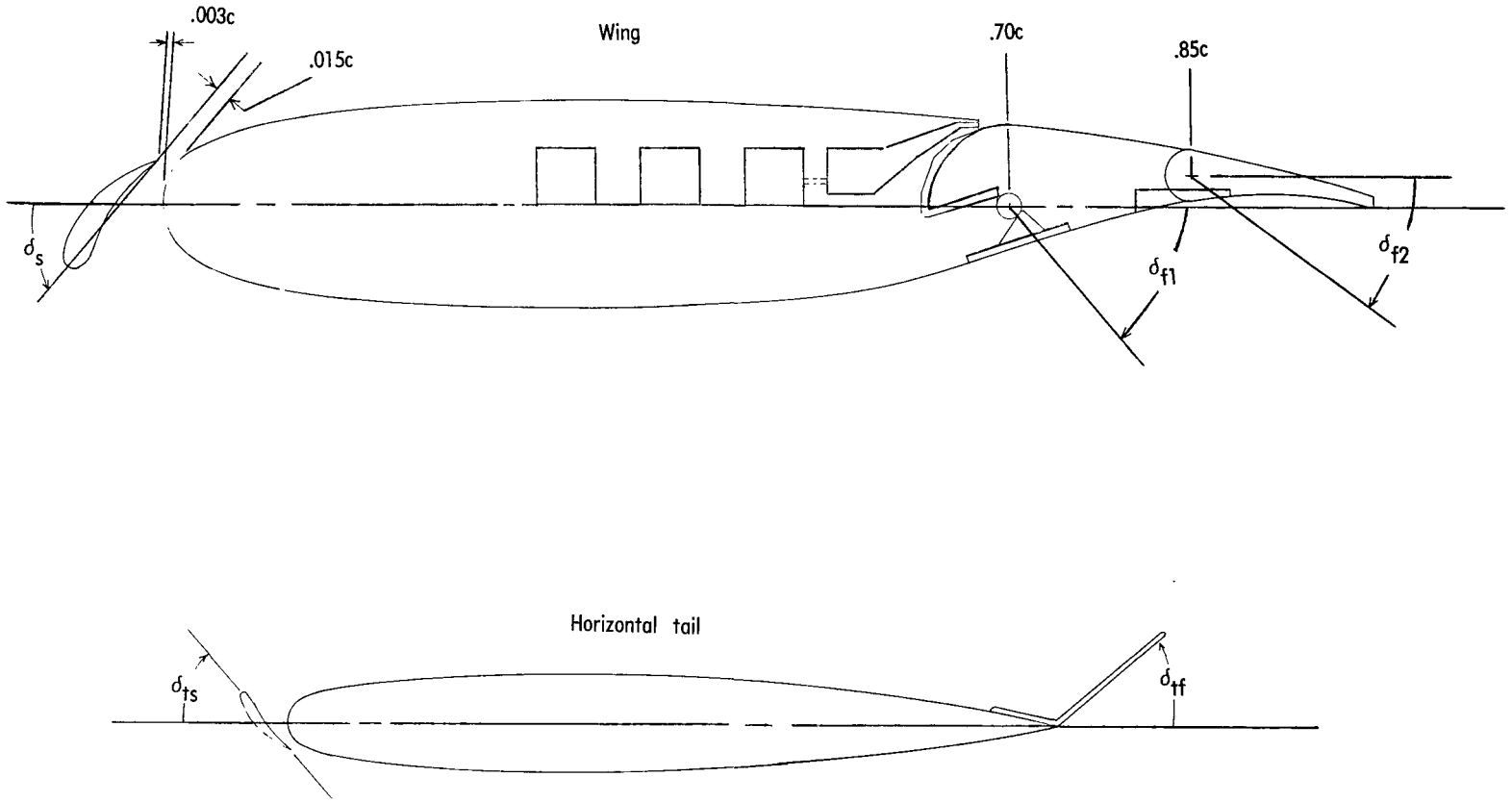

Figure 2.- Sketch of wing and horizontal-tail sections showing flap and slat details.

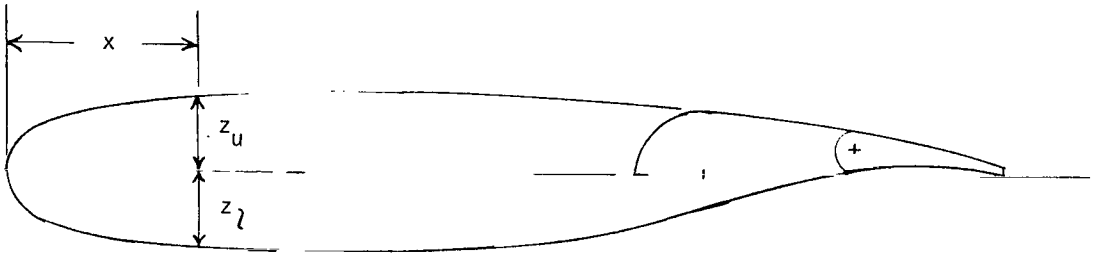

x, percent chord	z_u, percent chord	z_l, percent chord
0.00	0.00	0.00
.75	2.70	-2.70
1.25	3.40	-3.40
1.62	3.79	-3.62
2.50	4.47	-4.48
5.00	5.65	-5.70
7.50	6.38	-6.47
10.00	6.91	-7.02
12.50	7.31	-7.42
15.00	7.62	-7.74
17.50	7.86	-7.97
20.00	8.05	-8.16
25.00	8.31	-8.39
30.00	8.45	-8.49
32.00	8.48	-8.50
35.00	8.50	-8.48
40.00	8.47	-8.39
45.00	8.36	-8.19
50.00	8.19	-7.88
55.00	7.94	-7.38
60.00	7.62	-6.56
62.50	7.43	-5.97
65.00	7.22	-5.21
66.00	7.13	-4.85
67.50	6.99	-4.28
70.00	6.74	-3.40
72.50	6.46	-2.58
75.00	6.15	-1.83
77.50	5.82	-1.14
80.00	5.46	- .53
82.50	5.06	.01
85.00	4.63	.46
87.50	4.15	.80
90.00	3.63	1.02
92.50	3.05	1.10
95.00	2.42	.98
97.50	1.73	.63
100.00	.97	0

Figure 3.- Wing ordinates.

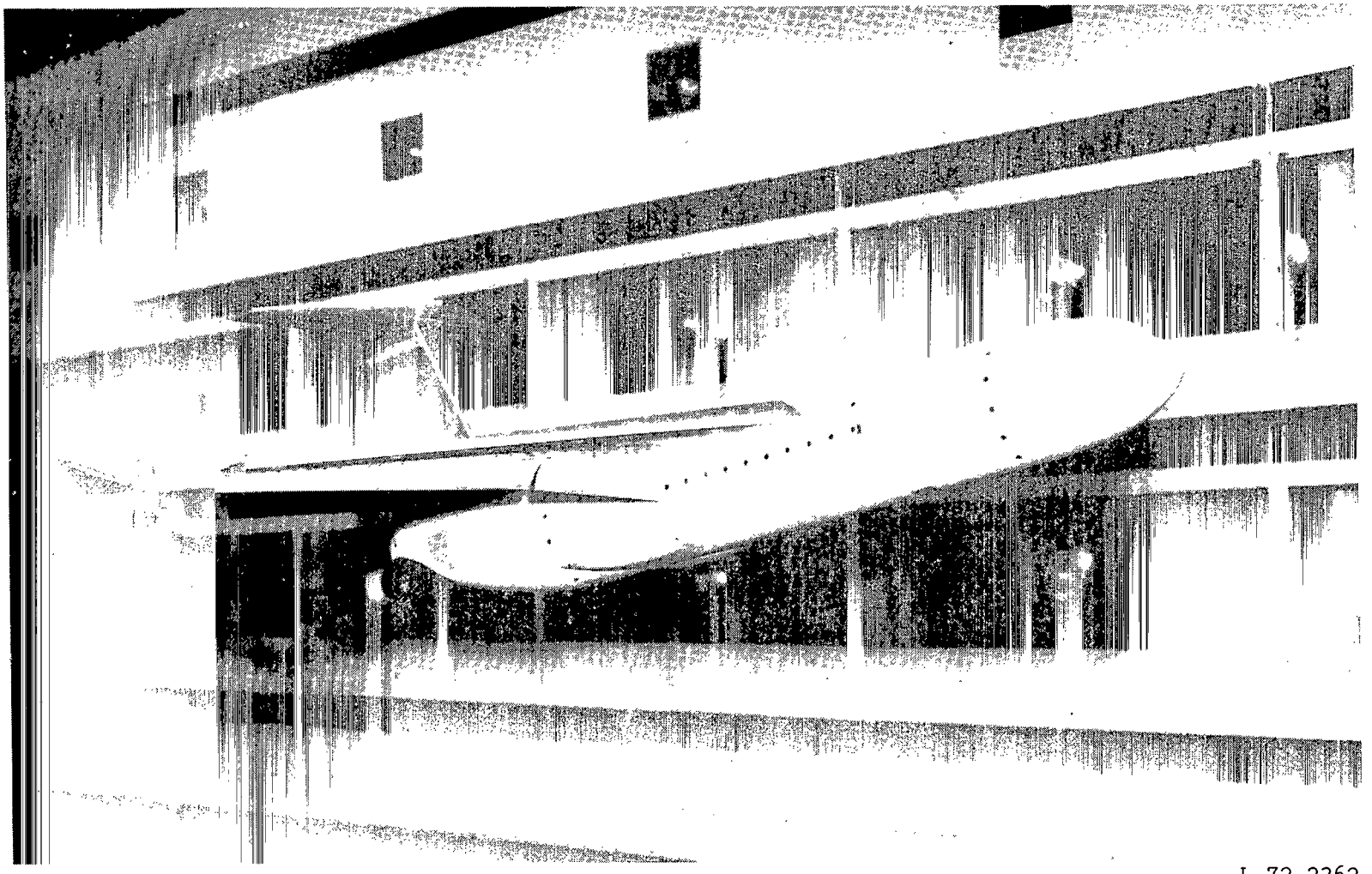

L-72-2362

(a) Three-quarter front view.

Figure 4.- Photographs of model.

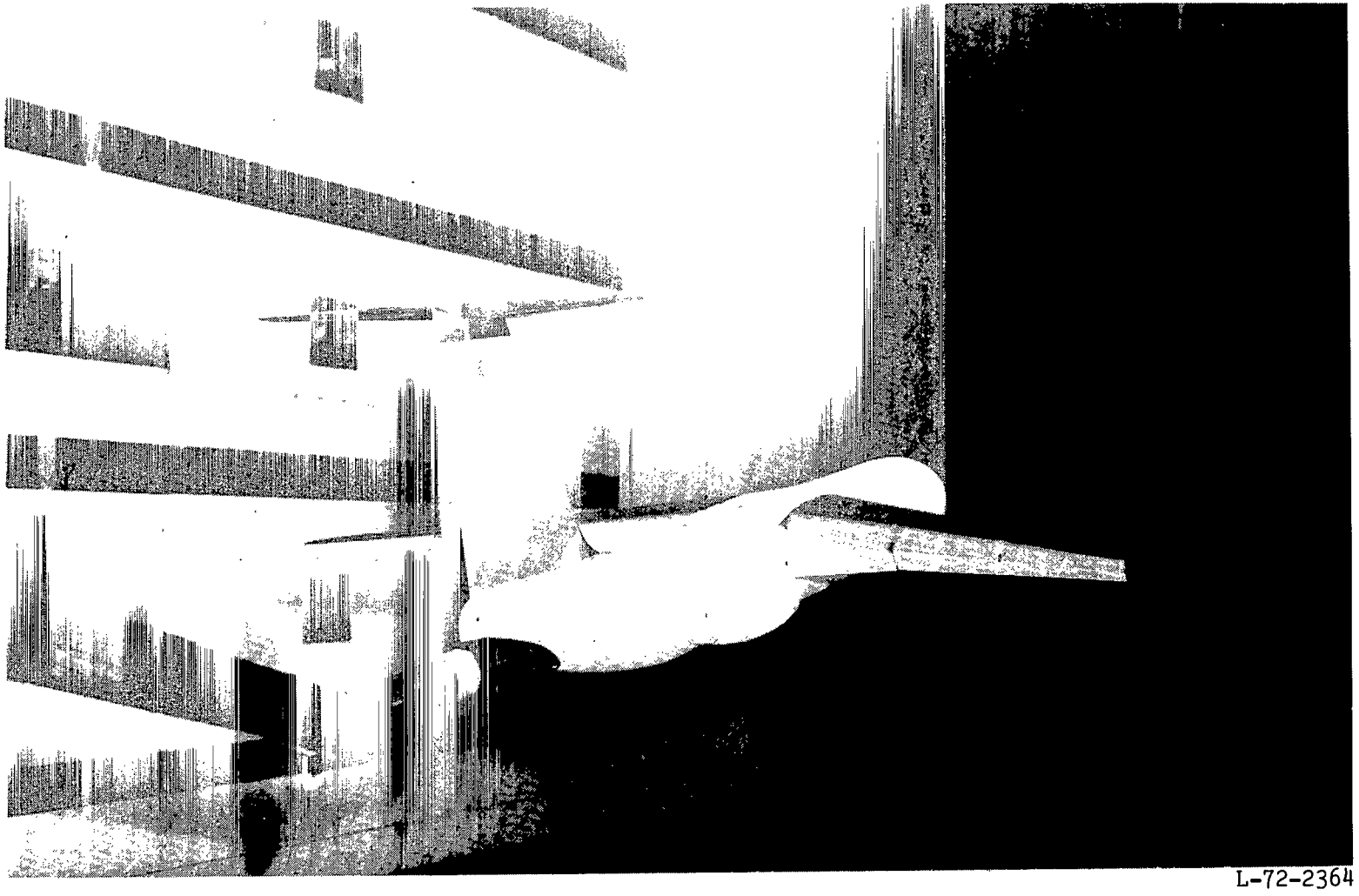

L-72-2364

(b) Three-quarter rear view.

Figure 4.- Concluded.

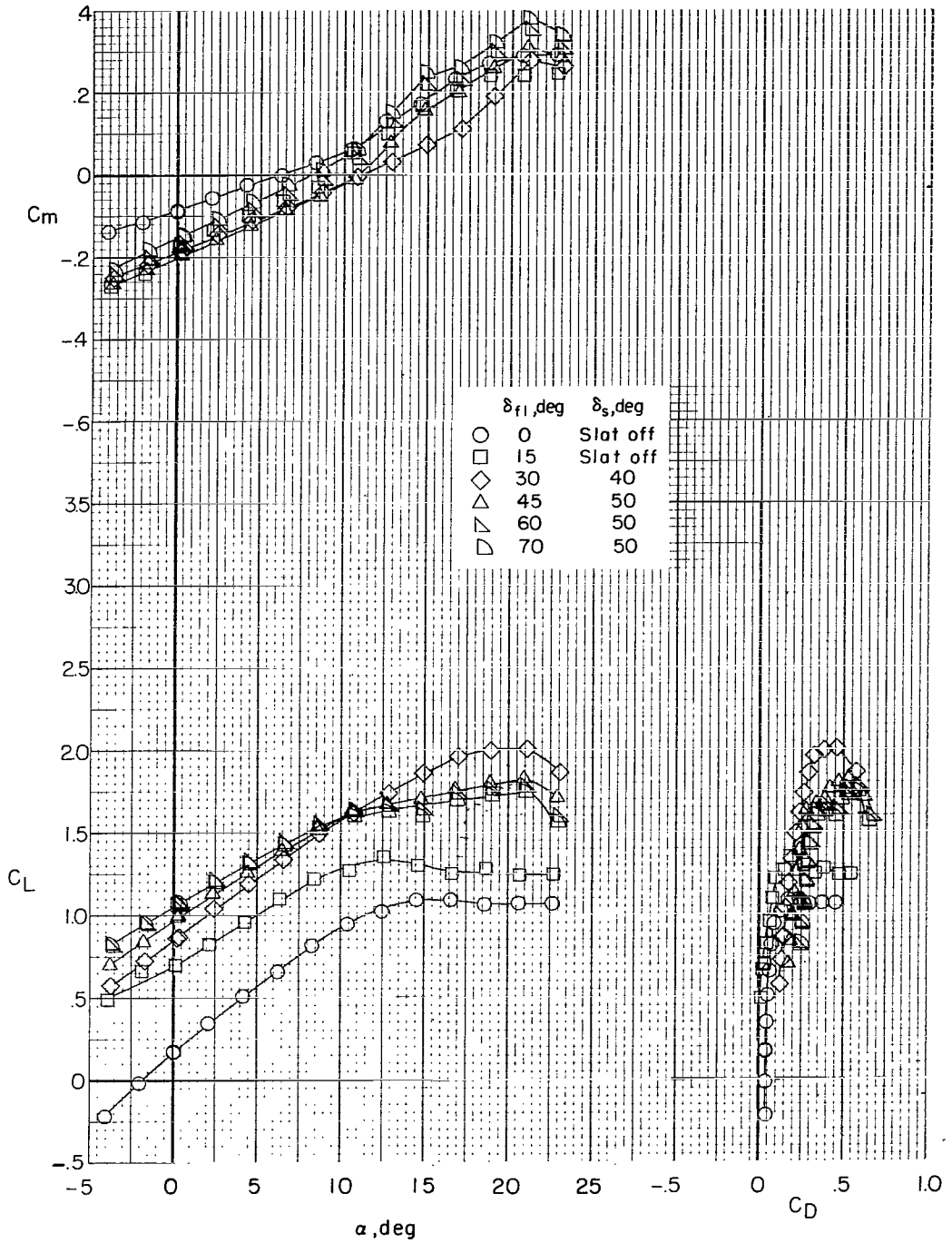

(a) $C_\mu = 0.$

Figure 5.- Effect of flap deflection on longitudinal characteristics of model. Tail off; $\delta_{f2} = 0^o$; slat chord, 0.15c.

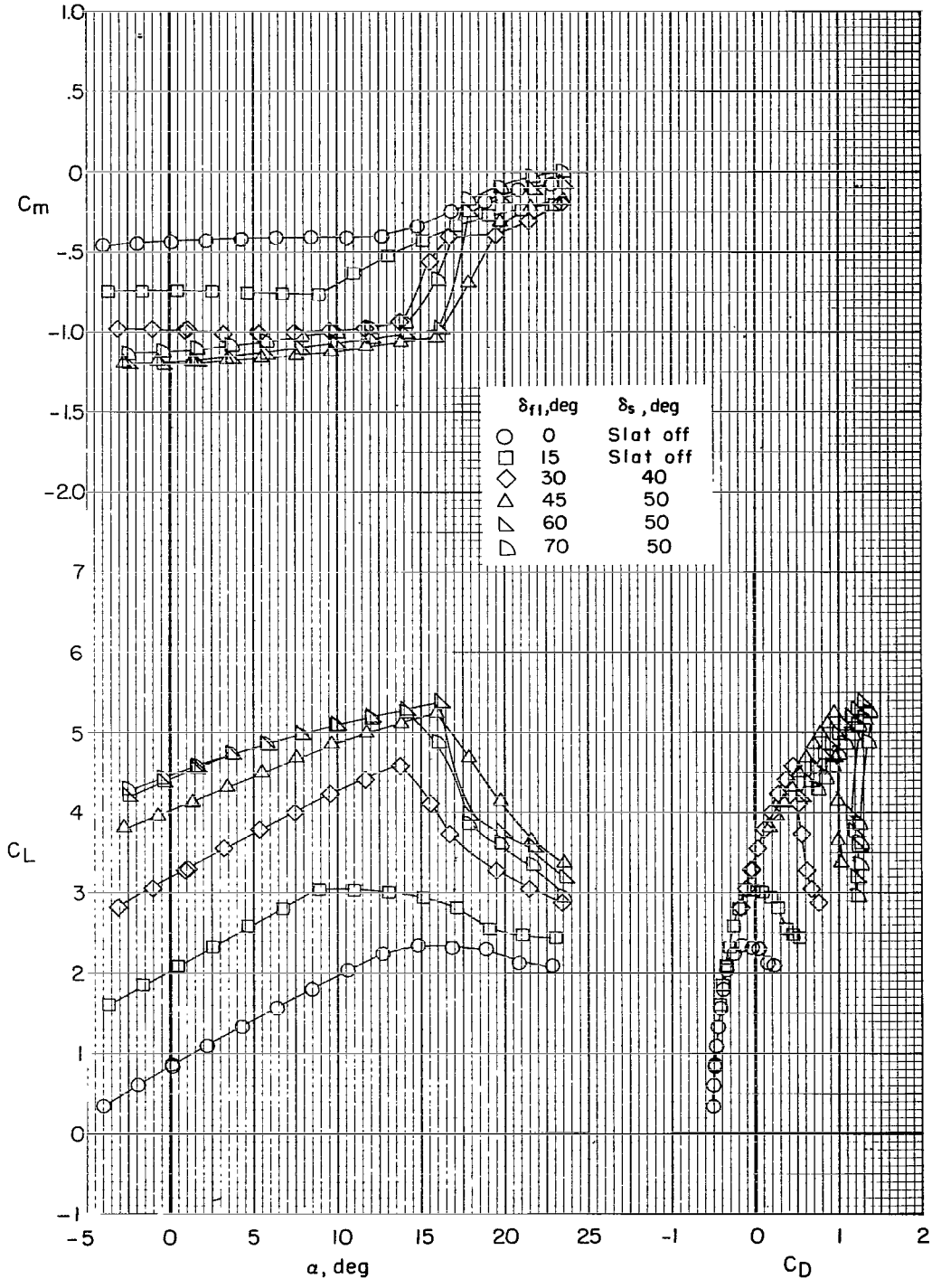

(b) C_μ = 0.61.

Figure 5.- Continued.

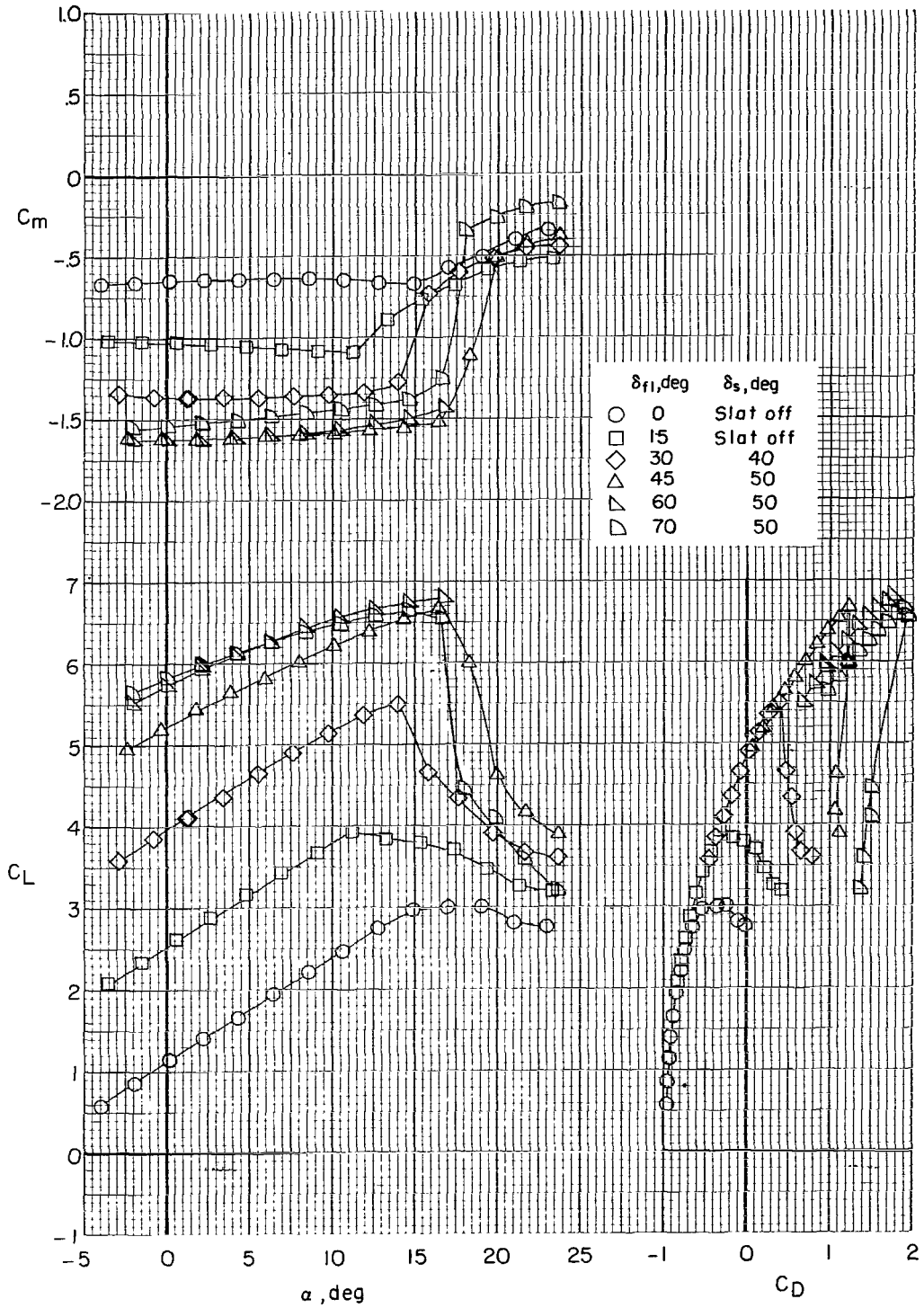

(c) C_μ = 1.11.

Figure 5.- Continued.

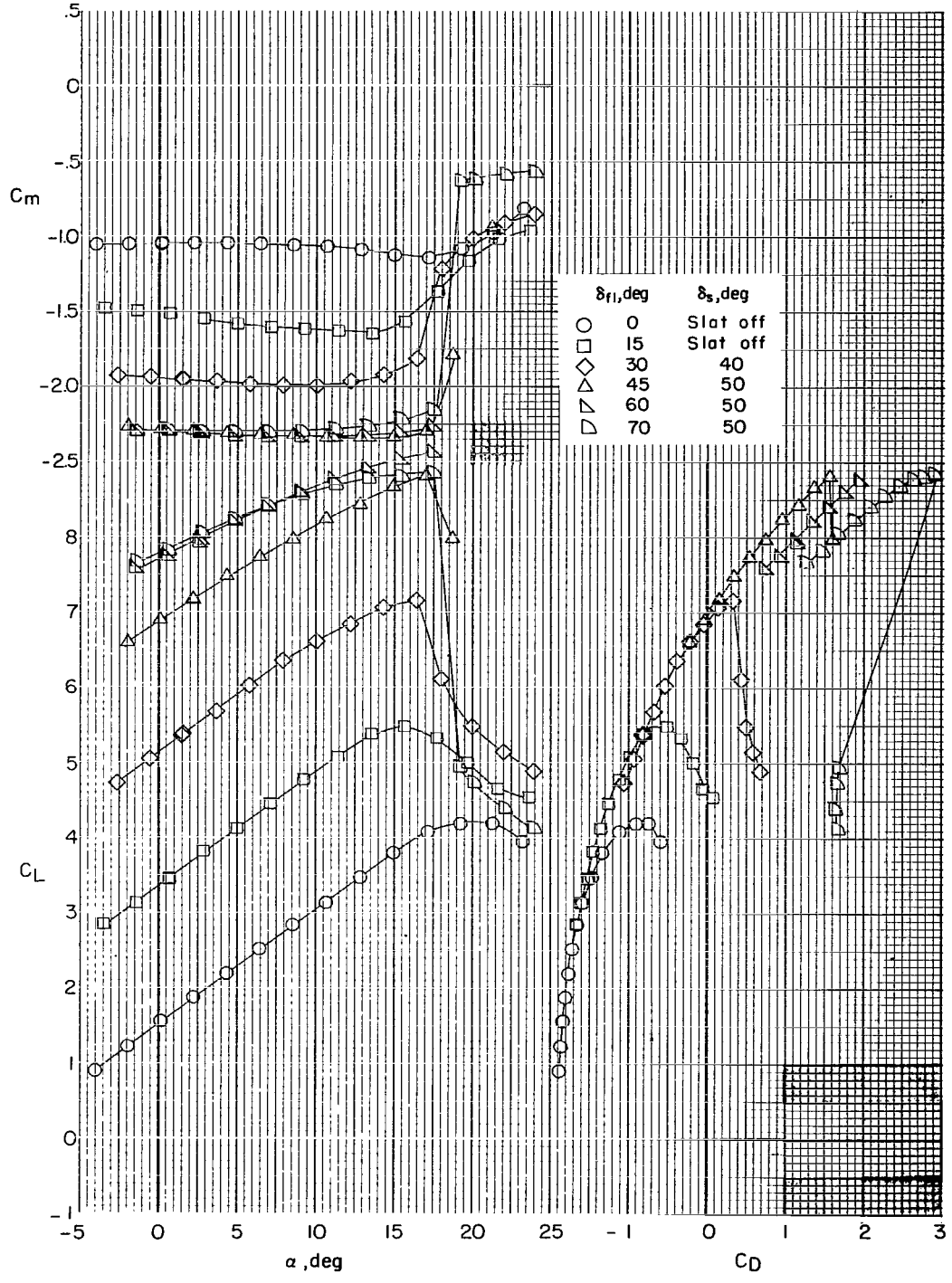

(d) C_μ = 2.20.

Figure 5.- Concluded.

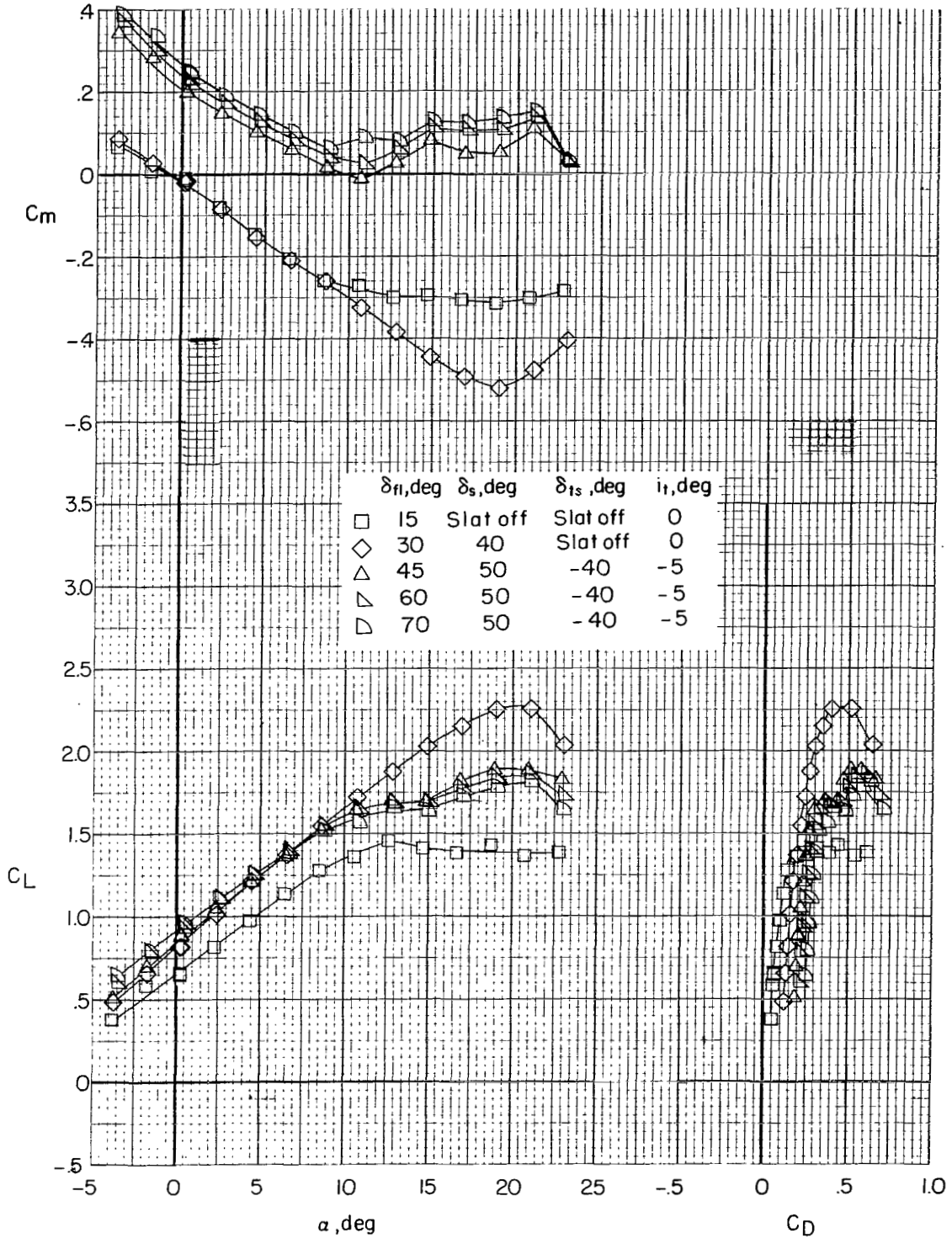

(a) $C_\mu = 0$.

Figure 6.- Effect of flap deflection on longitudinal characteristics of model. Tail on; tail flap off; $\delta_{f2} = 0^o$; slat chord, 0.15c.

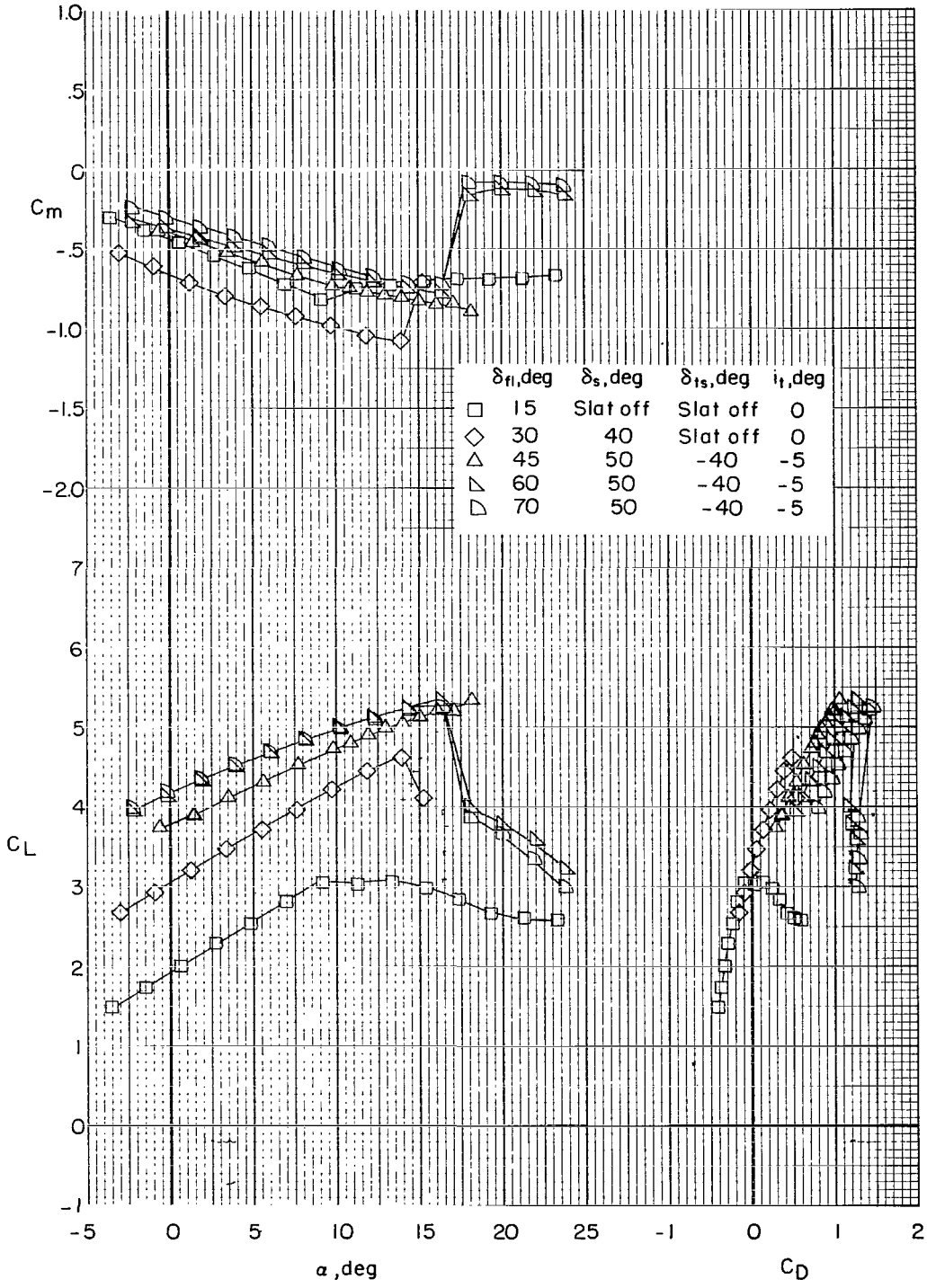

(b) $C_\mu = 0.60$.

Figure 6.- Continued.

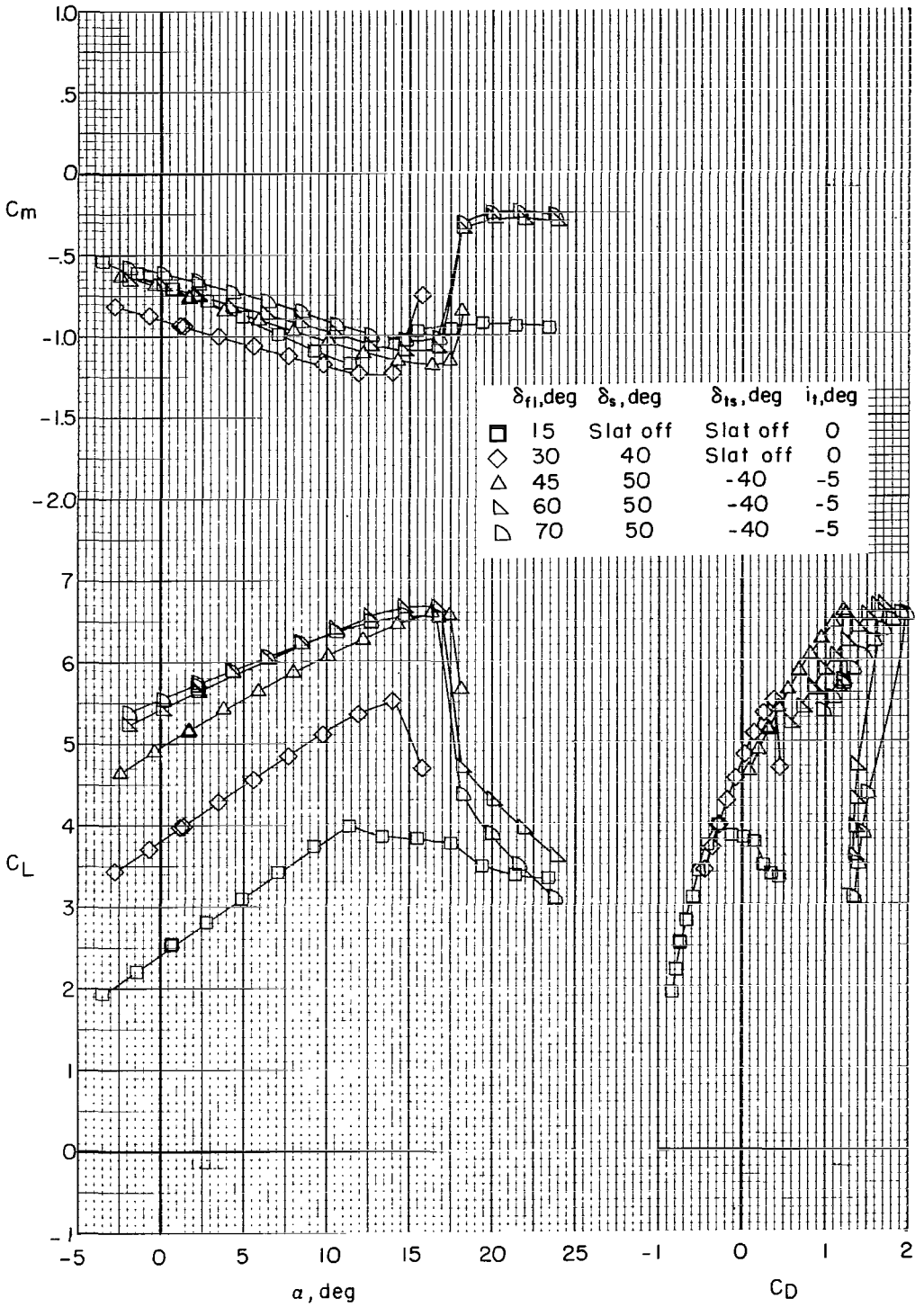

(c) C_μ = 1.11.

Figure 6.- Continued.

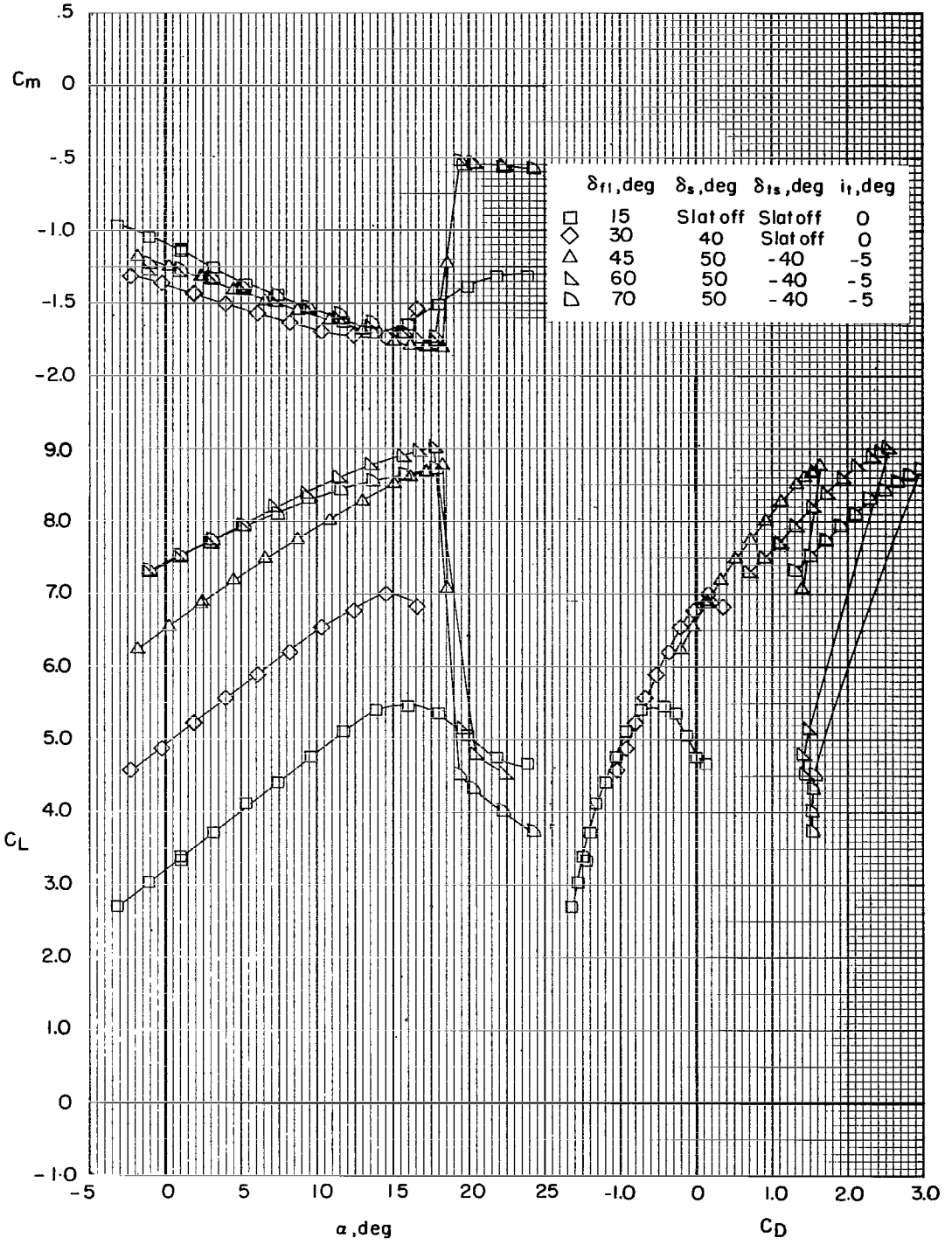

(d) C_μ = 2.20.

Figure 6.- Concluded.

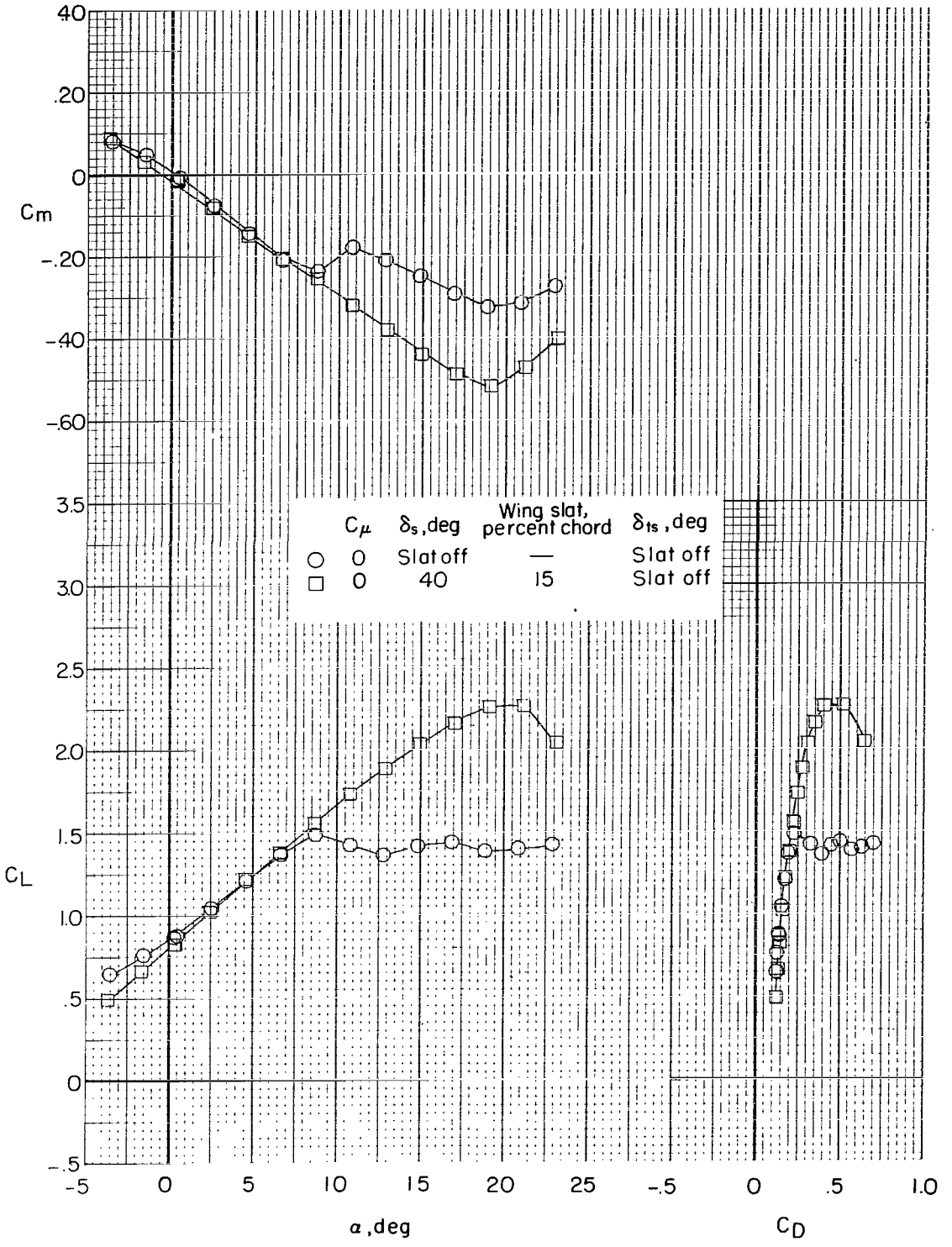

Figure 7.- Effect of wing slats on longitudinal characteristics of model. Tail on; tail flap off; $\delta_{f1} = 30^{o}$; $\delta_{f2} = 0^{o}$; $i_t = 0^{o}$.

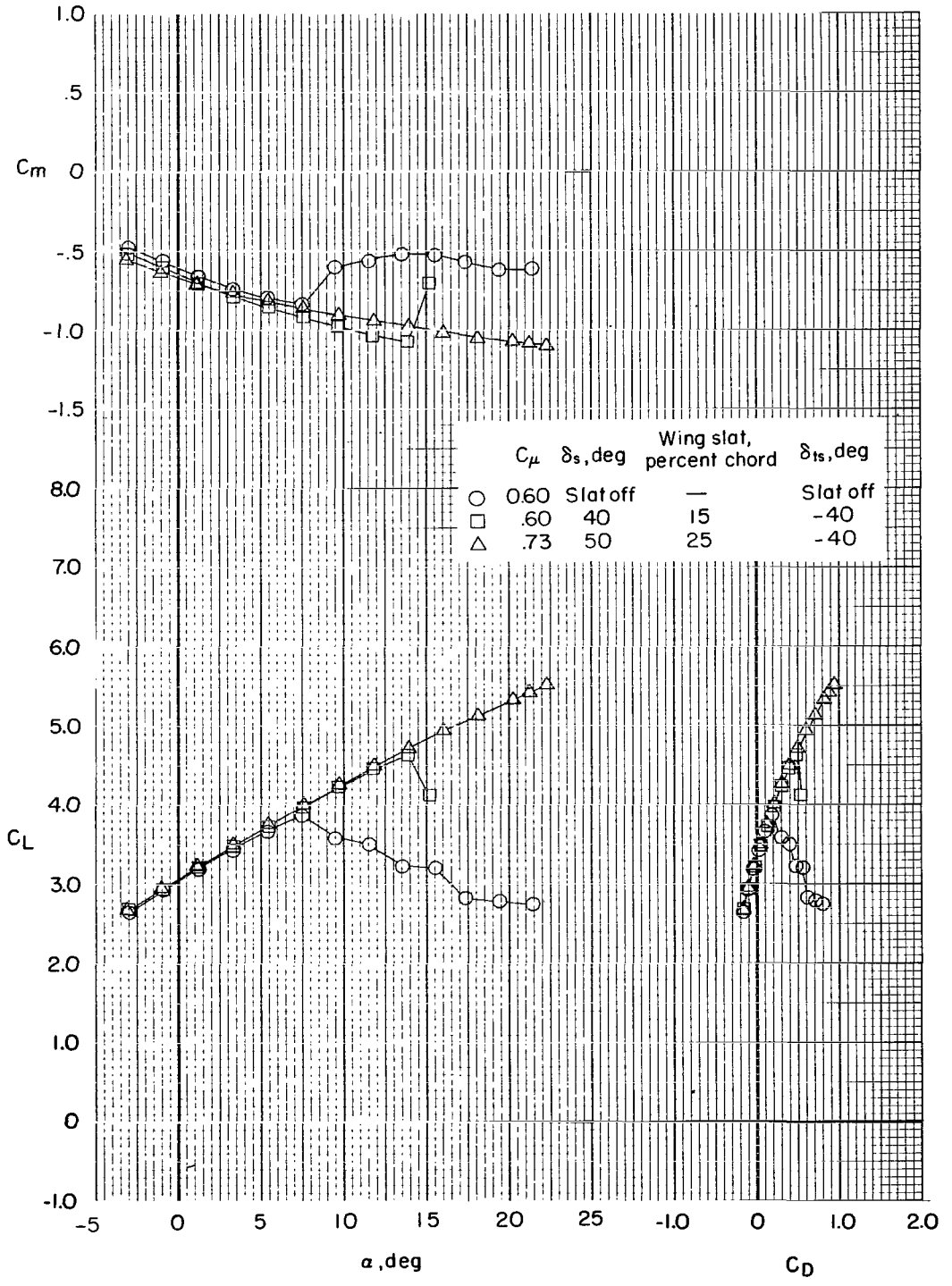

Figure 7.- Continued.

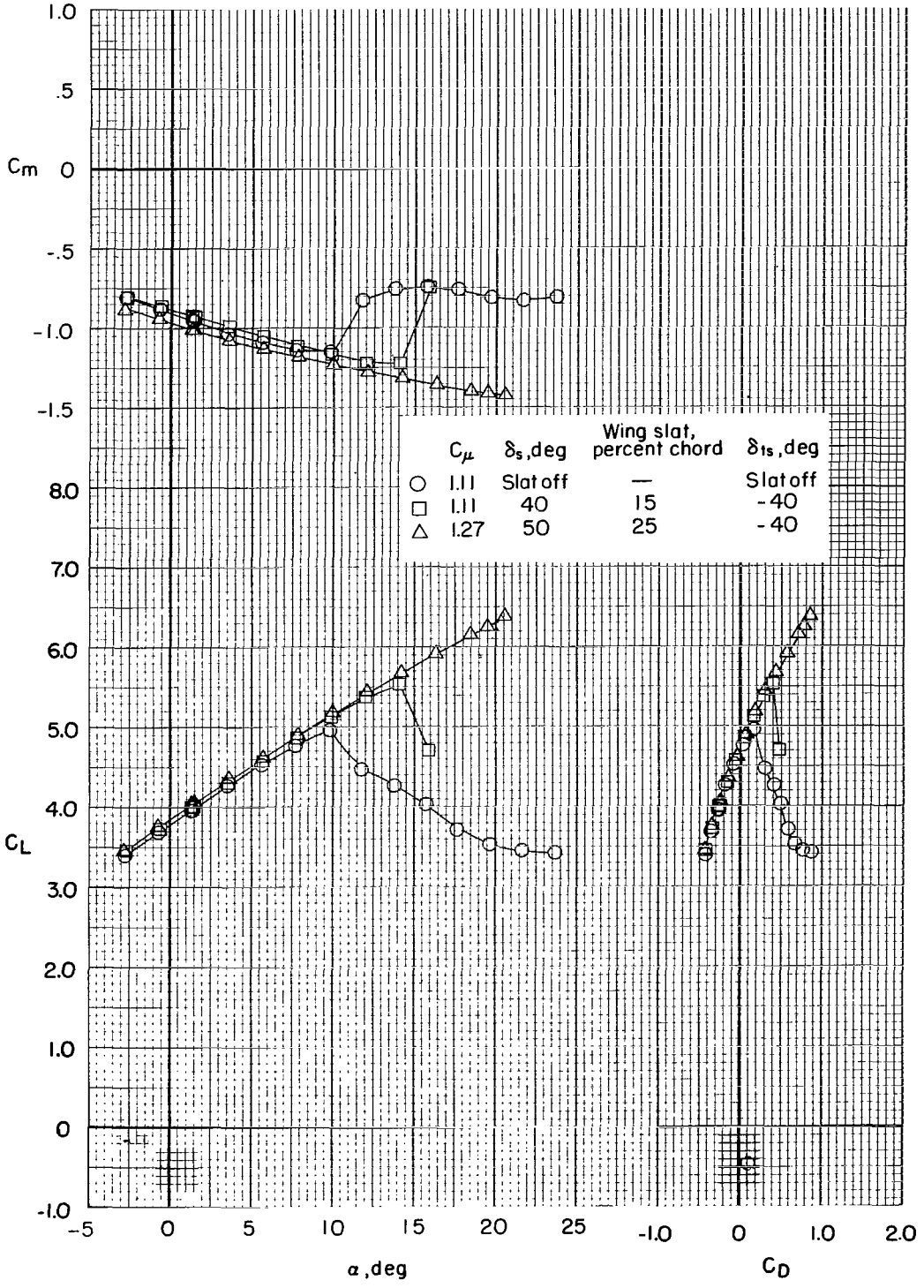

Figure 7.- Continued.

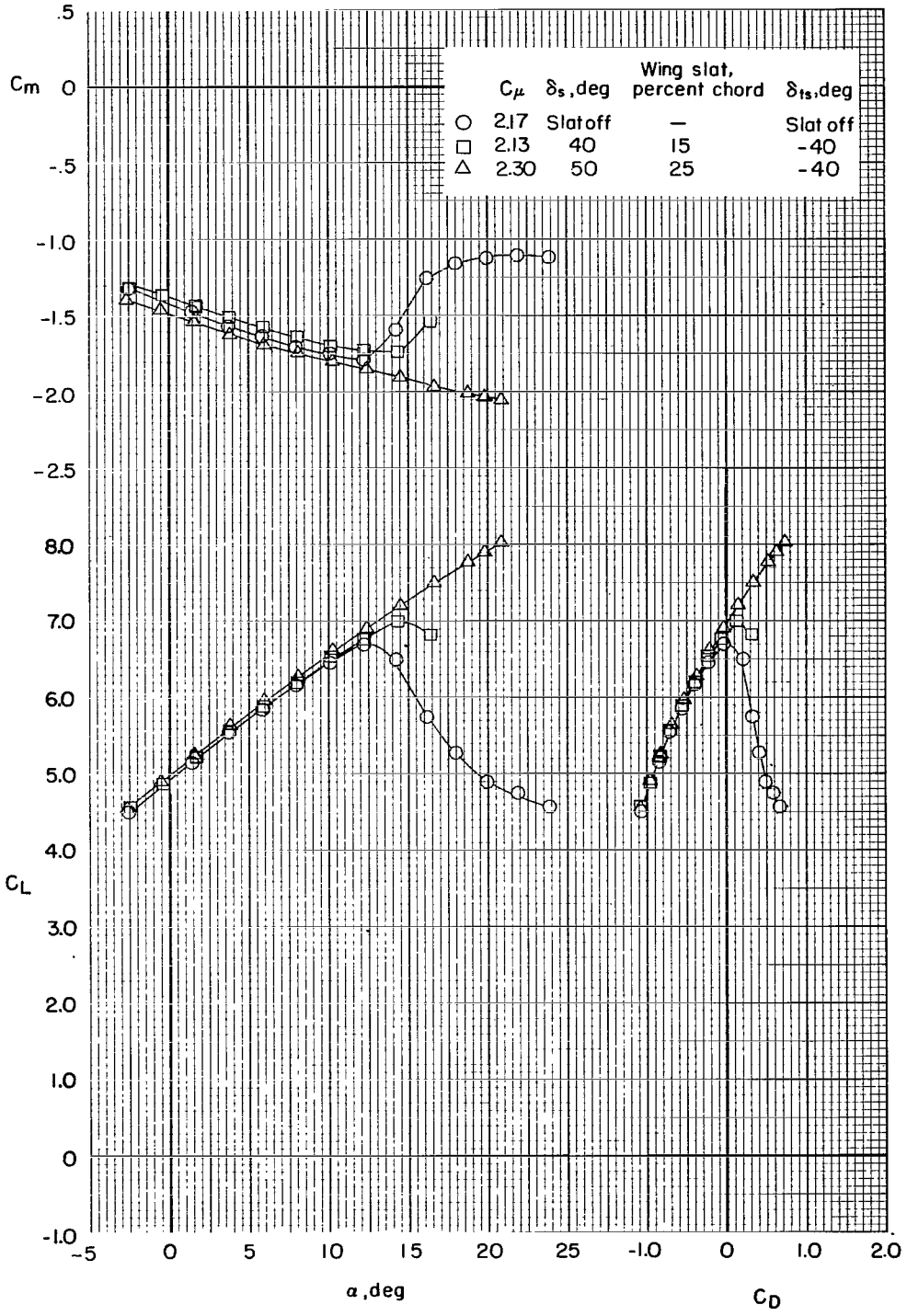

Figure 7.- Concluded.

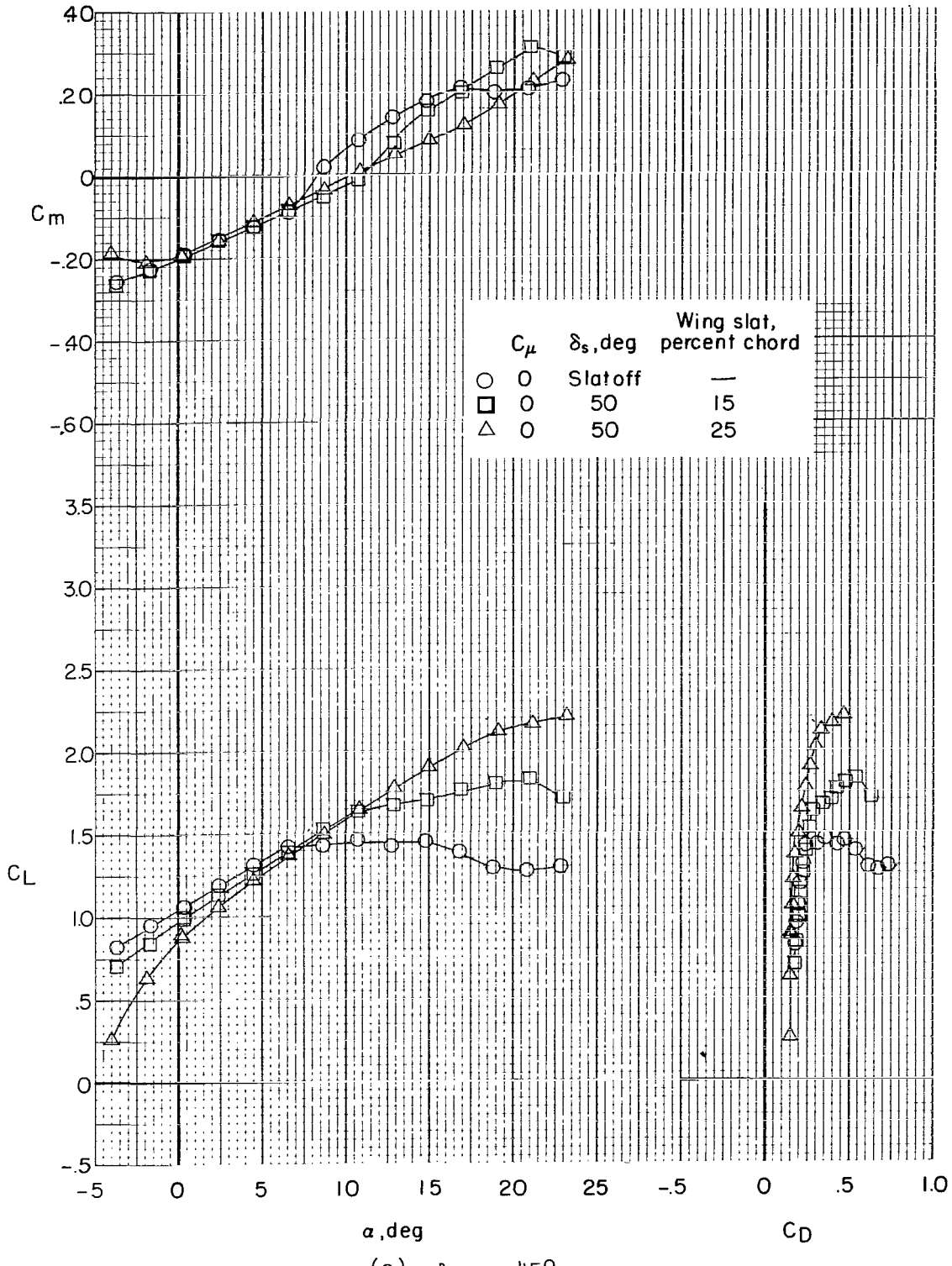

(a) $\delta_{f1} = 45^\circ$.

Figure 8.- Effect of wing-slat chord on longitudinal characteristics of model. Tail off; $\delta_{f2} = 0^\circ$.

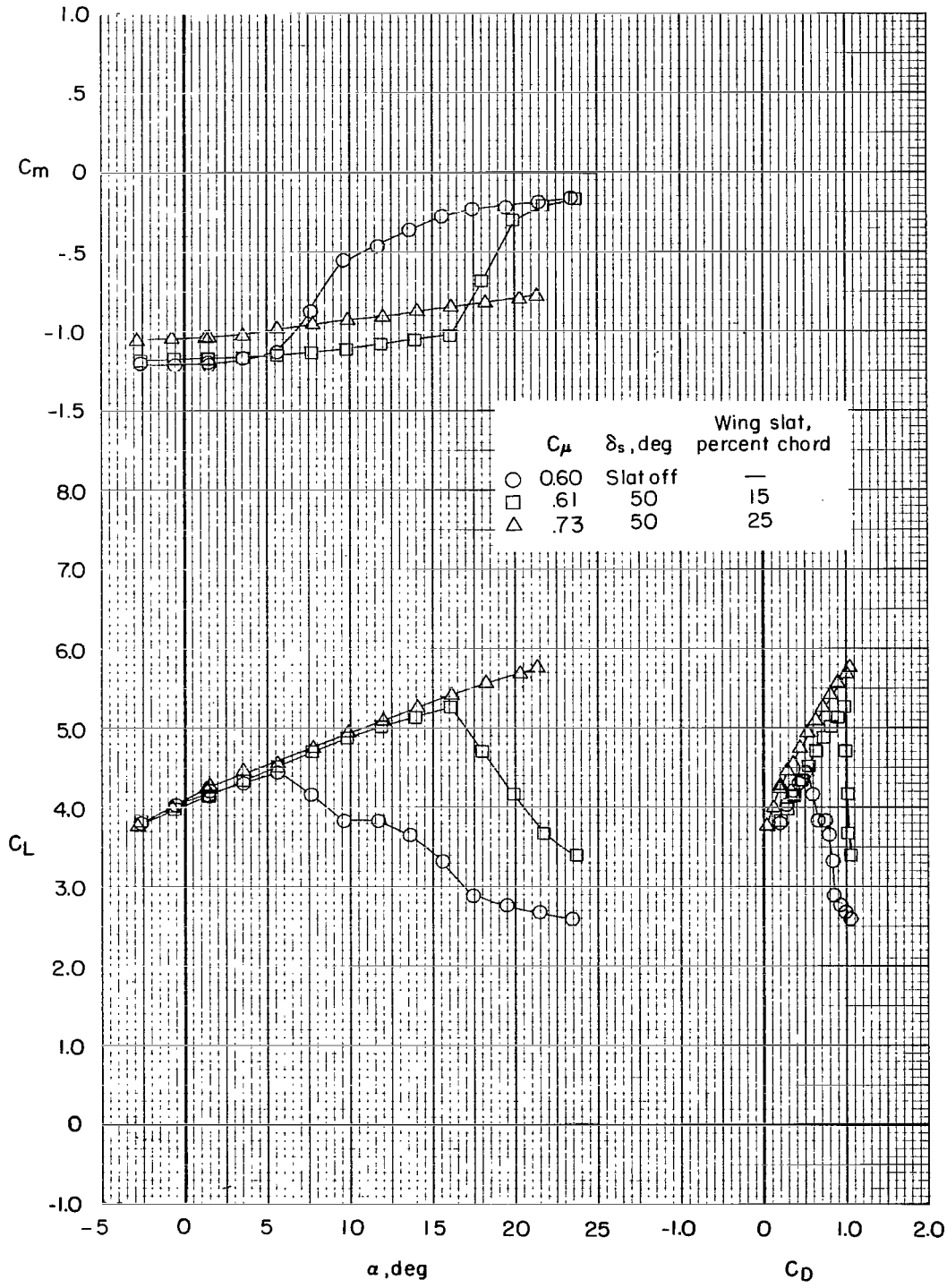

(a) Continued.

Figure 8.- Continued.

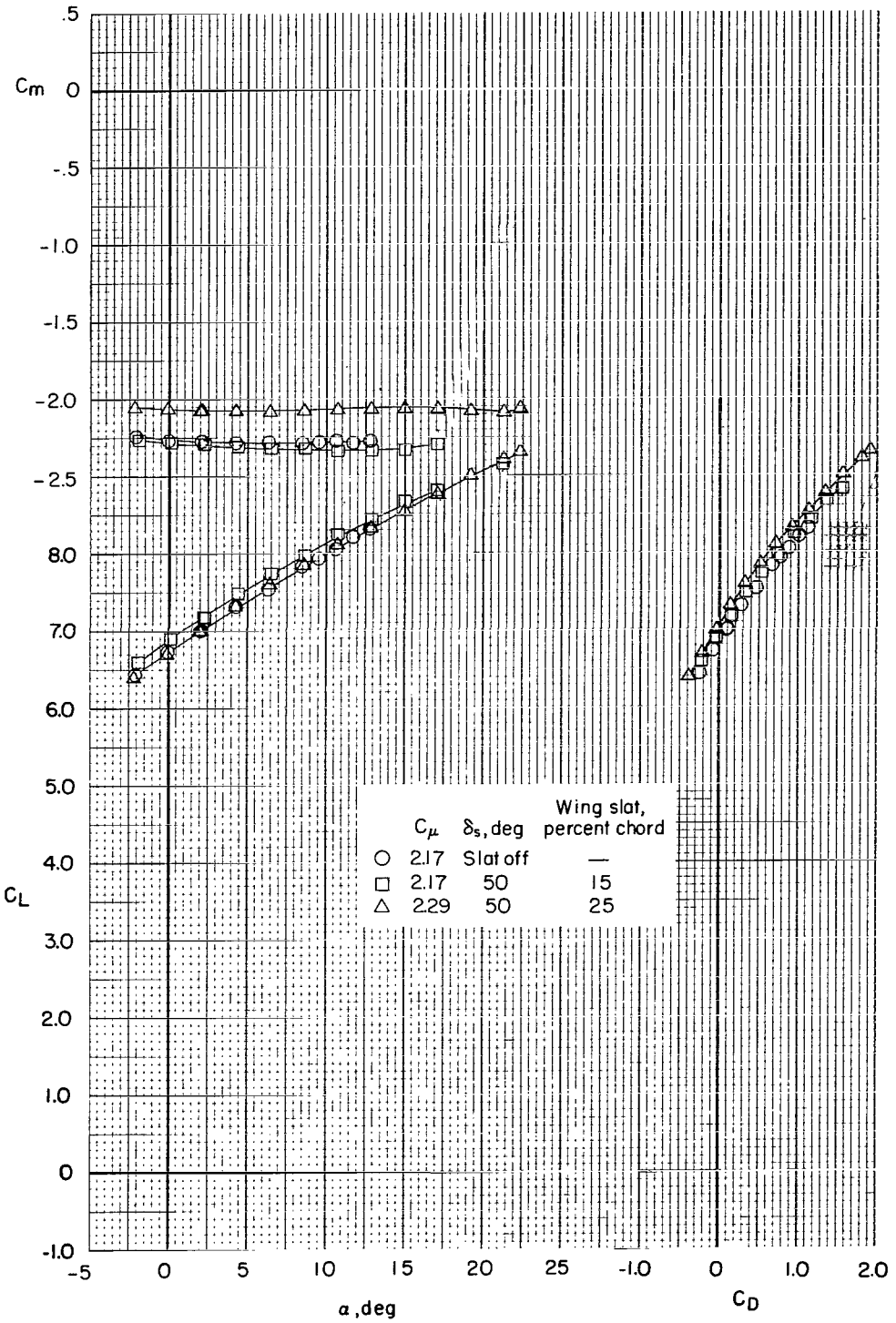

(a) Concluded.

Figure 8.- Continued.

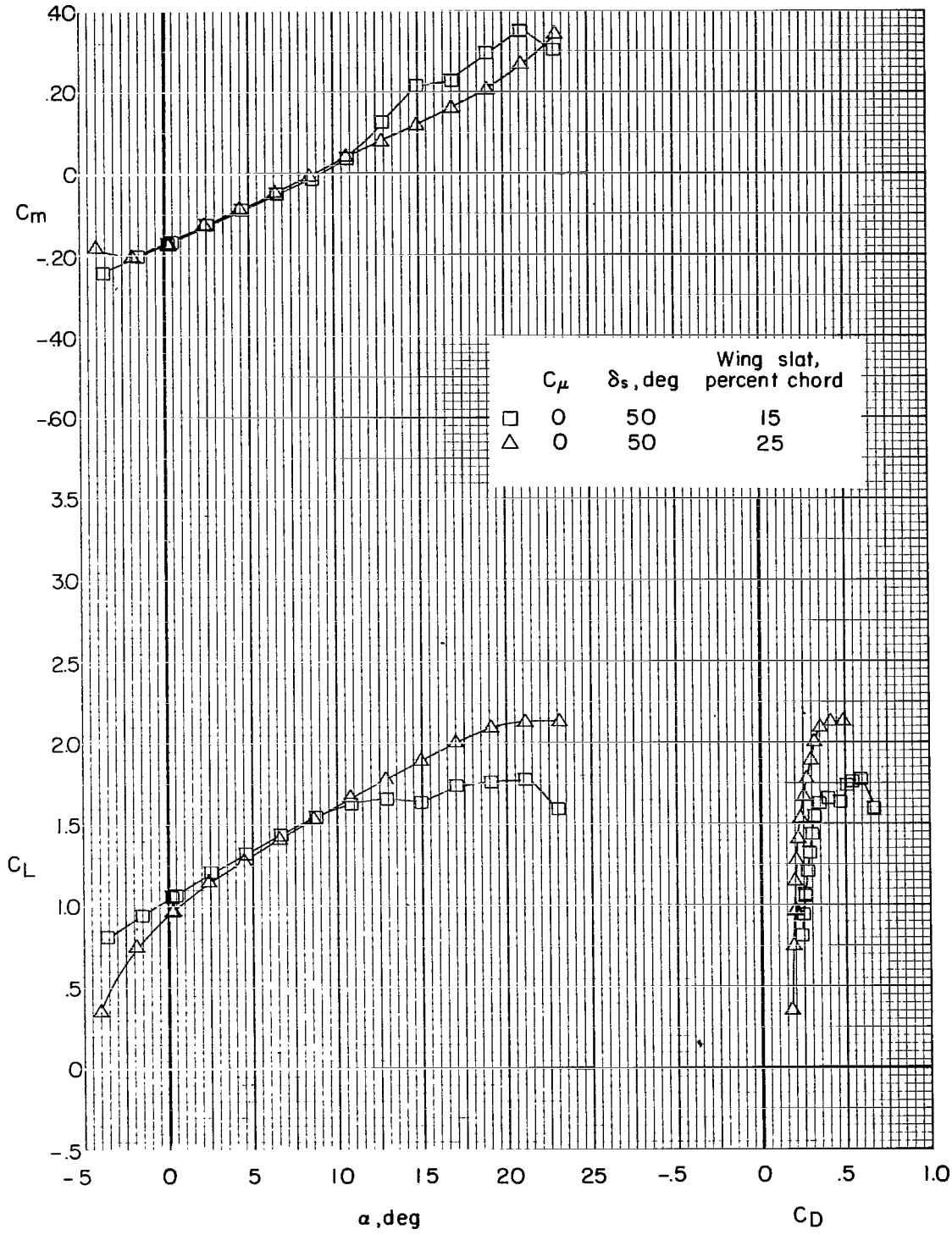

(b) $\delta_{f1} = 60^{\circ}$.

Figure 8.- Continued.

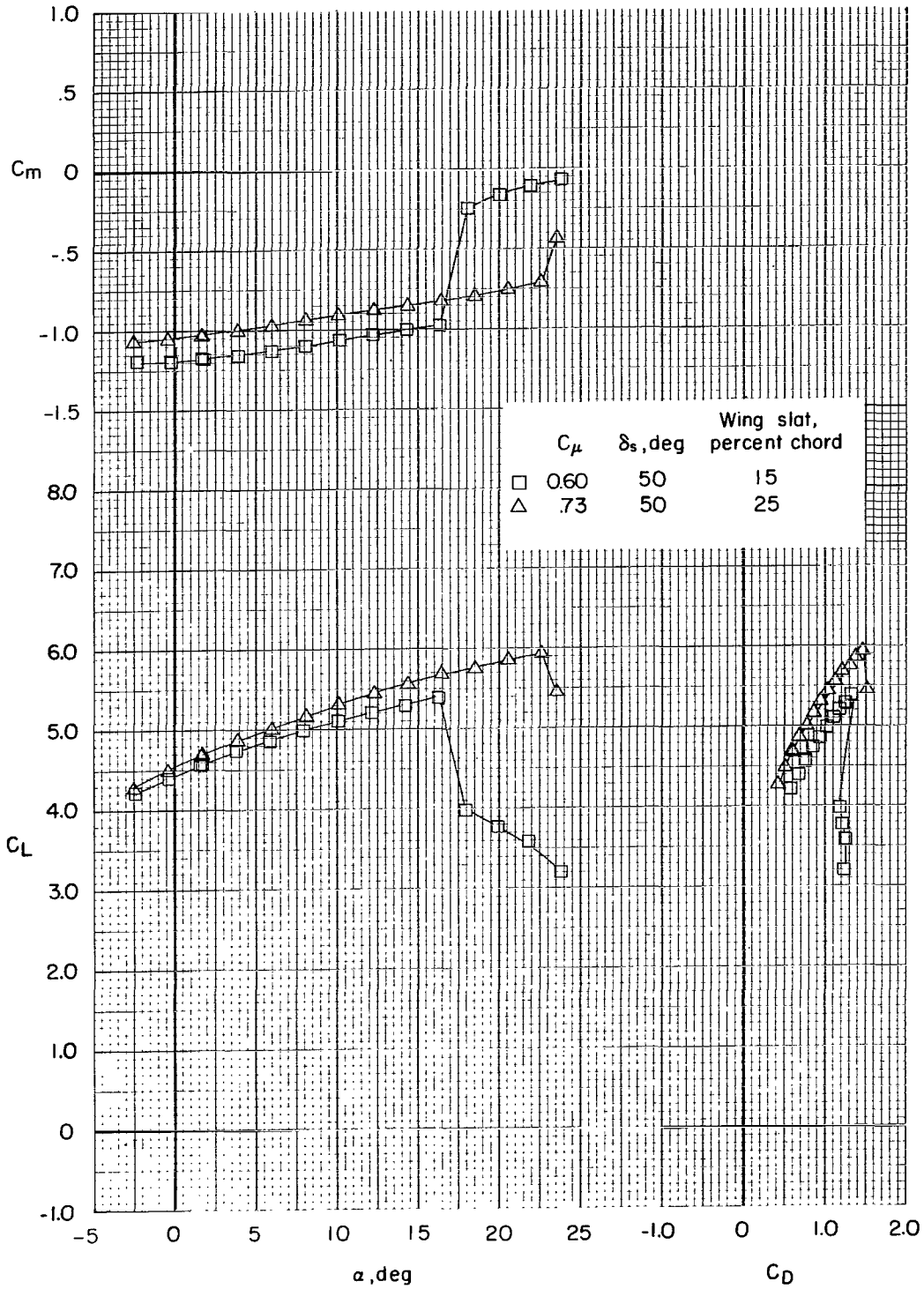

(b) Continued.

Figure 8.- Continued.

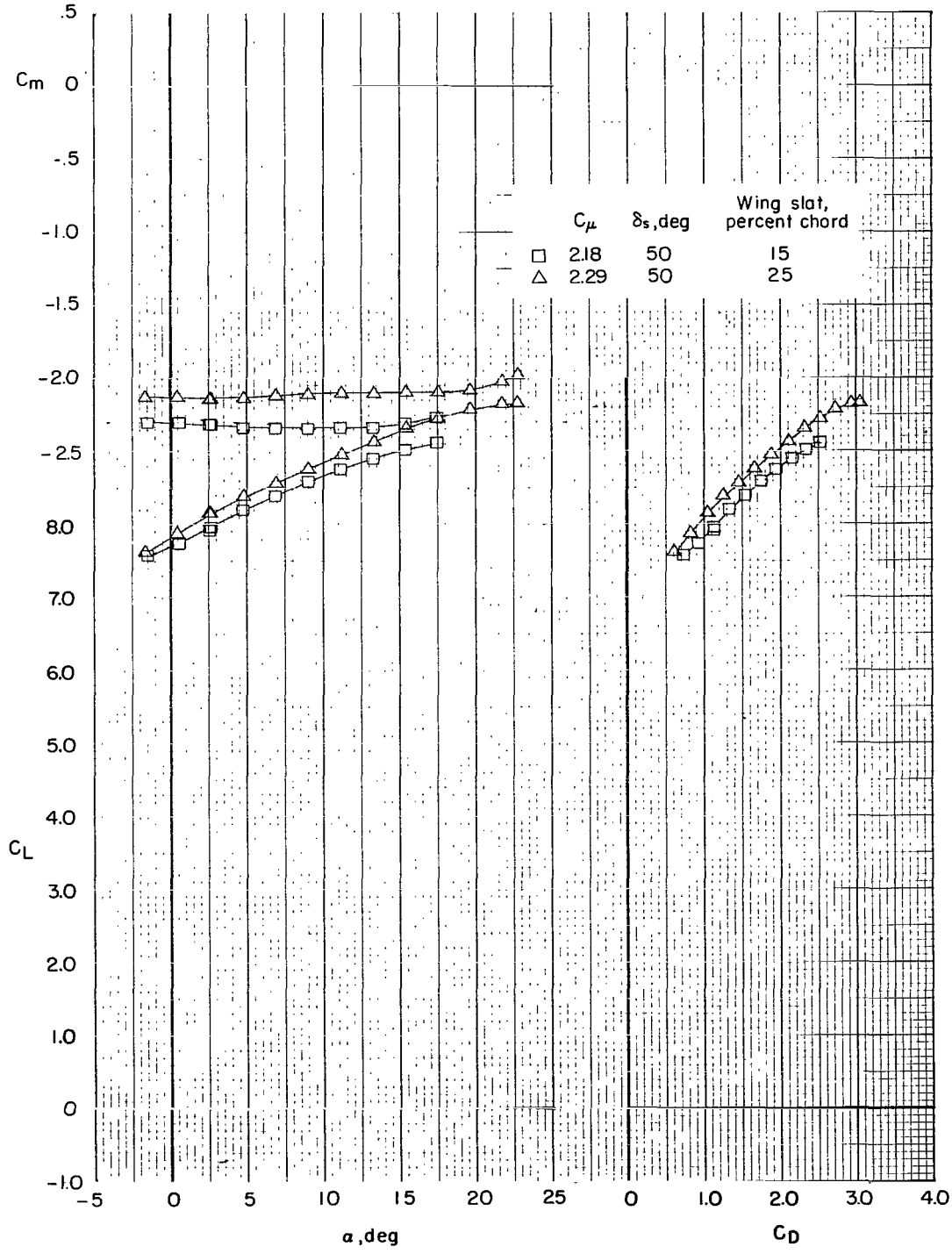

(b) Concluded.

Figure 8.- Continued.

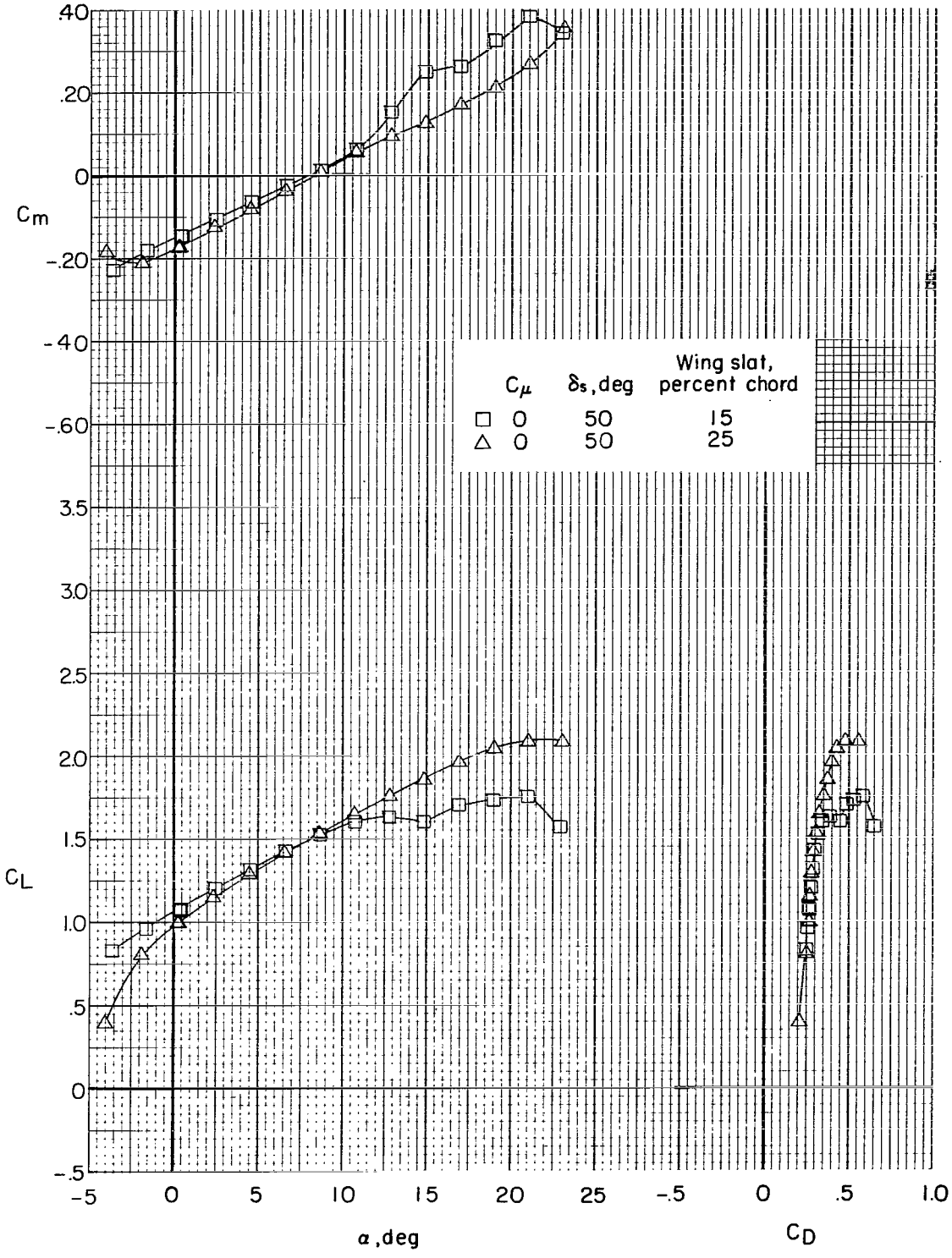

(c) $\delta_{f1} = 70^\circ$.

Figure 8.- Continued.

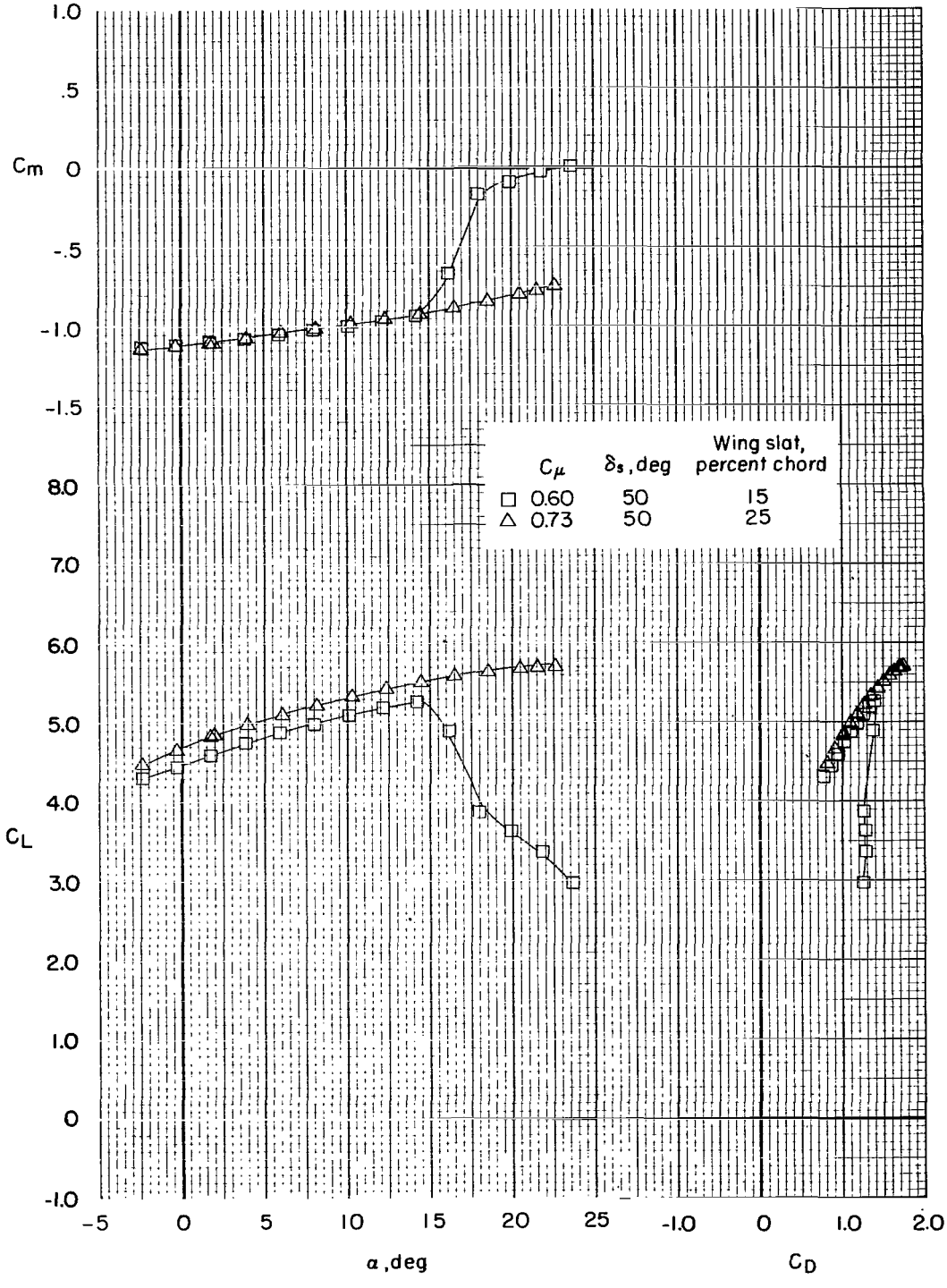

(c) Continued.

Figure 8.- Continued.

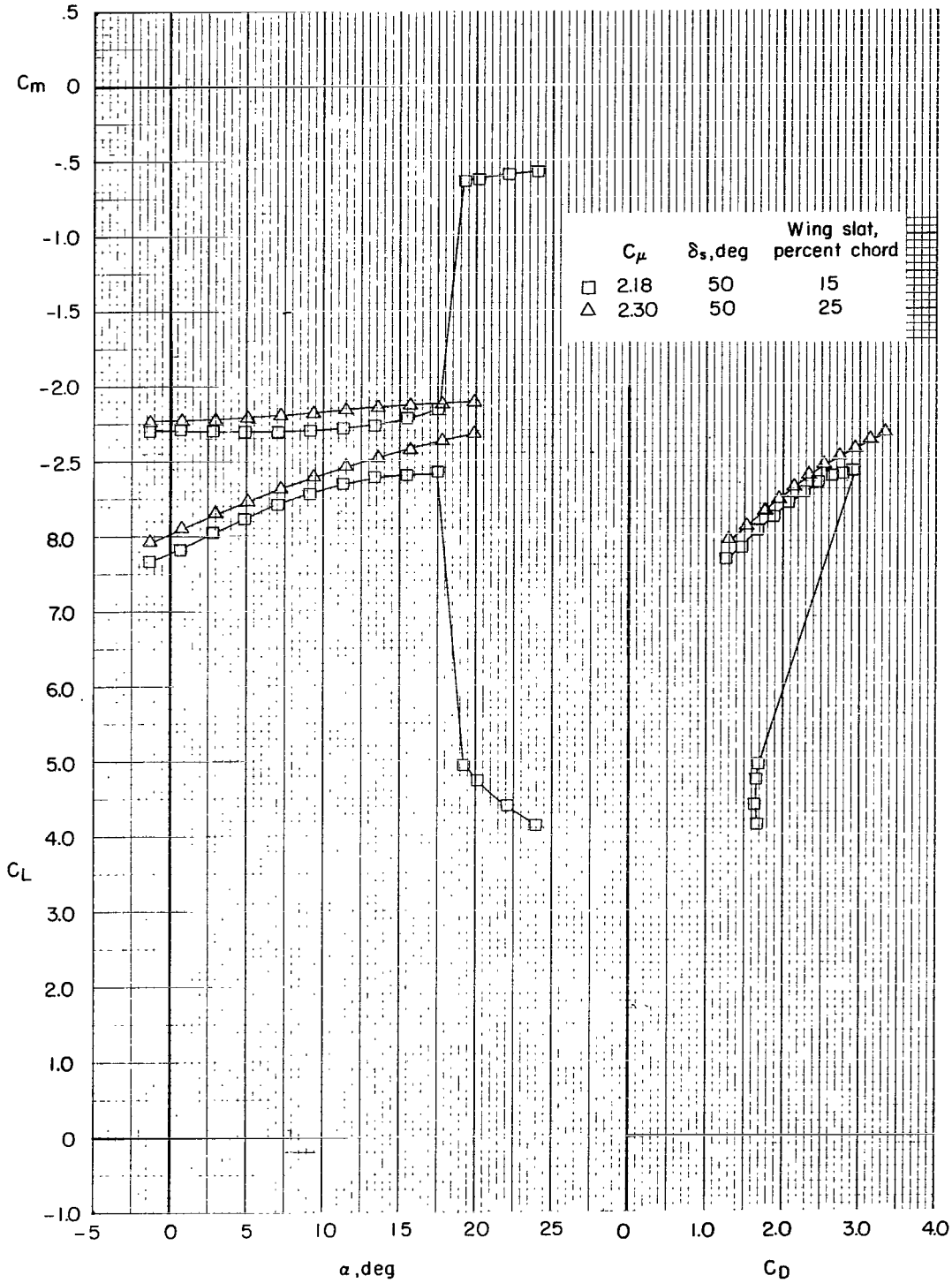

(c) Concluded.

Figure 8.- Concluded.

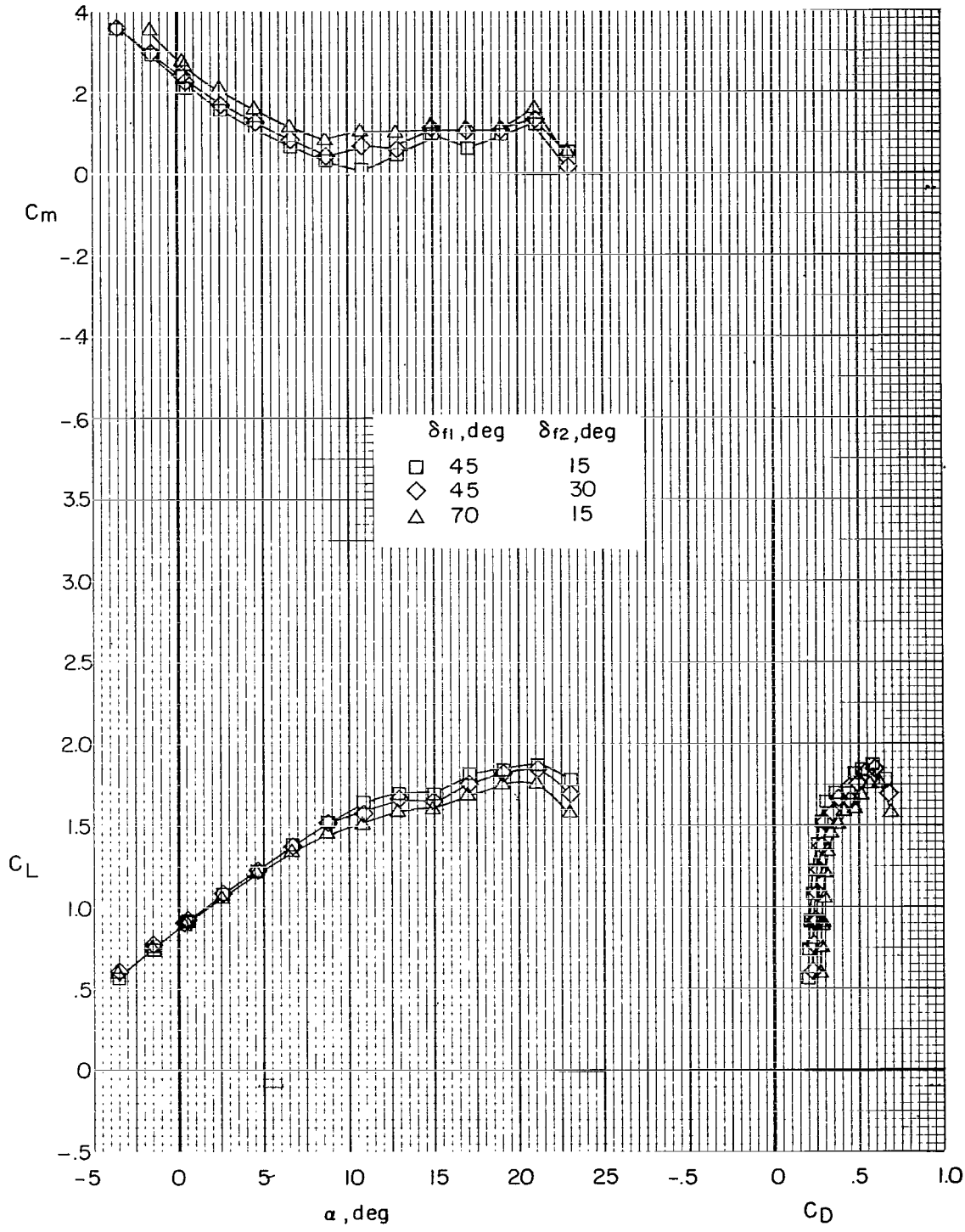

(a) $C_\mu = 0$.

Figure 9.- Effect of combined deflections of flap and flaperon on longitudinal characteristics of model. Tail flap off; $i_t = -5^\circ$; $\delta_{ts} = -40^\circ$; $\delta_s = 50^\circ$; slat chord, 0.15c.

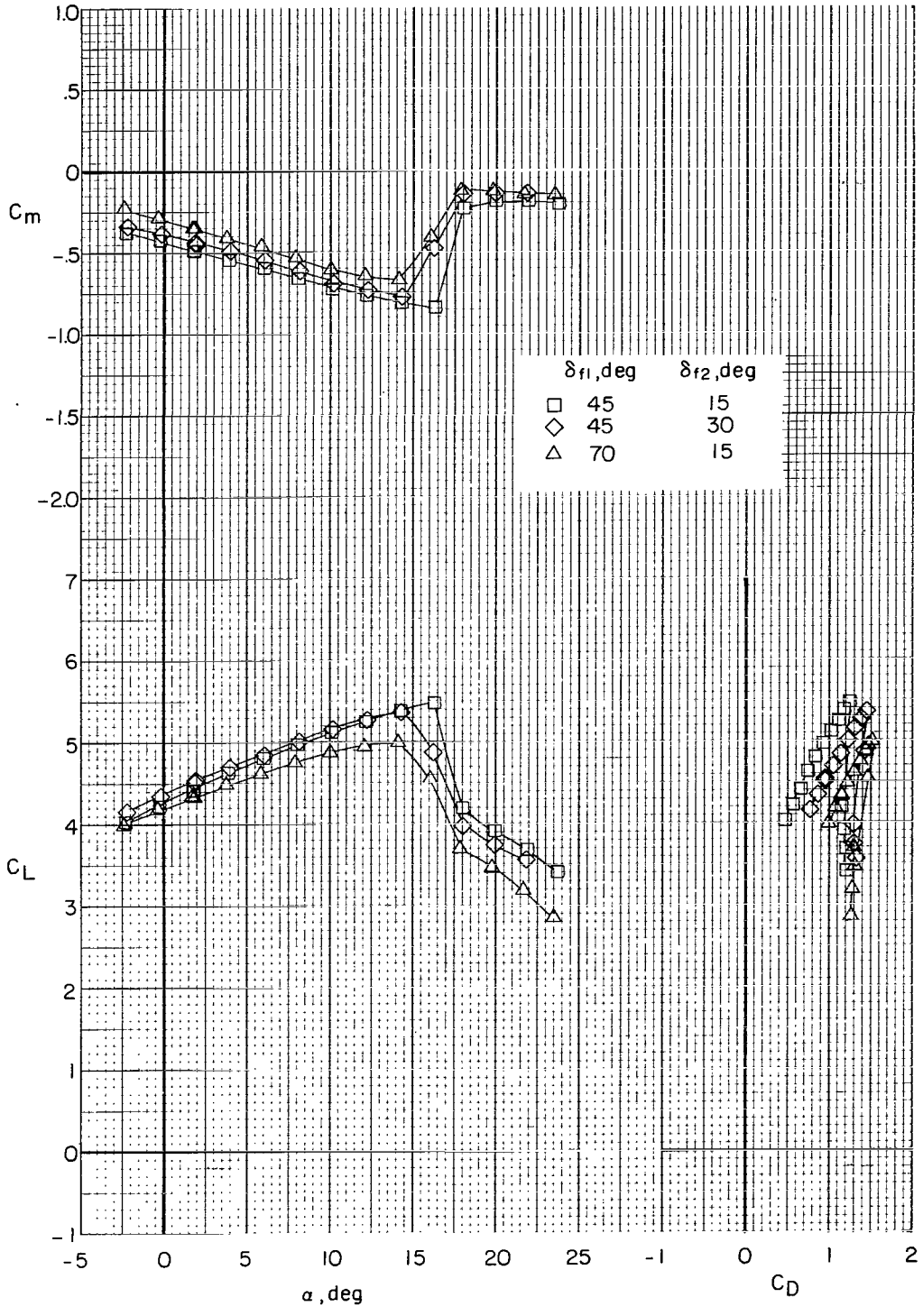

(b) $C_\mu = 0.61$.

Figure 9.- Continued.

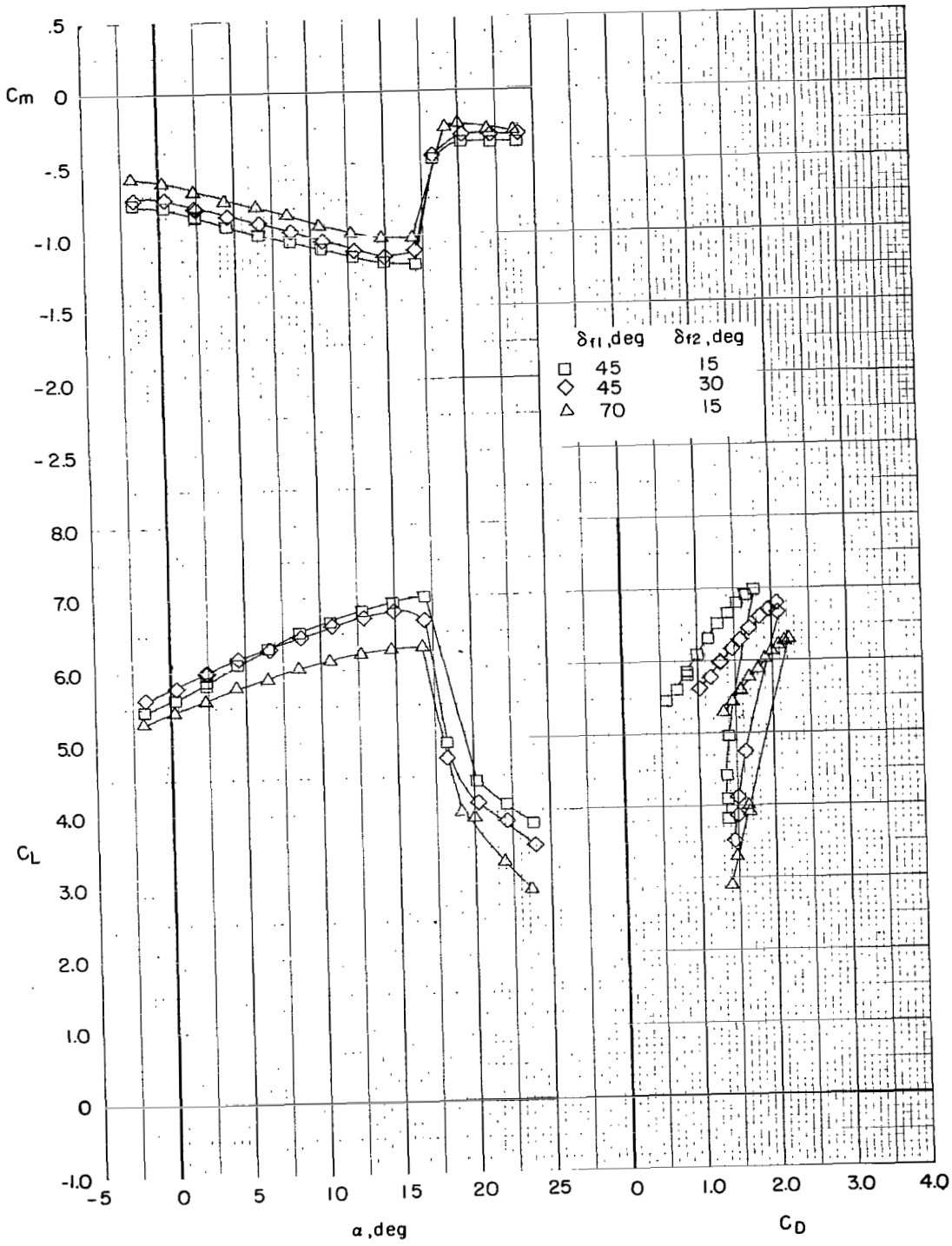

(c) C_μ = 1.11.

Figure 9.- Concluded.

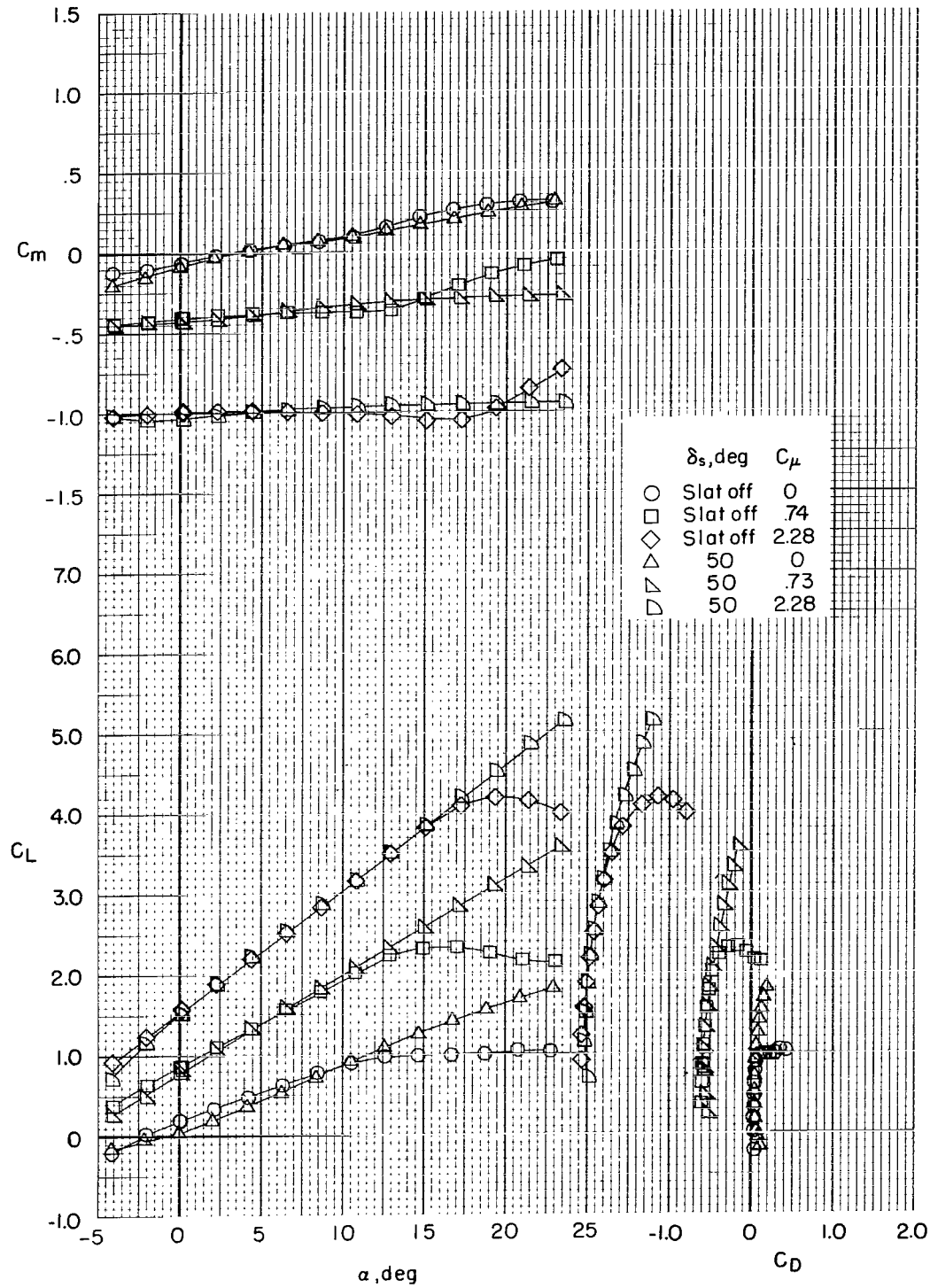

Figure 10.- Effect of 0.25-chord wing slats on longitudinal characteristics of model. Tail off; $\delta_{f1} = 0^o$; $\delta_{f2} = 0^o$.

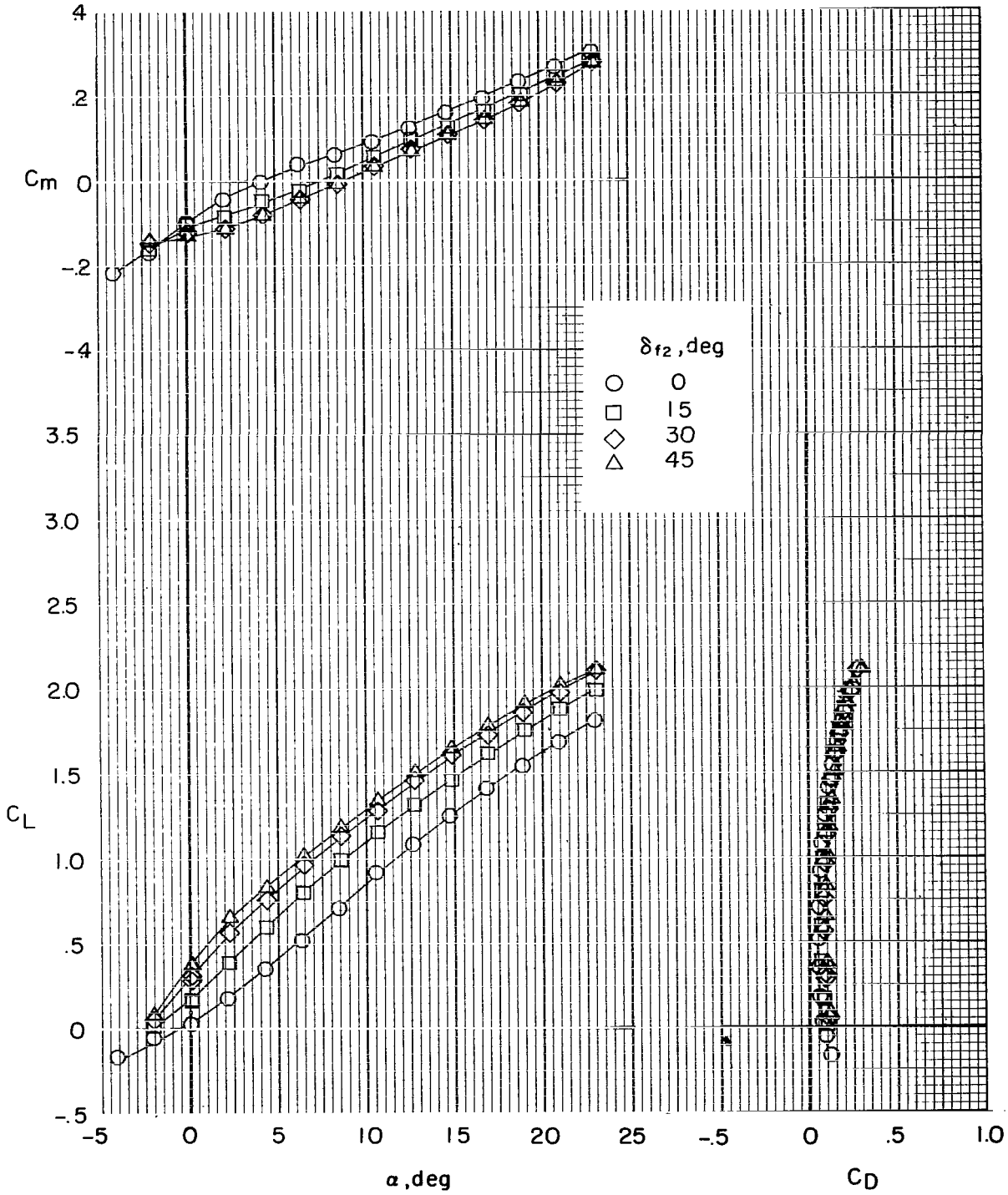

(a) $C_\mu = 0$.

Figure 11.- Effect of flaperon deflection on longitudinal characteristics of model with flaps undeflected. Tail off; $\delta_s = 50^\circ$ (0.25c).

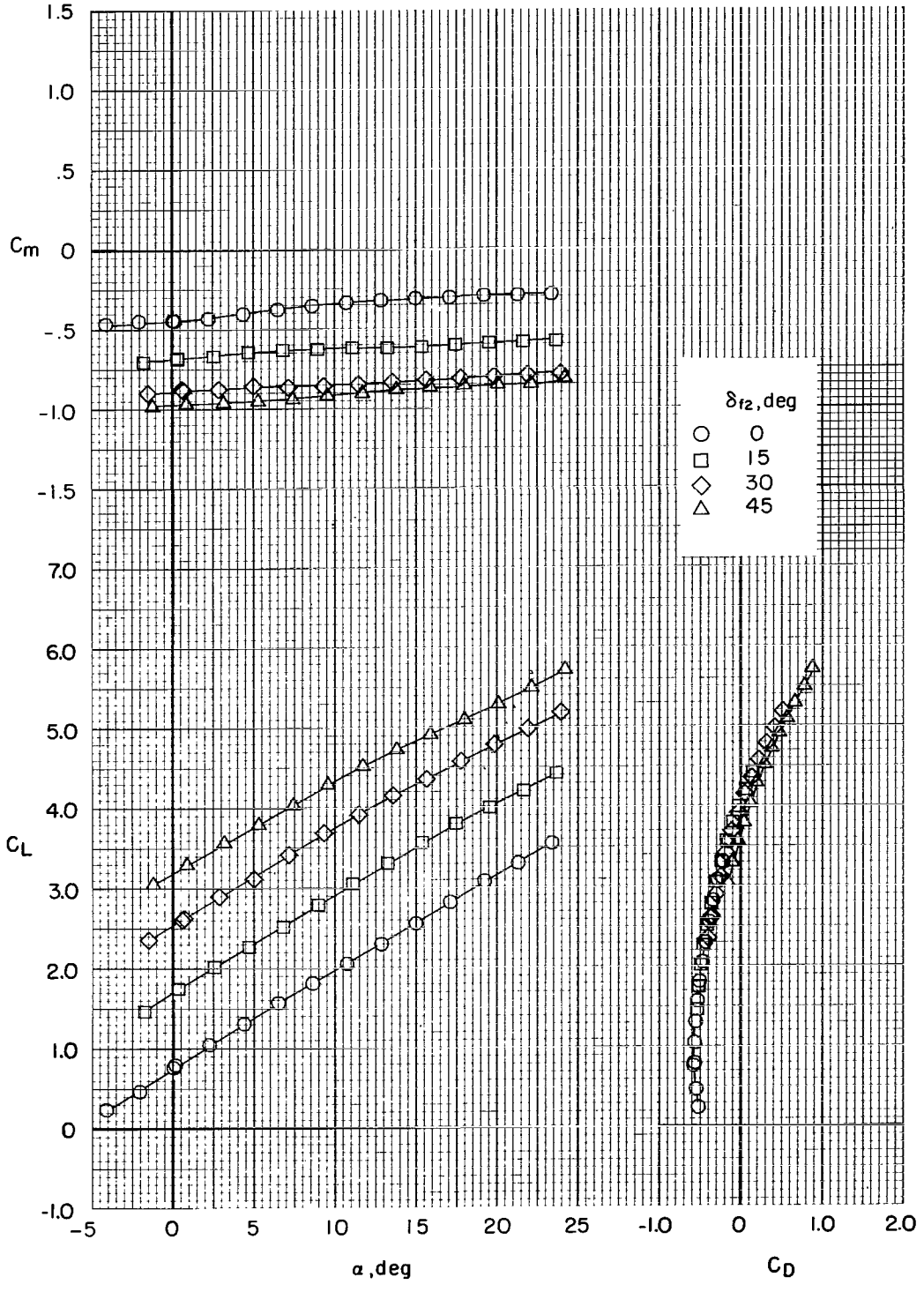

(b) $C_\mu = 0.73$.

Figure 11.- Continued.

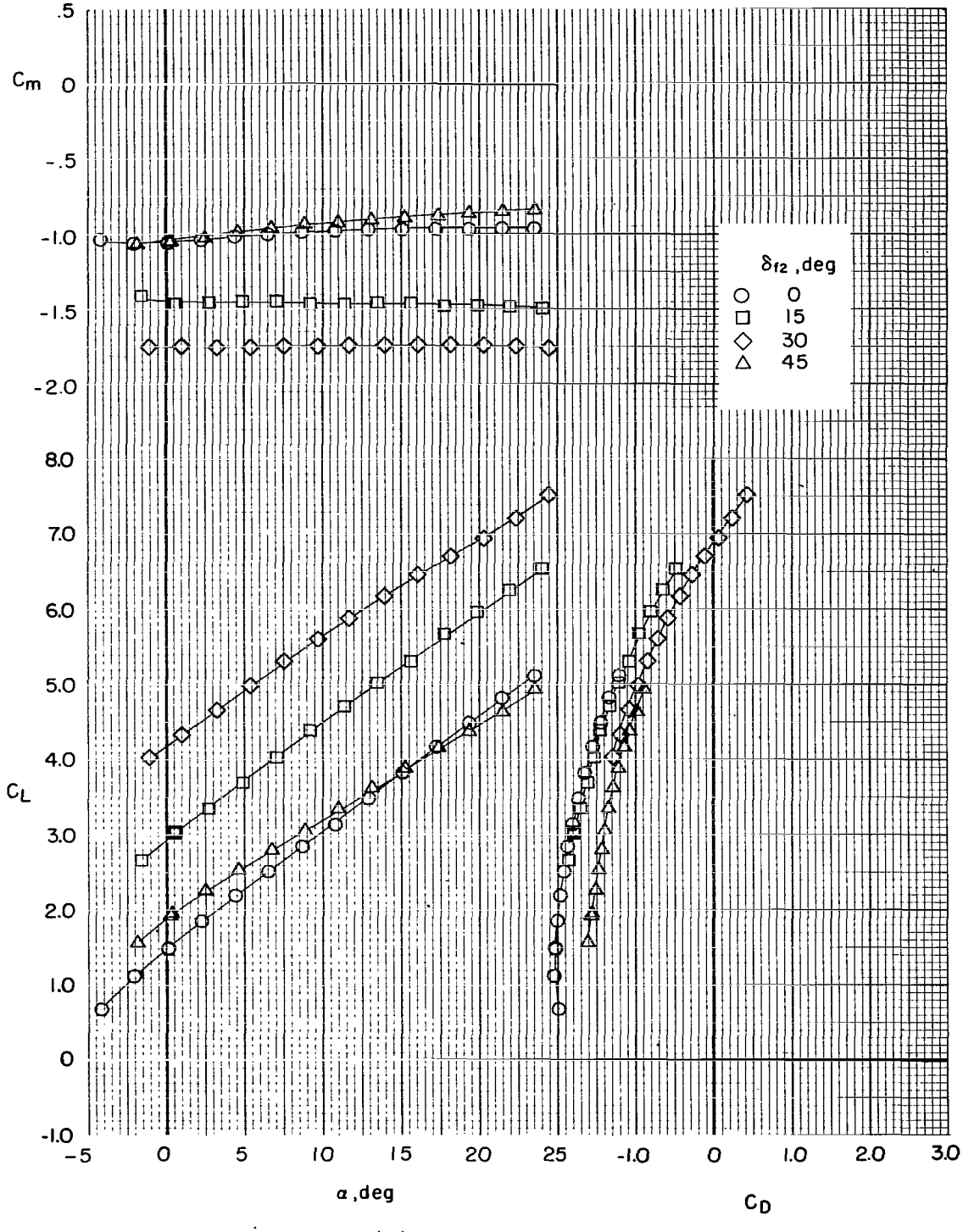

(c) C_μ = 2.29.

Figure 11.- Concluded.

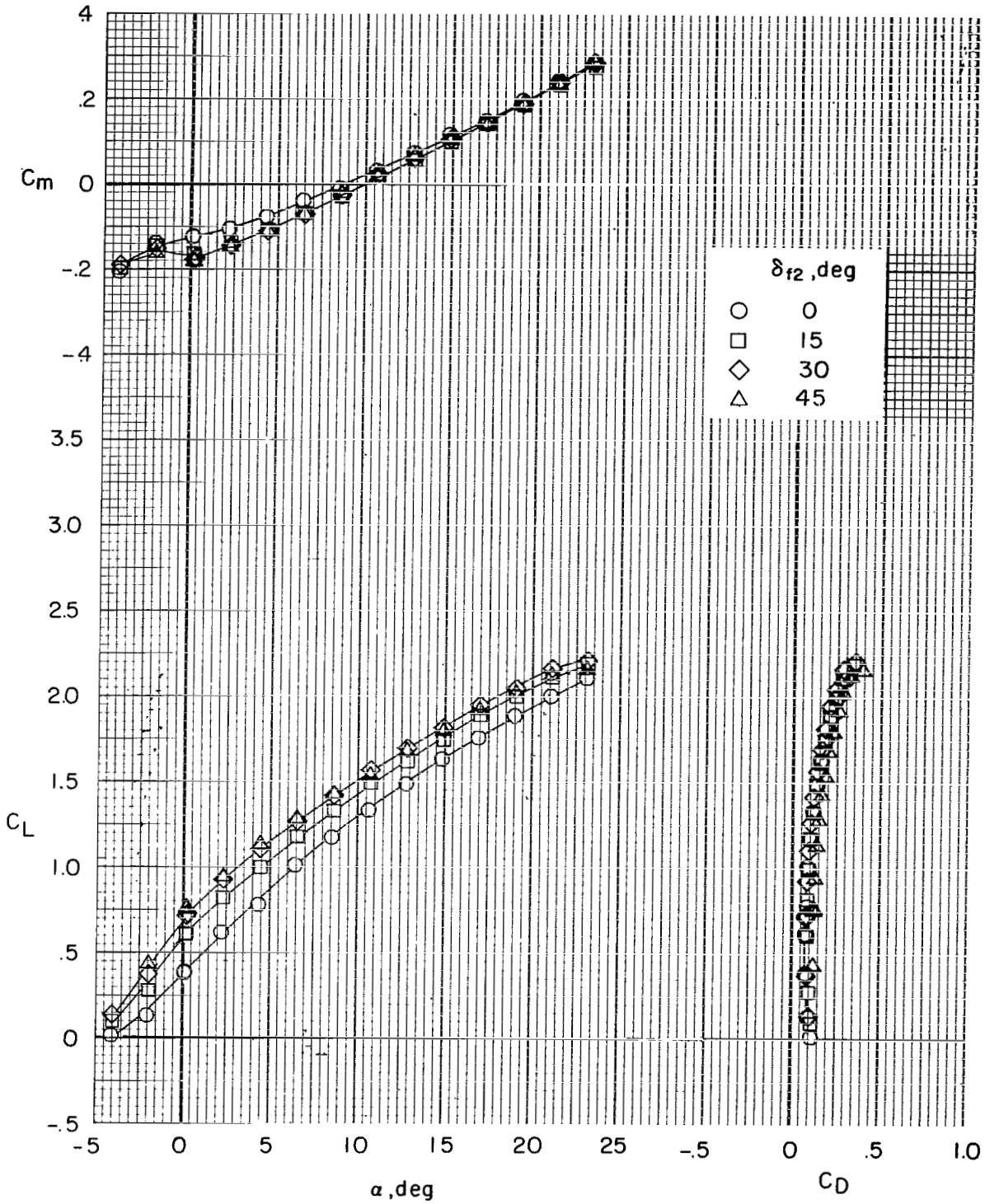

(a) $C_\mu = 0$.

Figure 12.- Effect of flaperon deflection on longitudinal characteristics of model with flaps deflected 15°. Tail off; $\delta_s = 50°$ (0.25c).

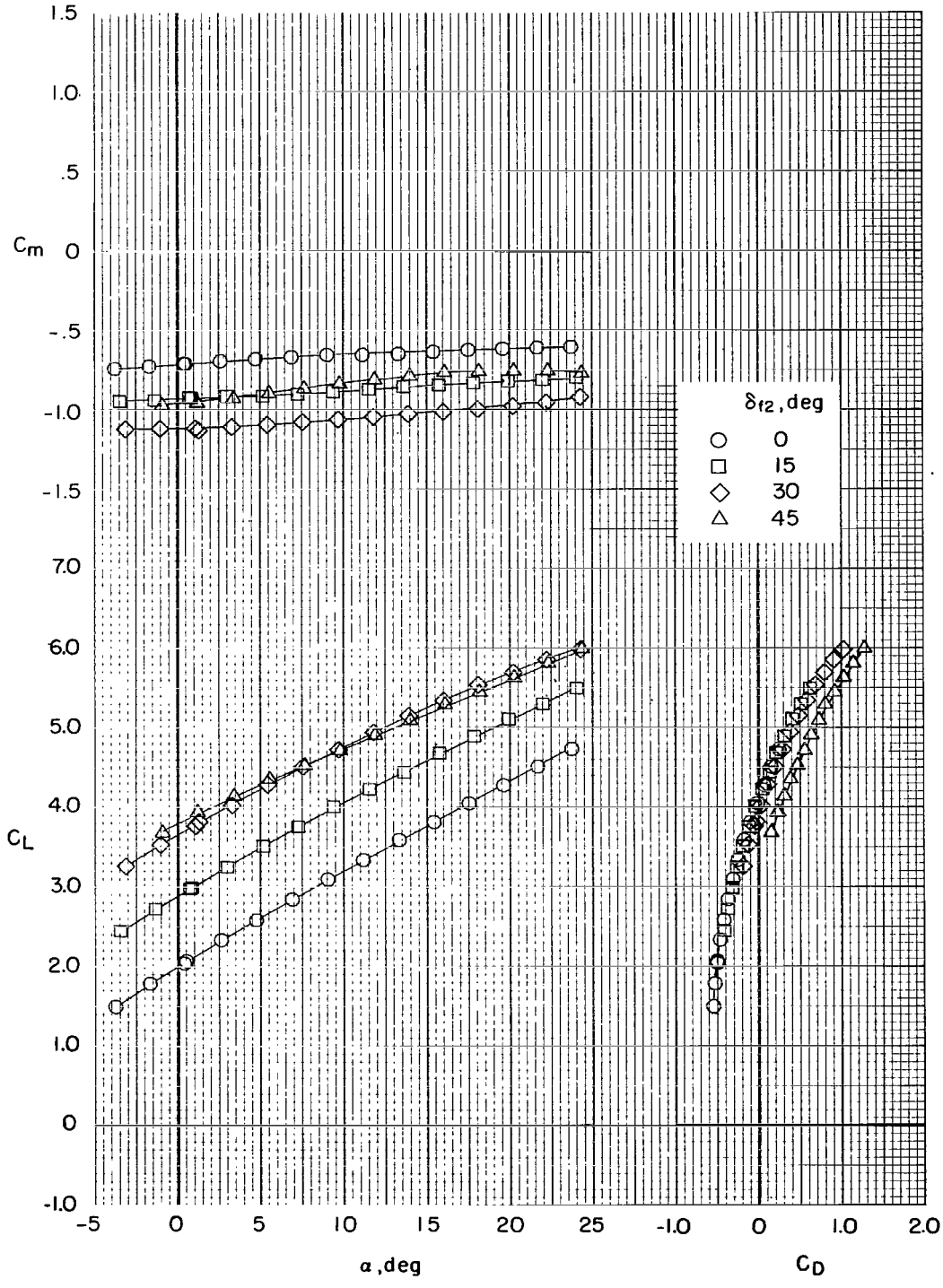

(b) C_μ = 0.73.

Figure 12.- Continued.

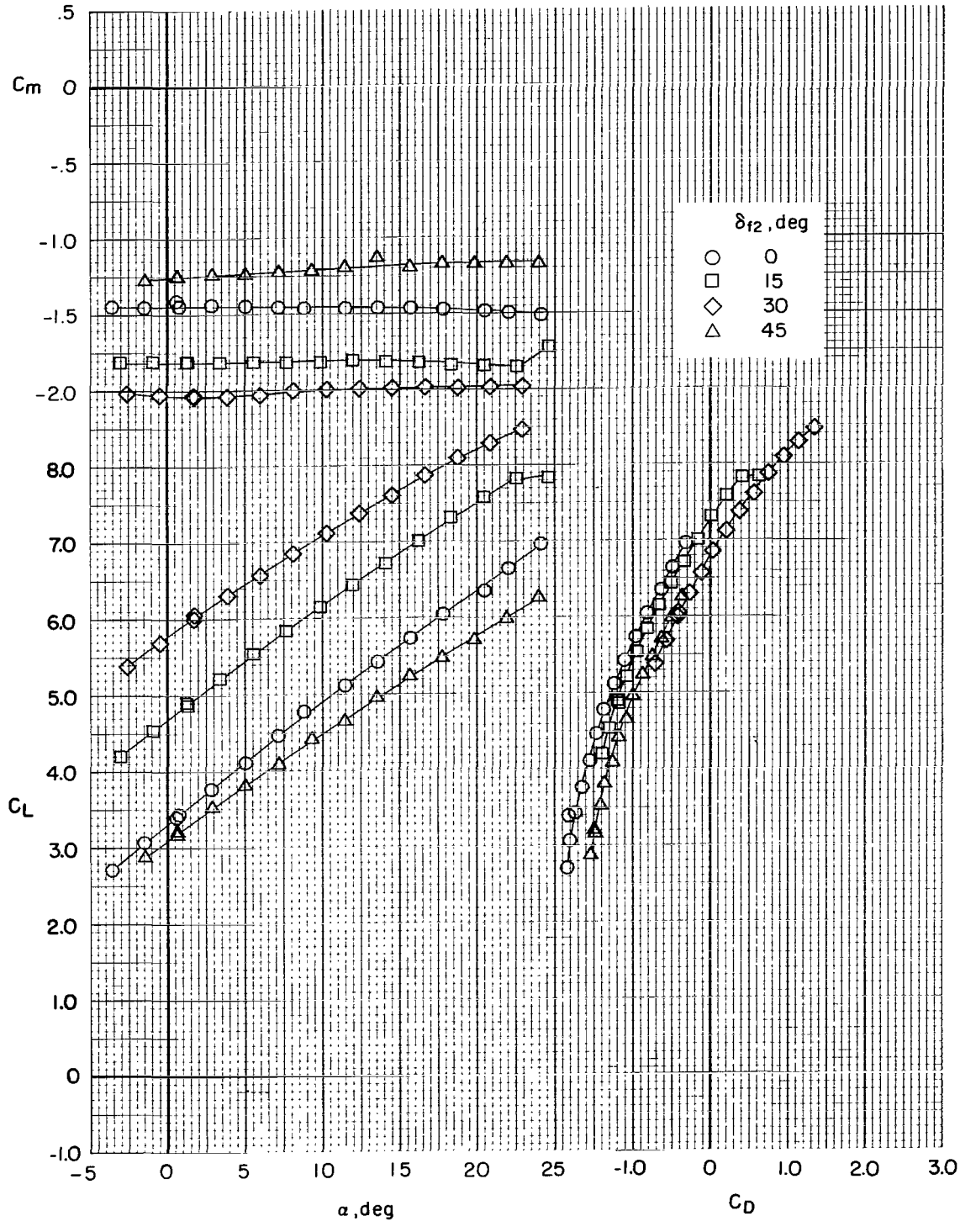

(c) C_μ = 2.29.

Figure 12.- Concluded.

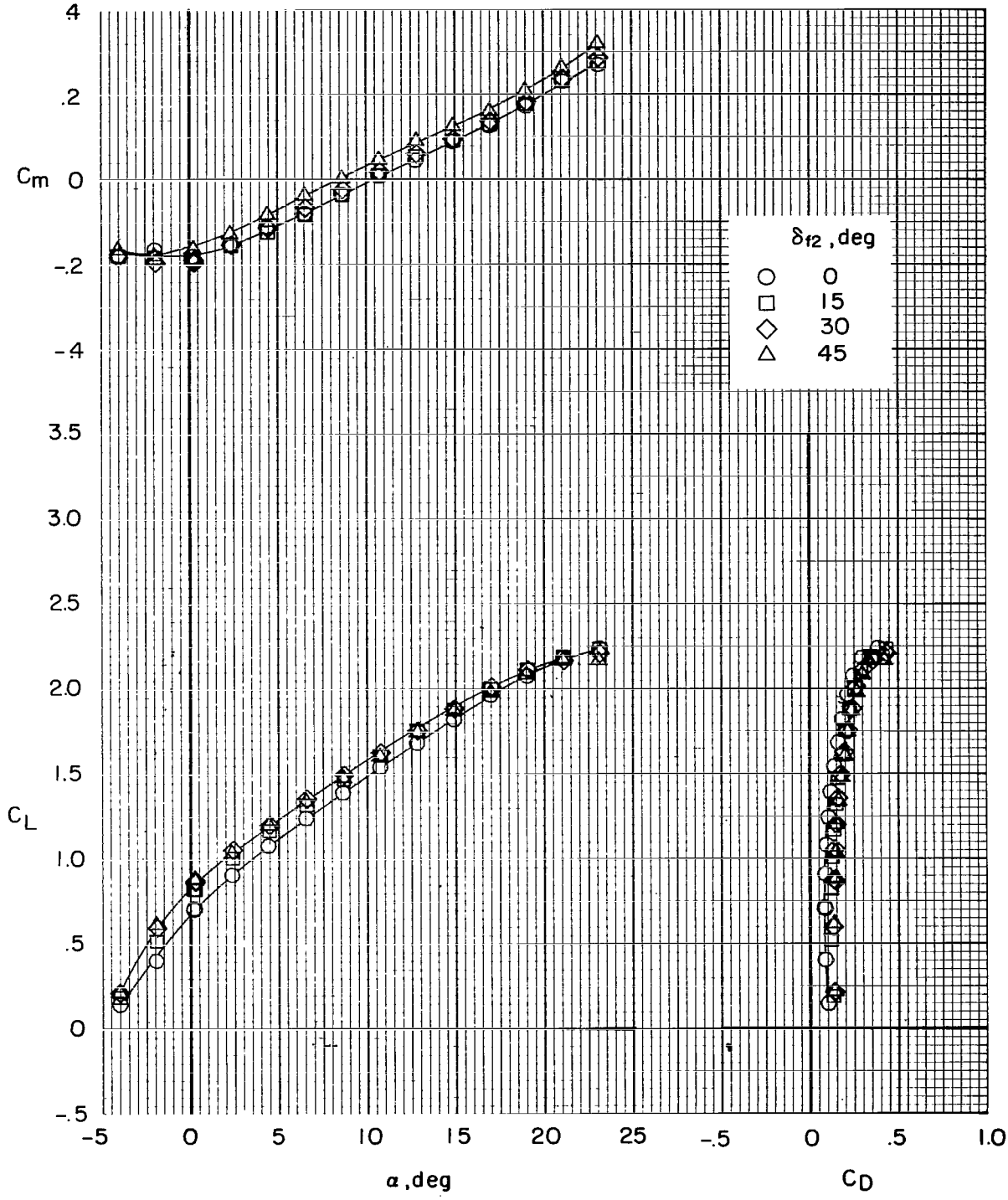

(a) C_μ = 0.

Figure 13.- Effect of flaperon deflection on longitudinal characteristics of model with flaps deflected 30°. Tail off; δ_s = 50° (0.25c).

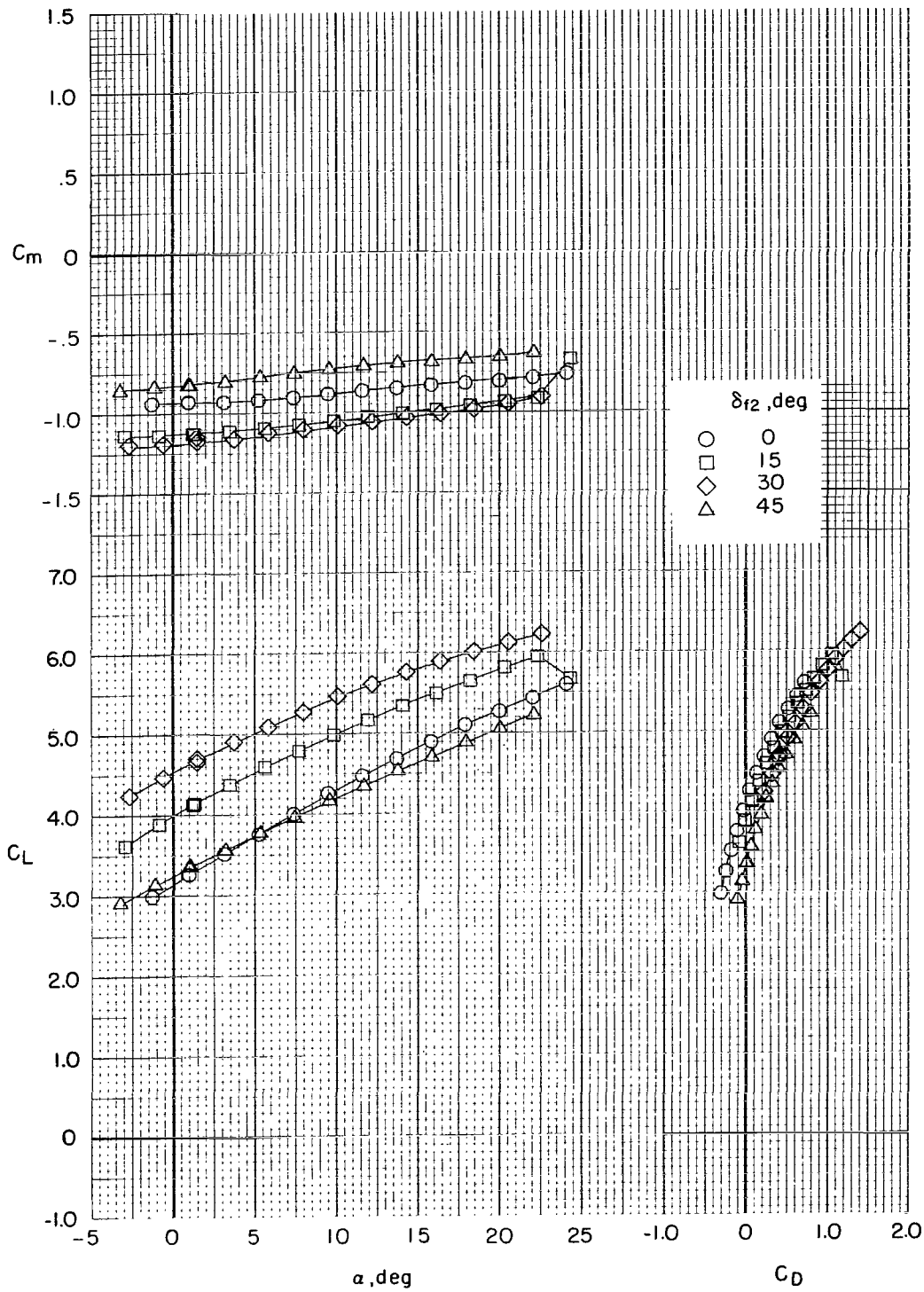

(b) C_μ = 0.73.

Figure 13.- Continued.

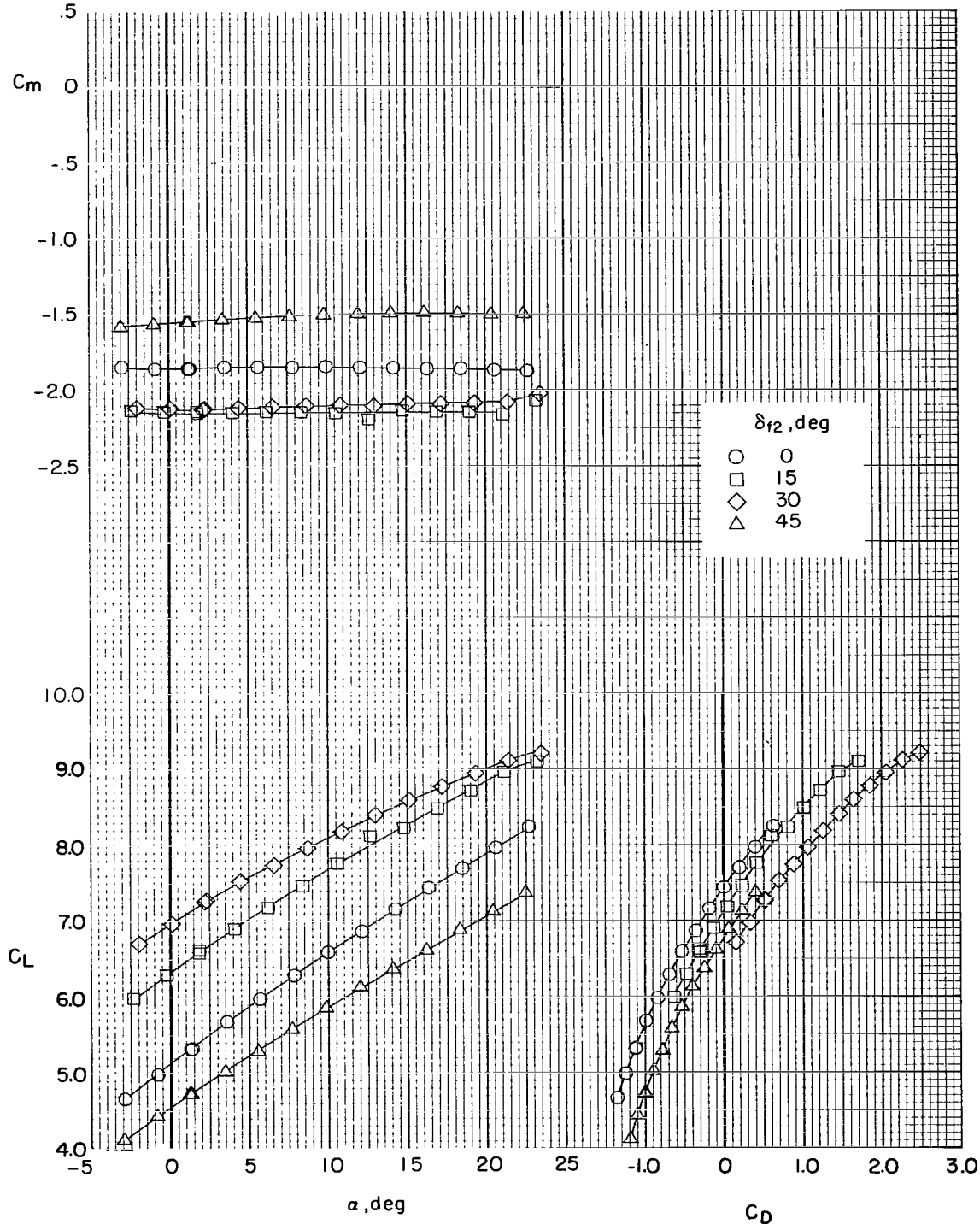

(c) C_μ = 2.29.

Figure 13.- Concluded.

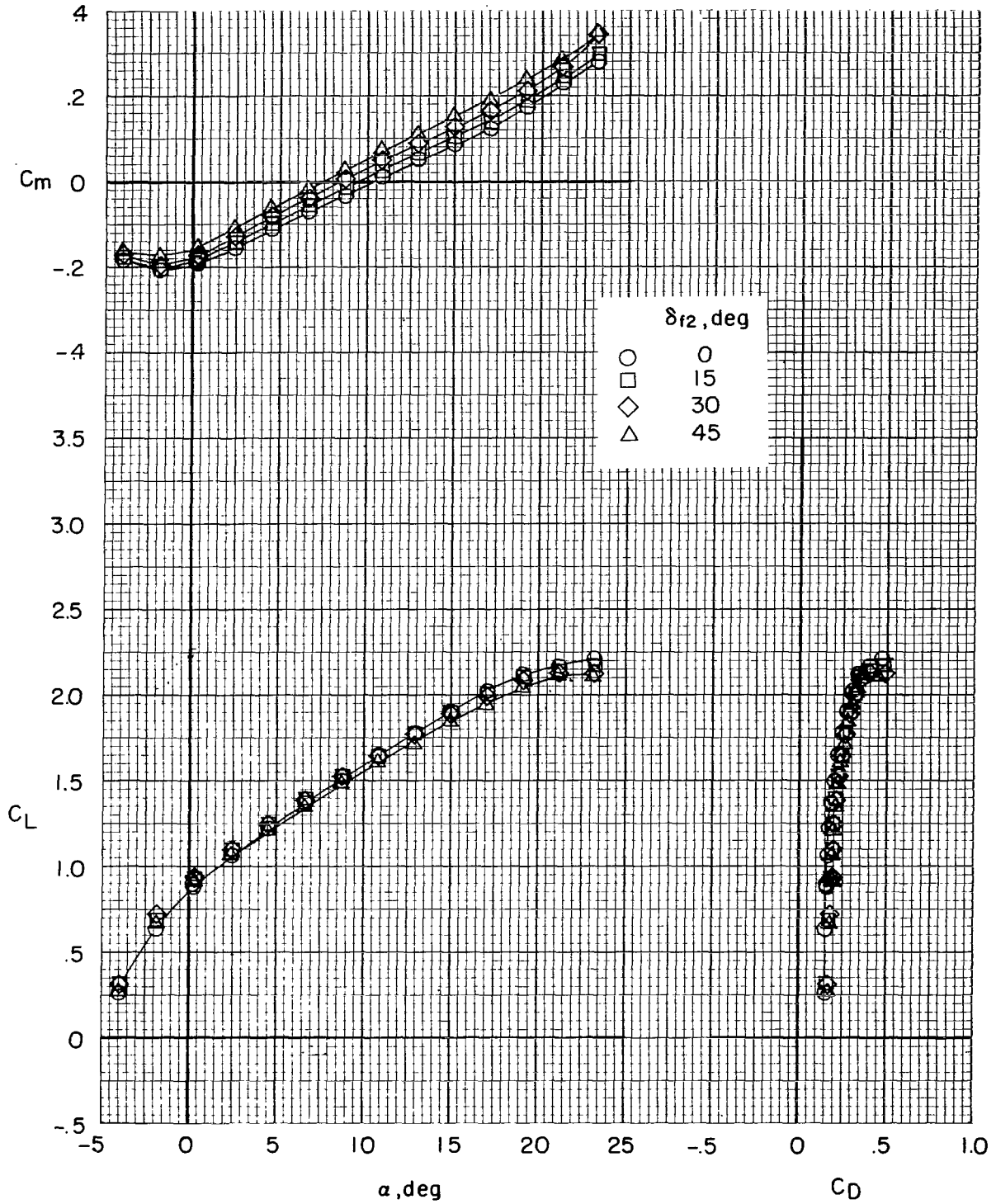

(a) $C_\mu = 0$.

Figure 14.- Effect of flaperon deflection on longitudinal characteristics of model with flaps deflected 45°. Tail off; $\delta_s = 50°$ (0.25c).

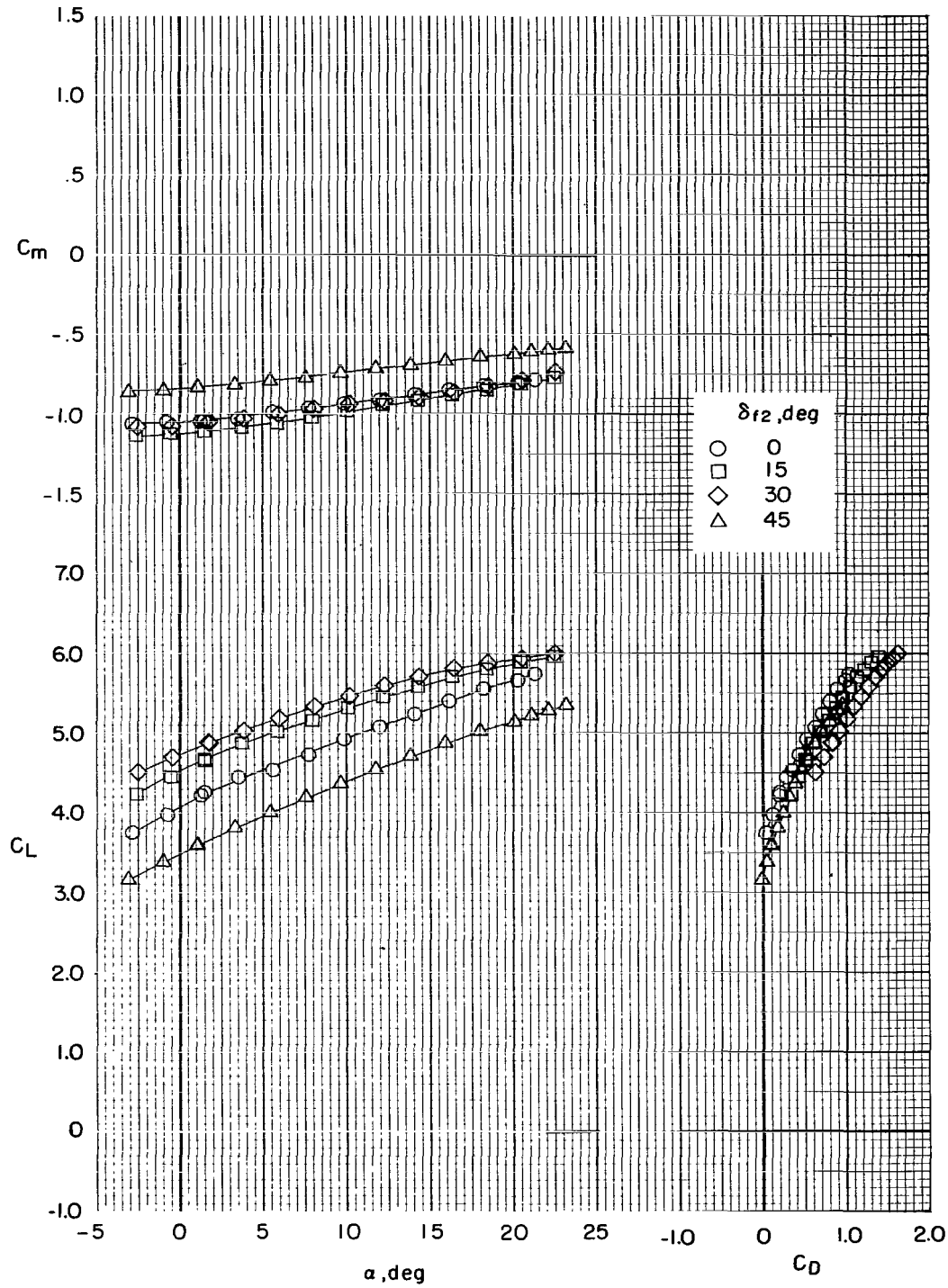

(b) C_μ = 0.73.

Figure 14.- Continued.

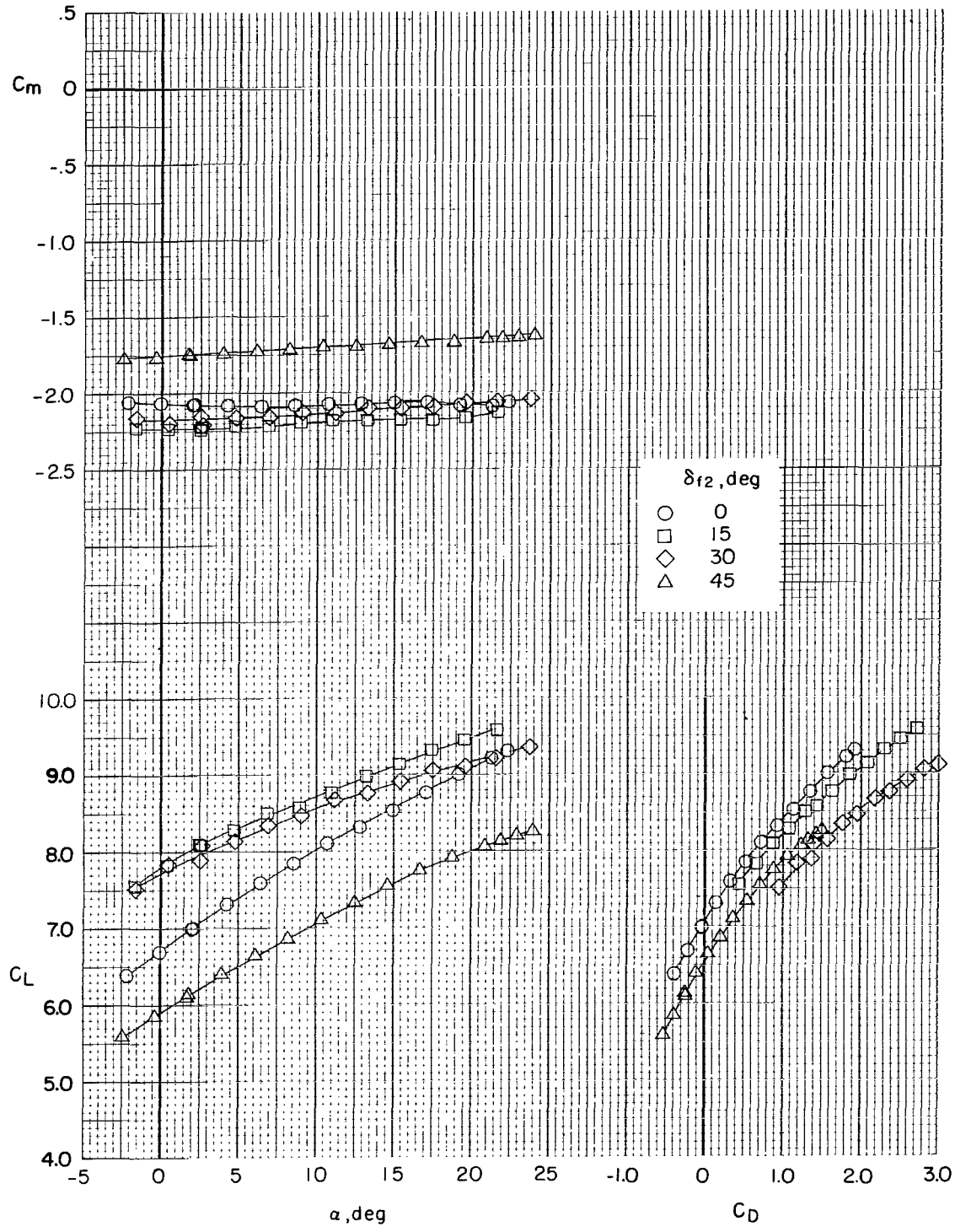

(c) C_μ = 2.29.

Figure 14.- Concluded.

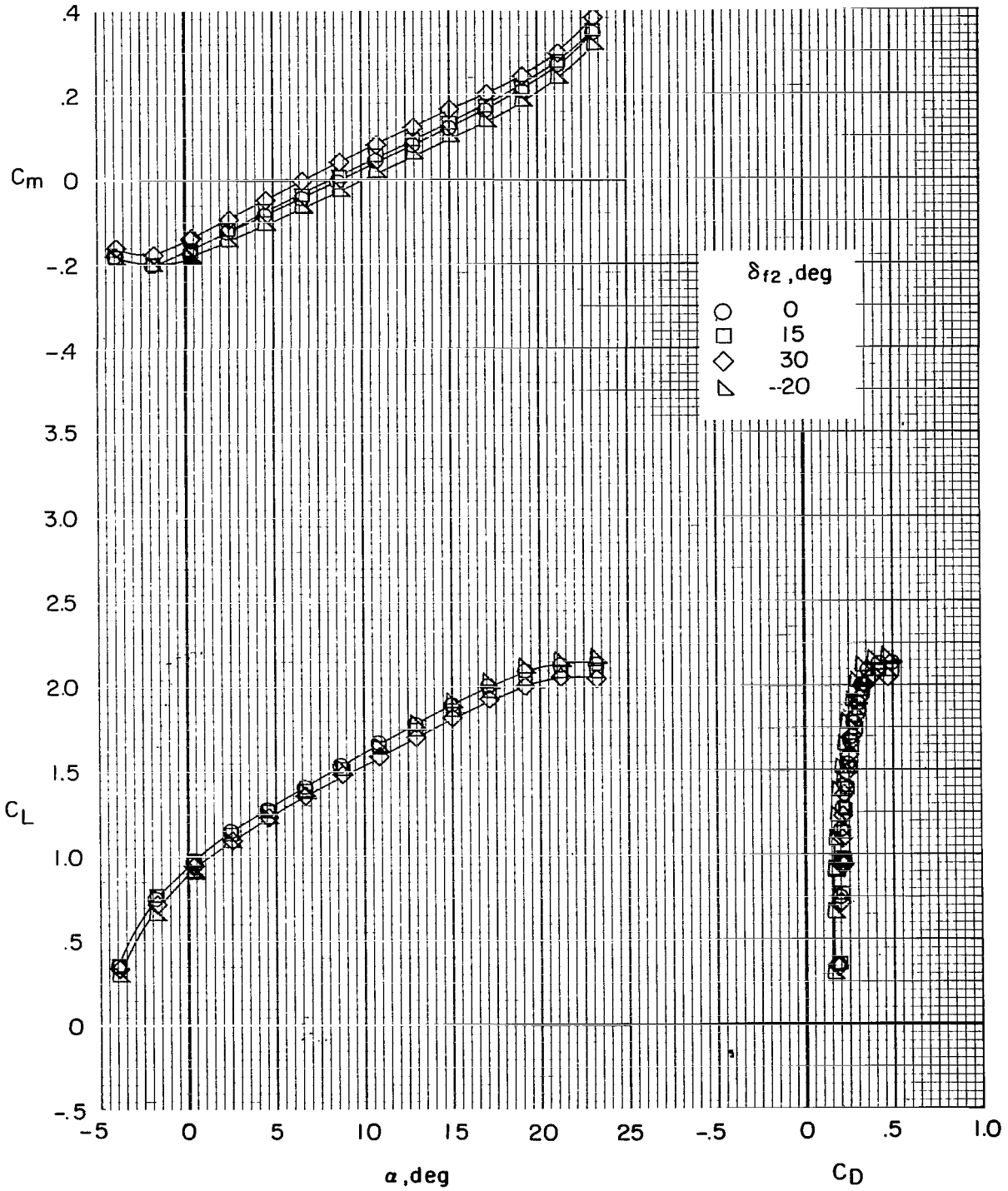

(a) $C_\mu = 0$.

Figure 15.- Effect of flaperon deflection on longitudinal characteristics of model with flaps deflected 60°. Tail off; $\delta_s = 50°$ (0.25c).

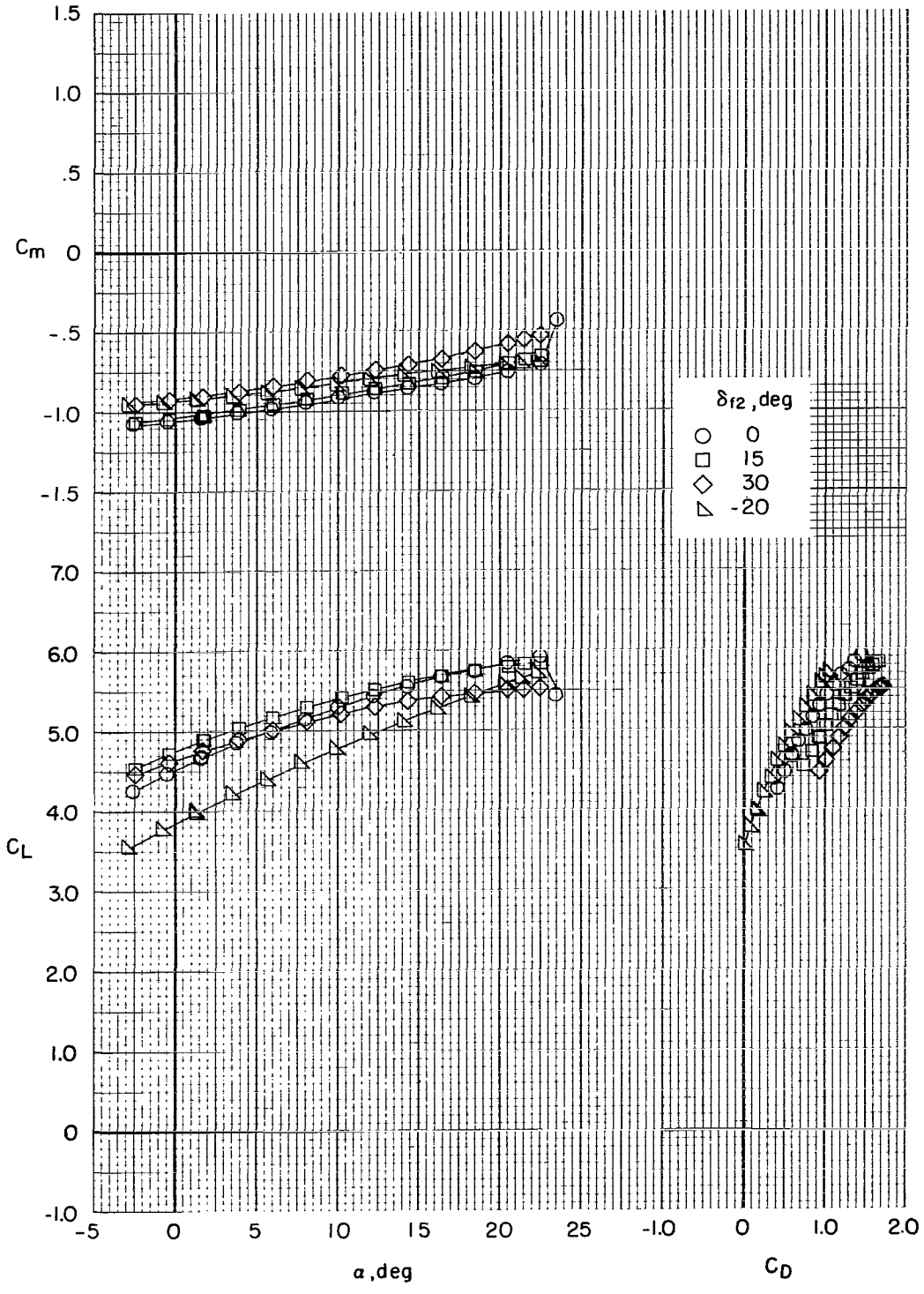

(b) C_μ = 0.73.

Figure 15.- Continued.

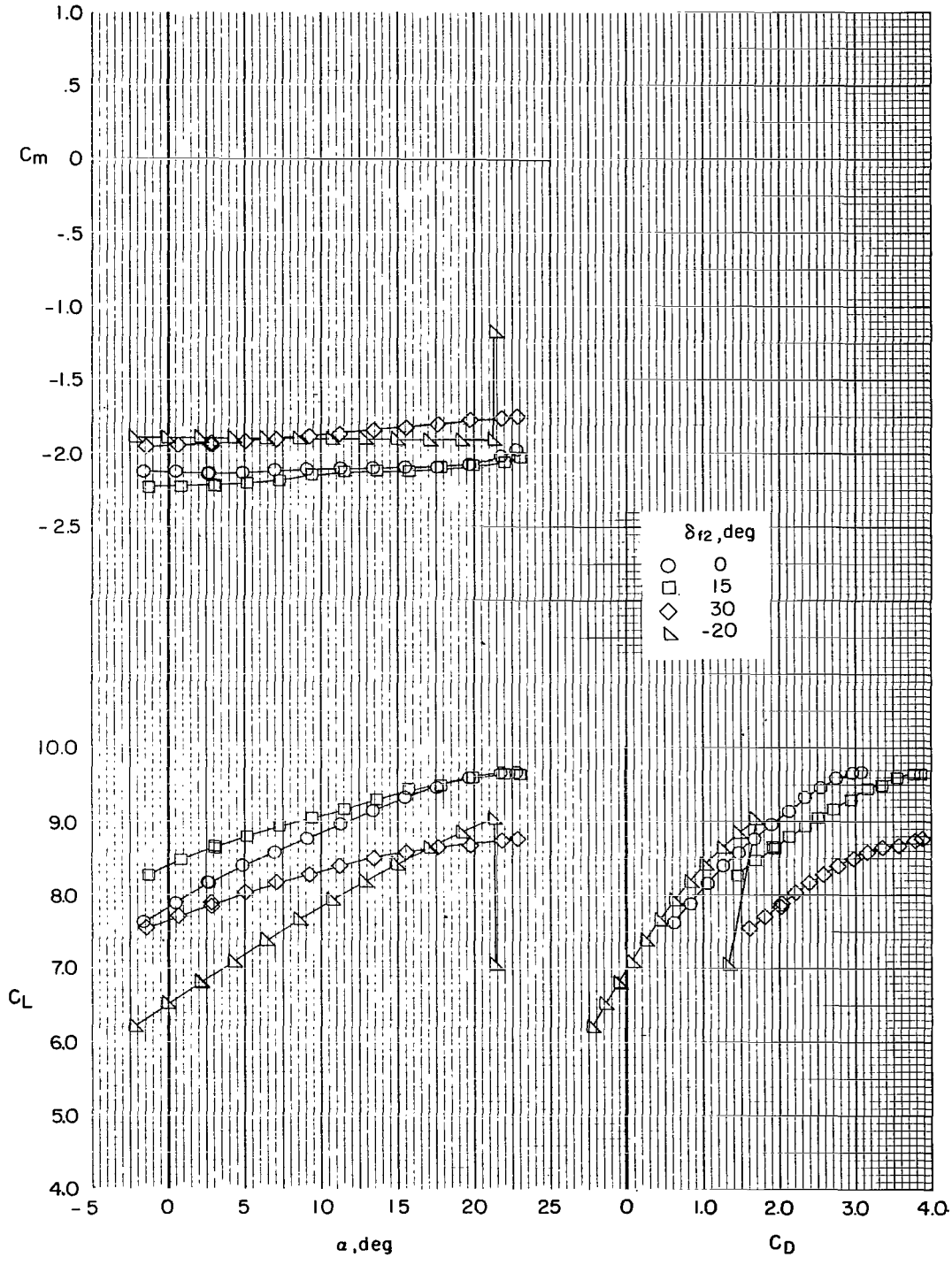

(c) C_μ = 2.29.

Figure 15.- Concluded.

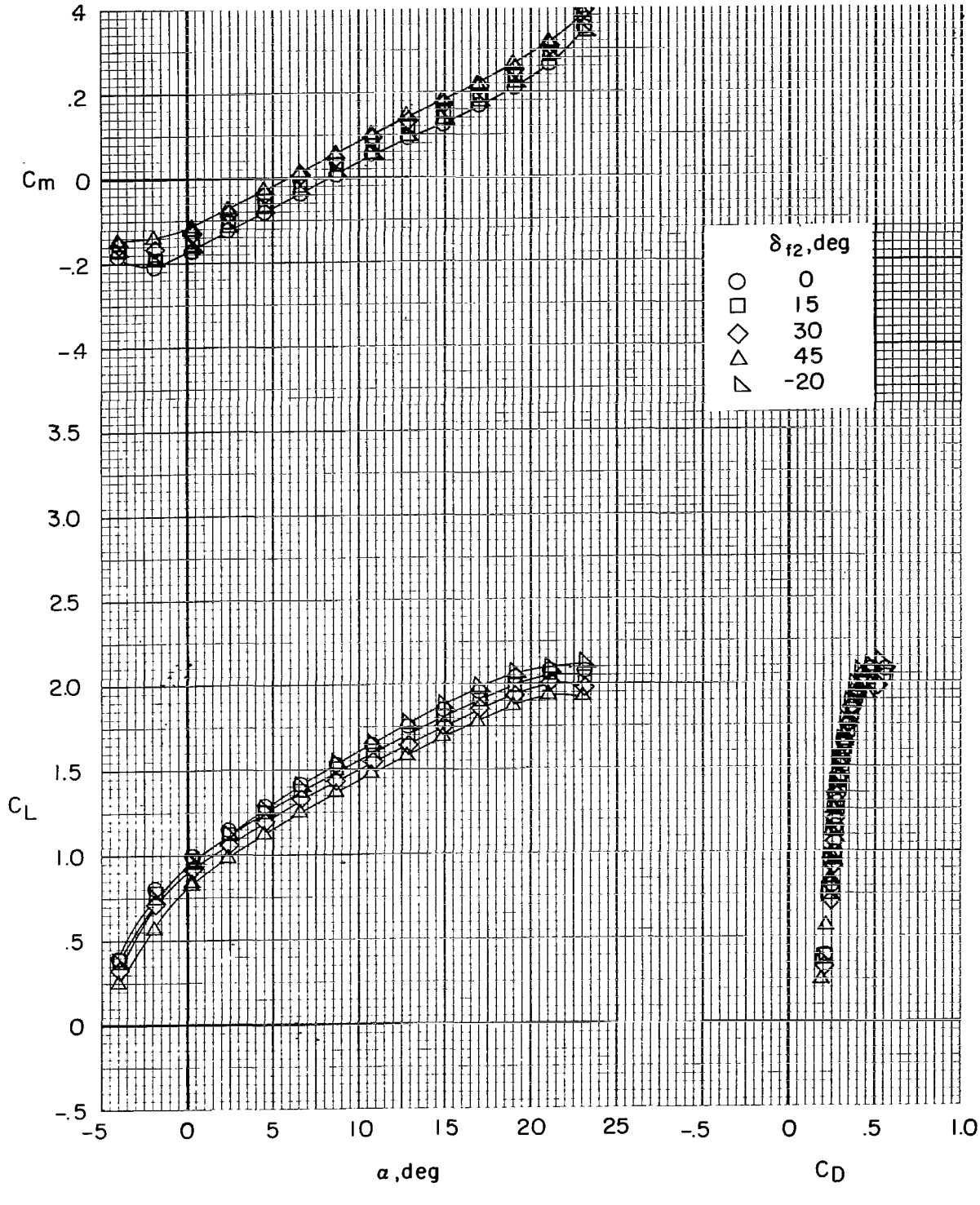

(a) $C_\mu = 0$.

Figure 16.- Effect of flaperon deflections on longitudinal characteristics of model with flaps deflected 70°. Tail off; $\delta_s = 50°$ (0.25c).

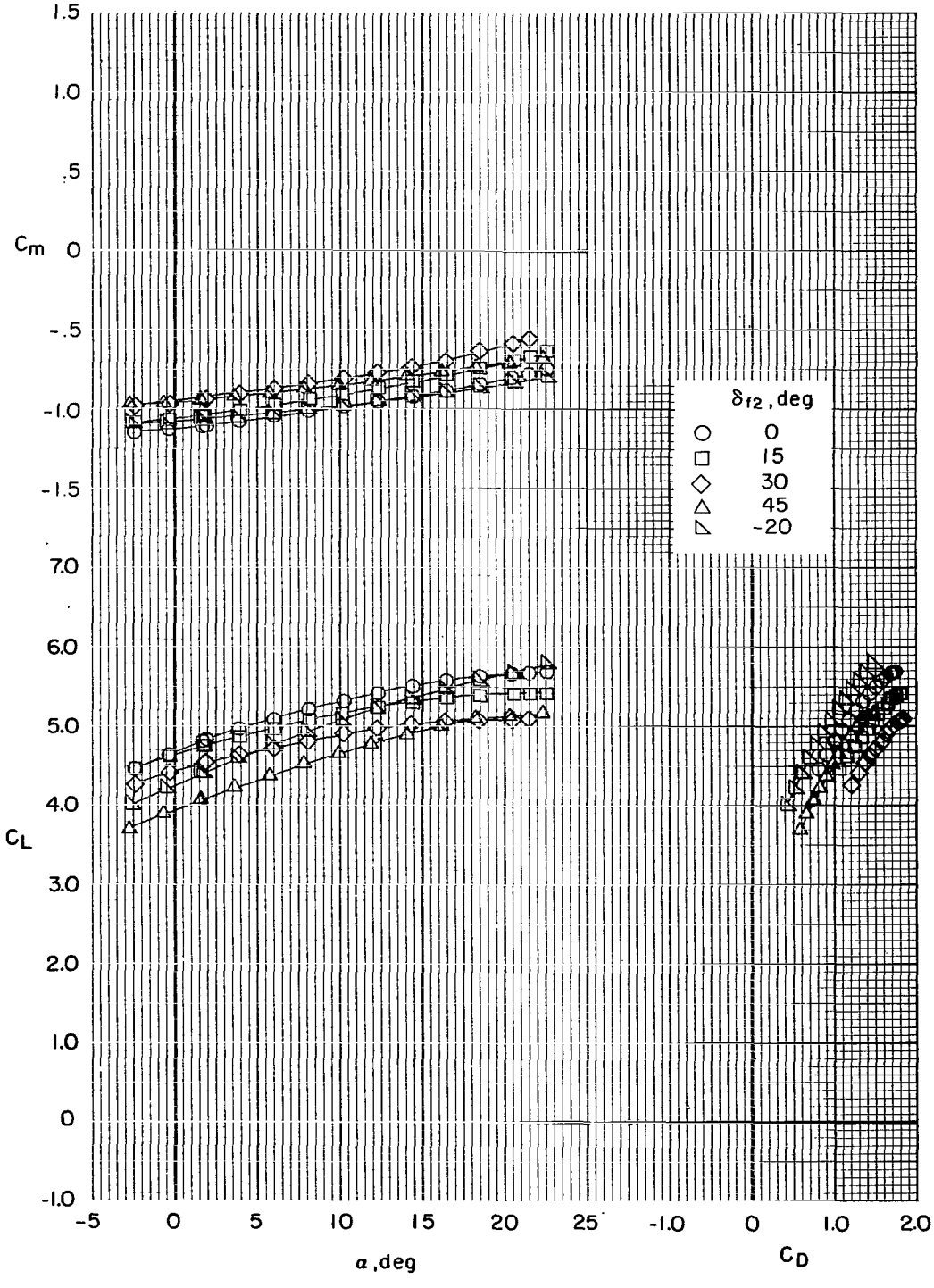

(b) $C_\mu = 0.73$.

Figure 16.- Continued.

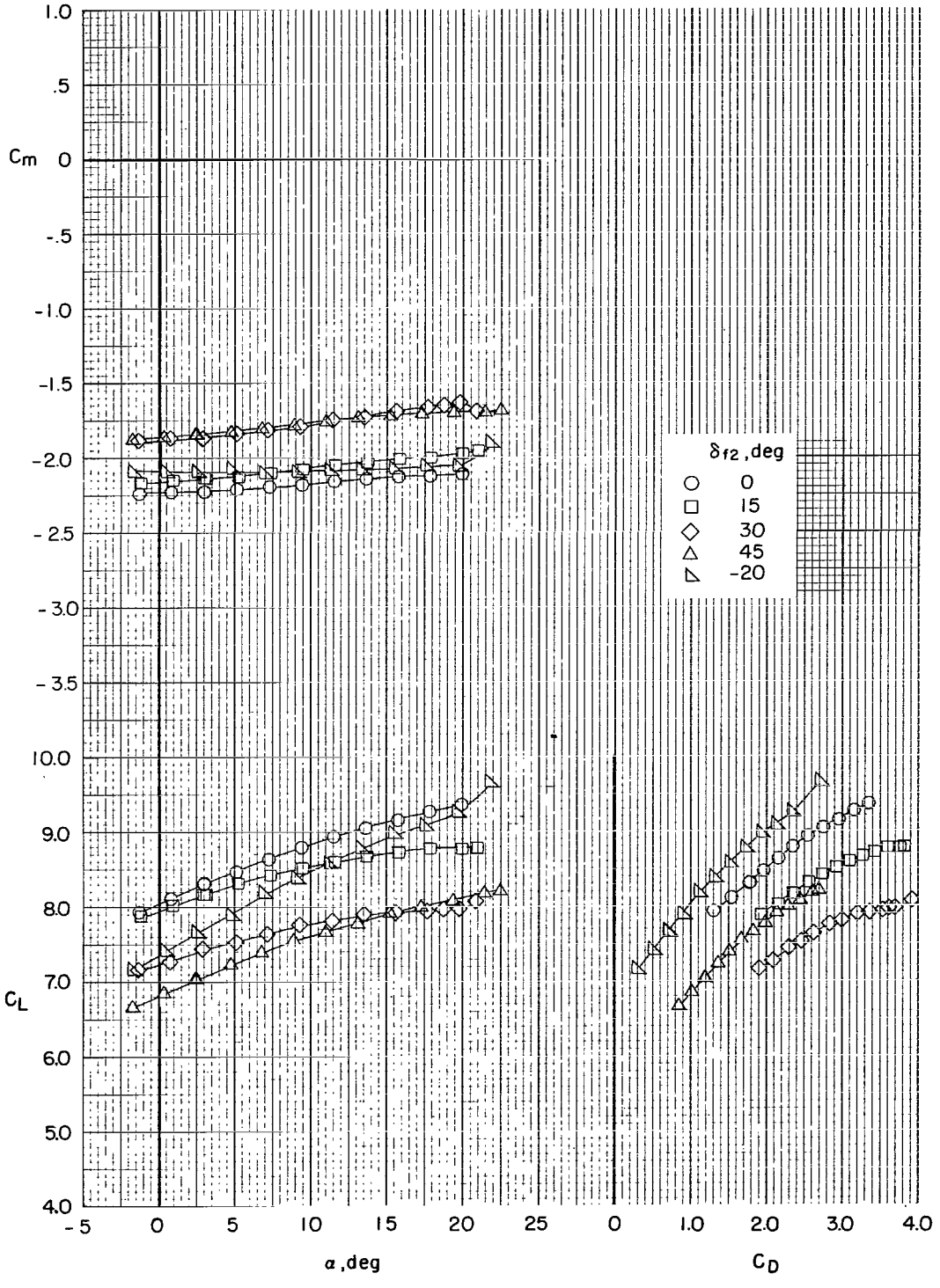

(c) C_μ = 2.29.

Figure 16.- Concluded.

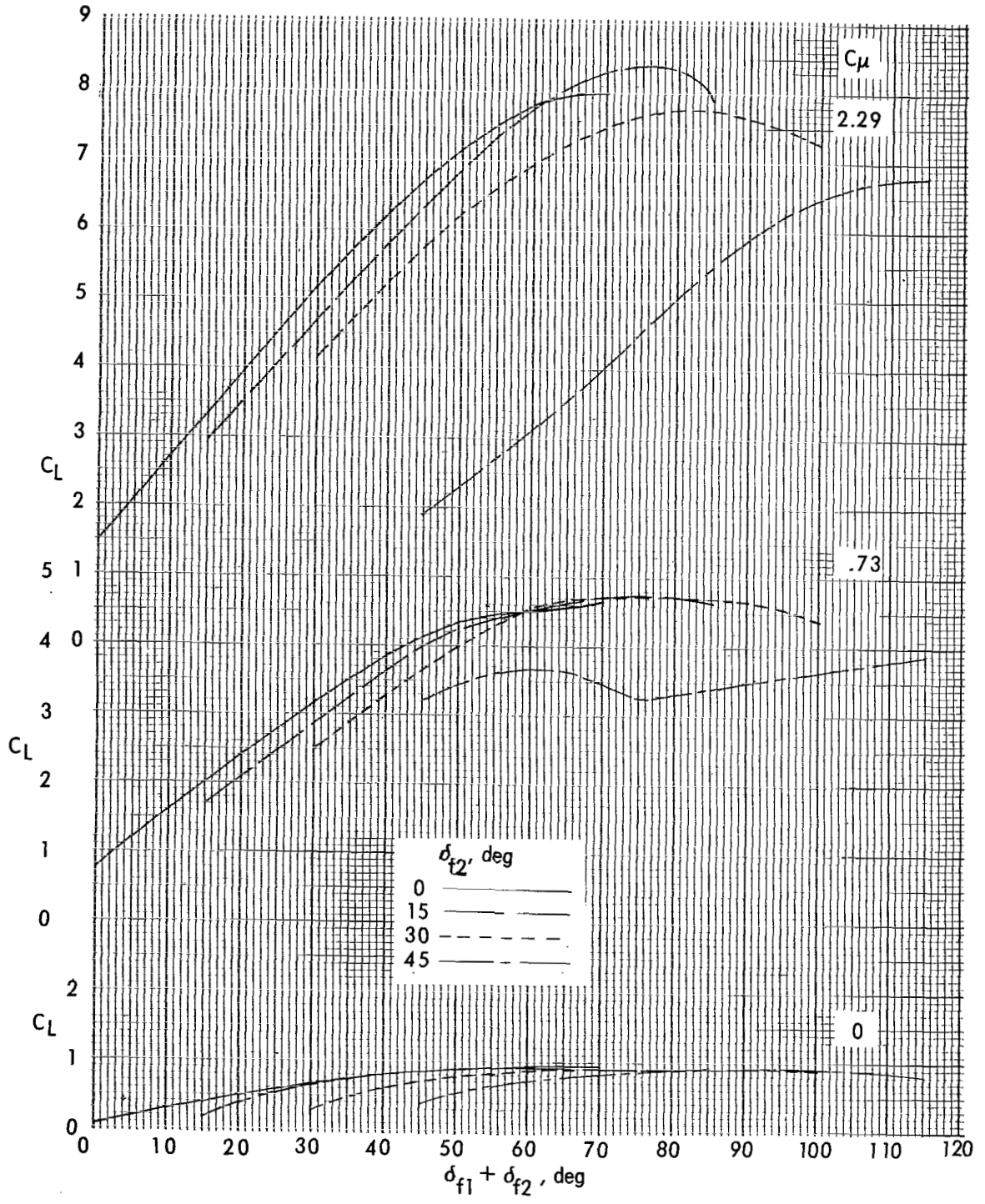

Figure 17.- Lift coefficient variation with combined flap and flaperon deflections. $\alpha = 0^o$.

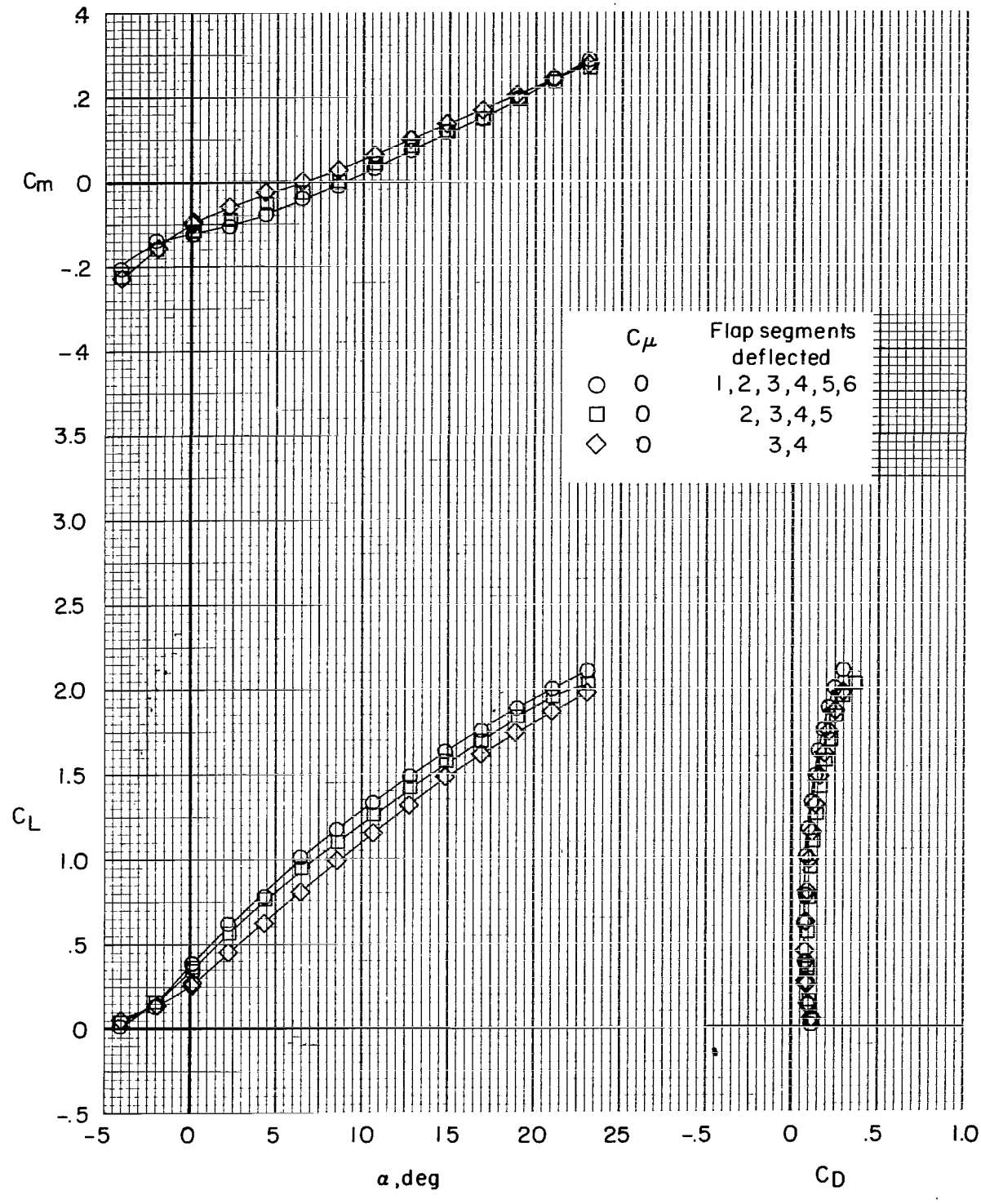

Figure 18.- Effect of partial-span flap deflection of 15° on longitudinal characteristics of model. Tail off; $\delta_{f2} = 0°$; $\delta_s = 50°$ (0.25c).

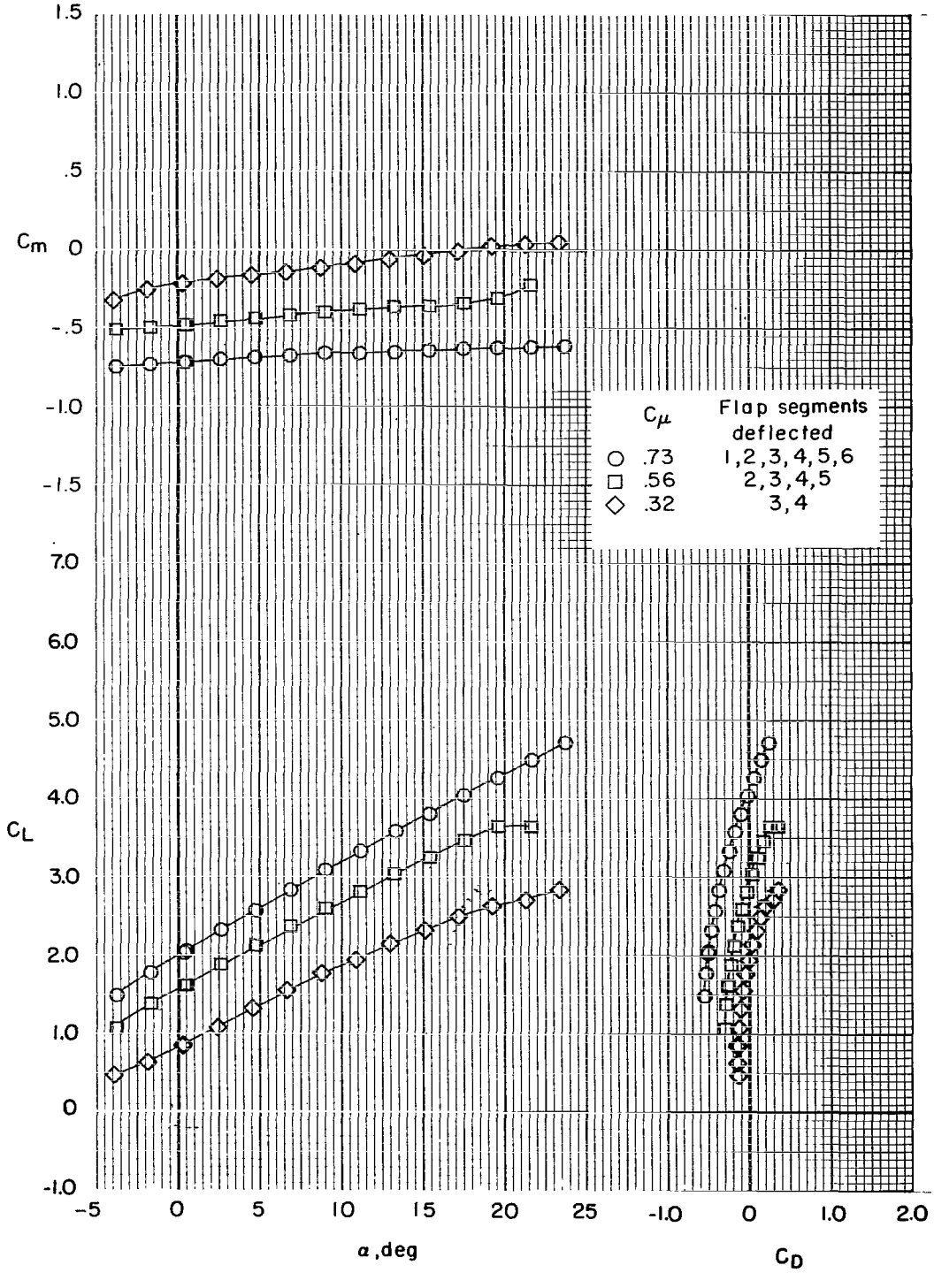

Figure 18.- Continued.

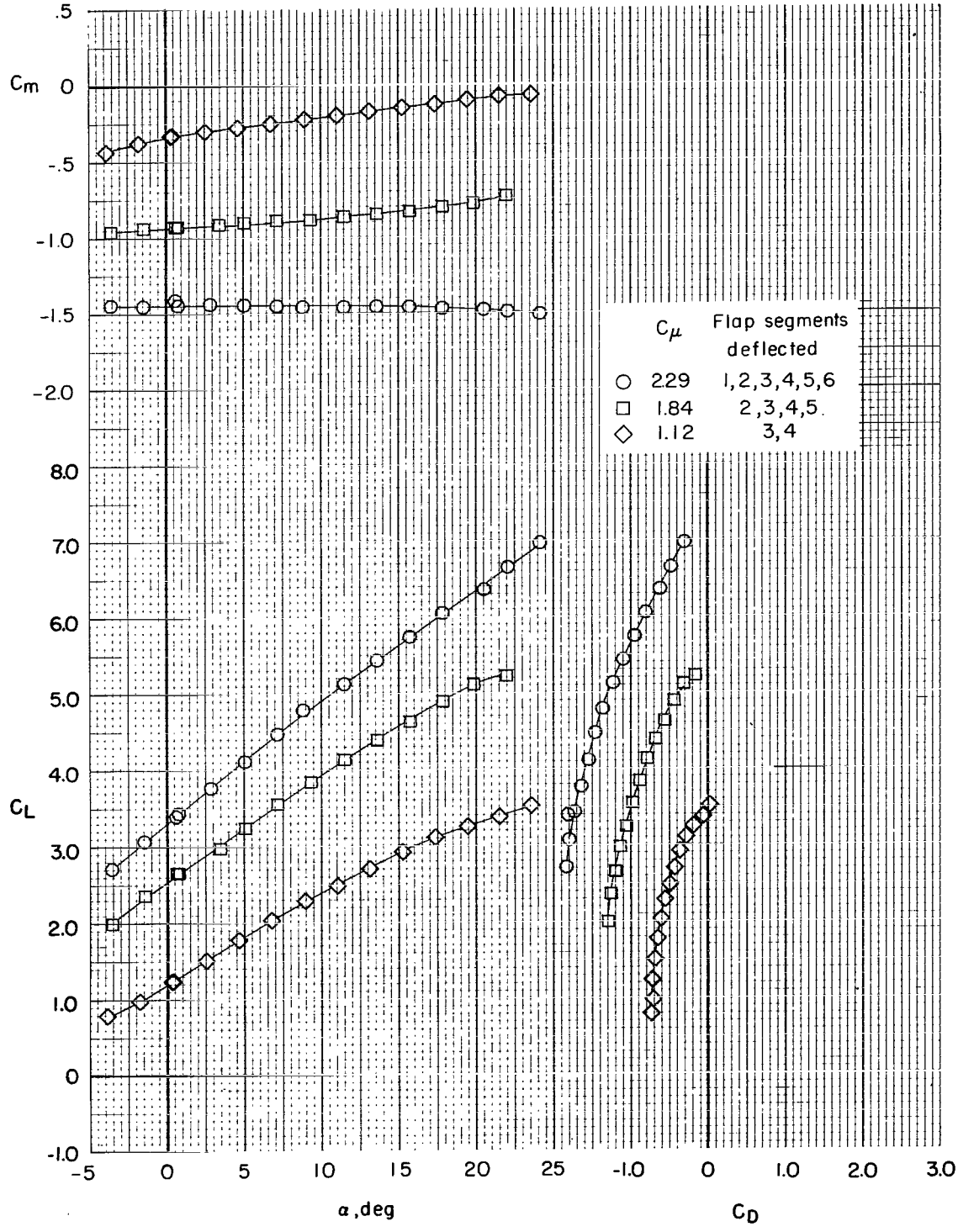

Figure 18.- Concluded.

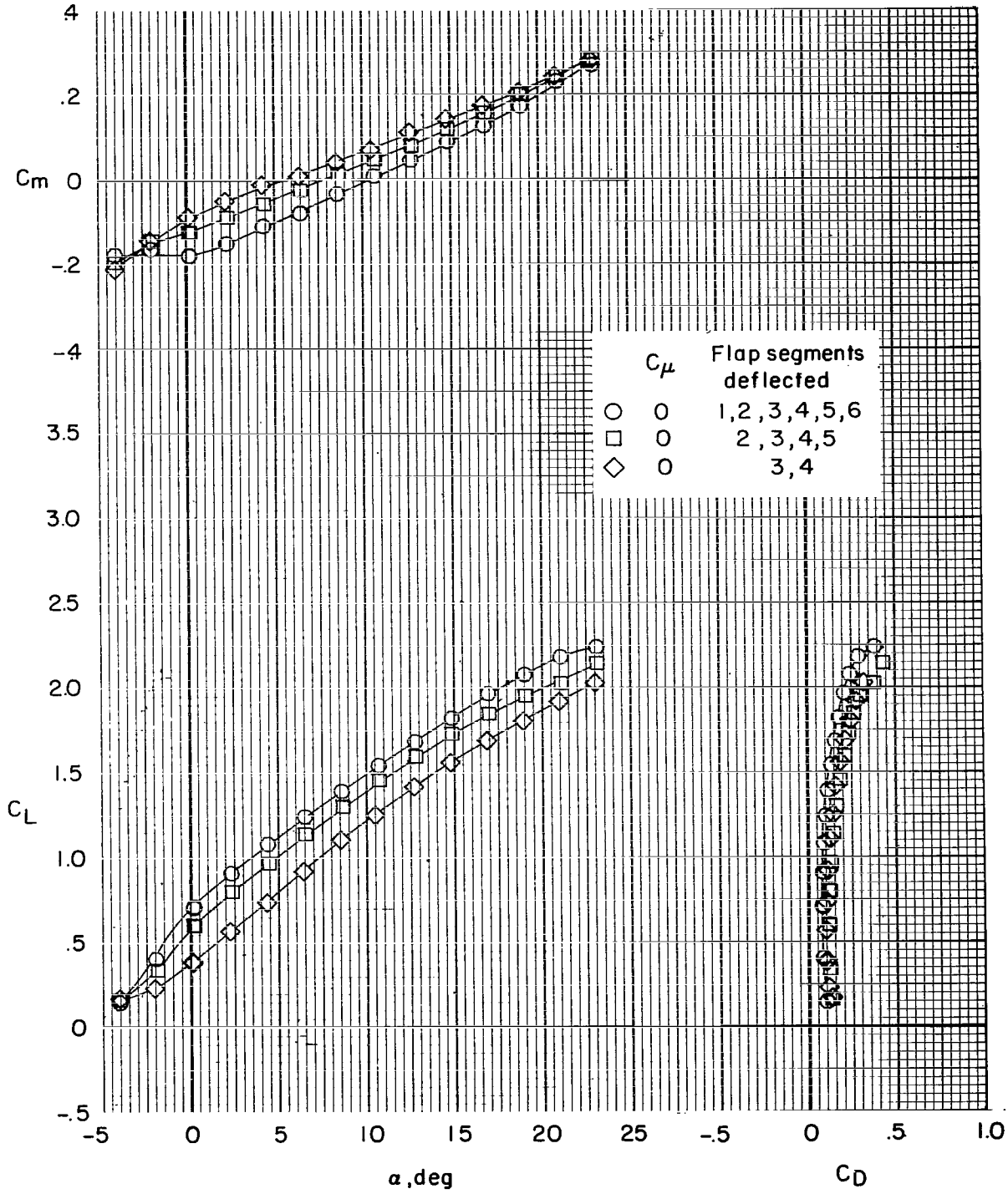

Figure 19.- Effect of partial-span flap deflection of 30° on longitudinal characteristics of model. Tail off; $\delta_{f2} = 0°$; $\delta_s = 50°$ (0.25c).

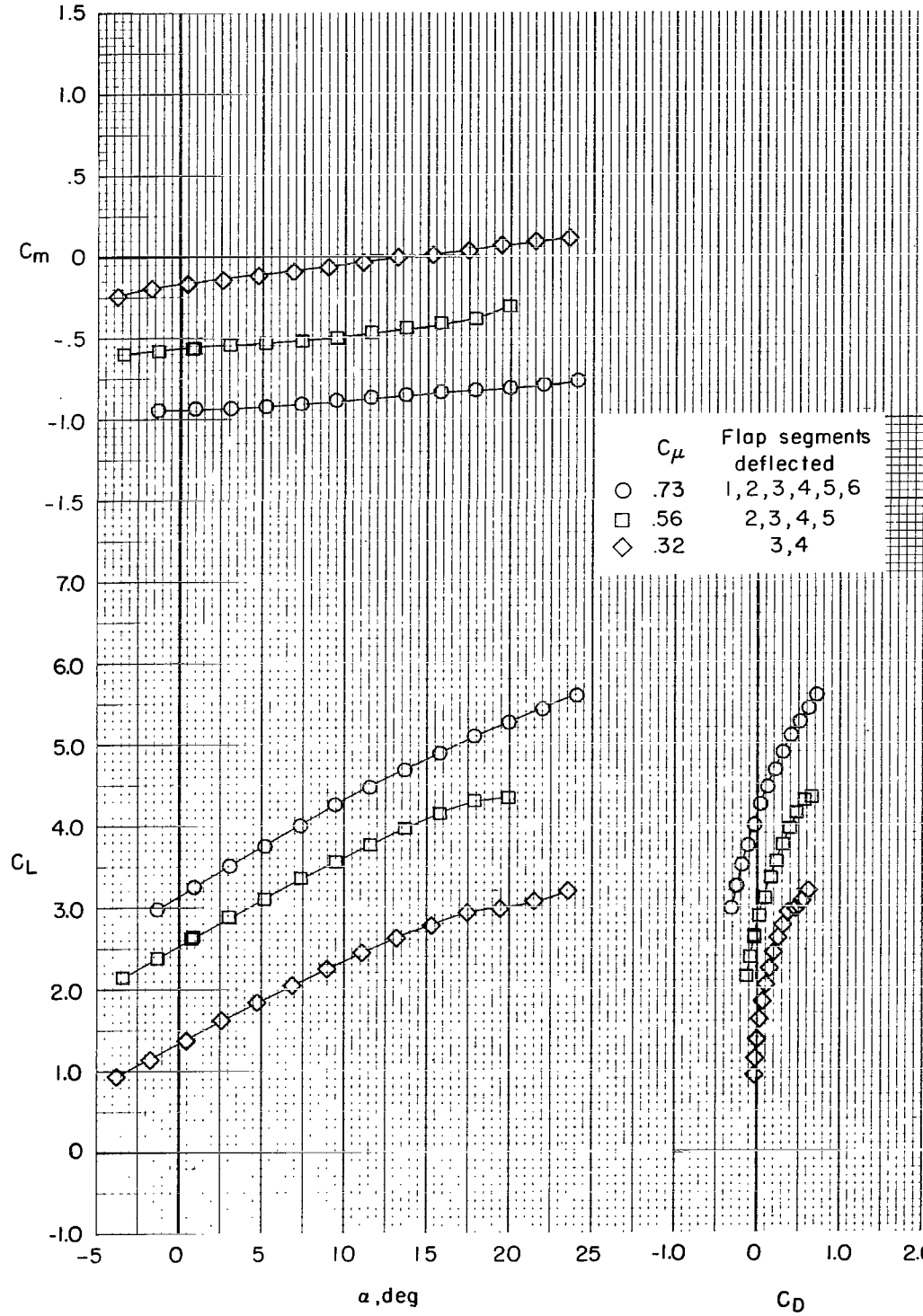

Figure 19.- Continued.

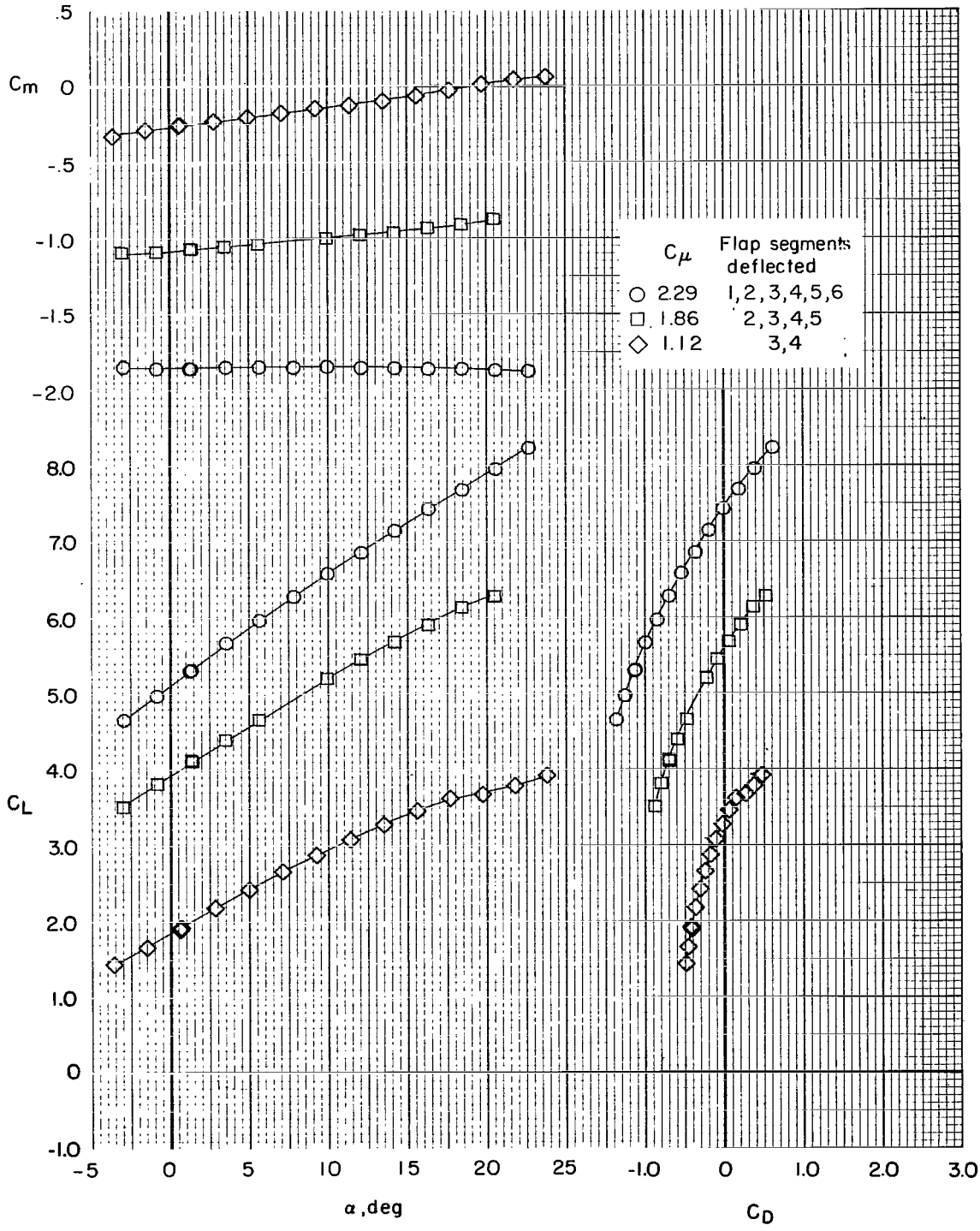

Figure 19.- Concluded.

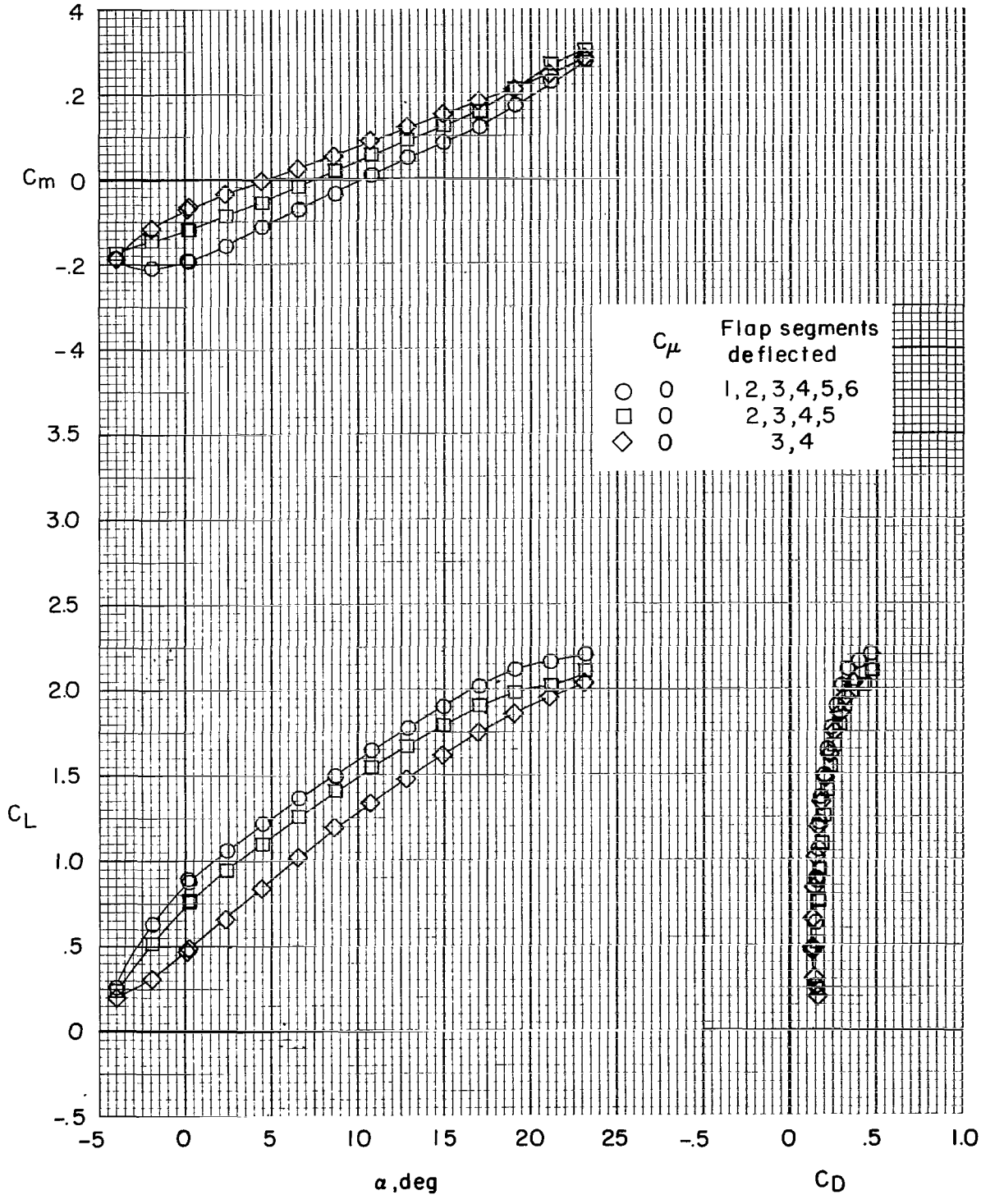

Figure 20.- Effect of partial-span flap deflection of 45° on longitudinal characteristics of model. Tail off; $\delta_{f2} = 0°$; $\delta_s = 50°$ (0.25c).

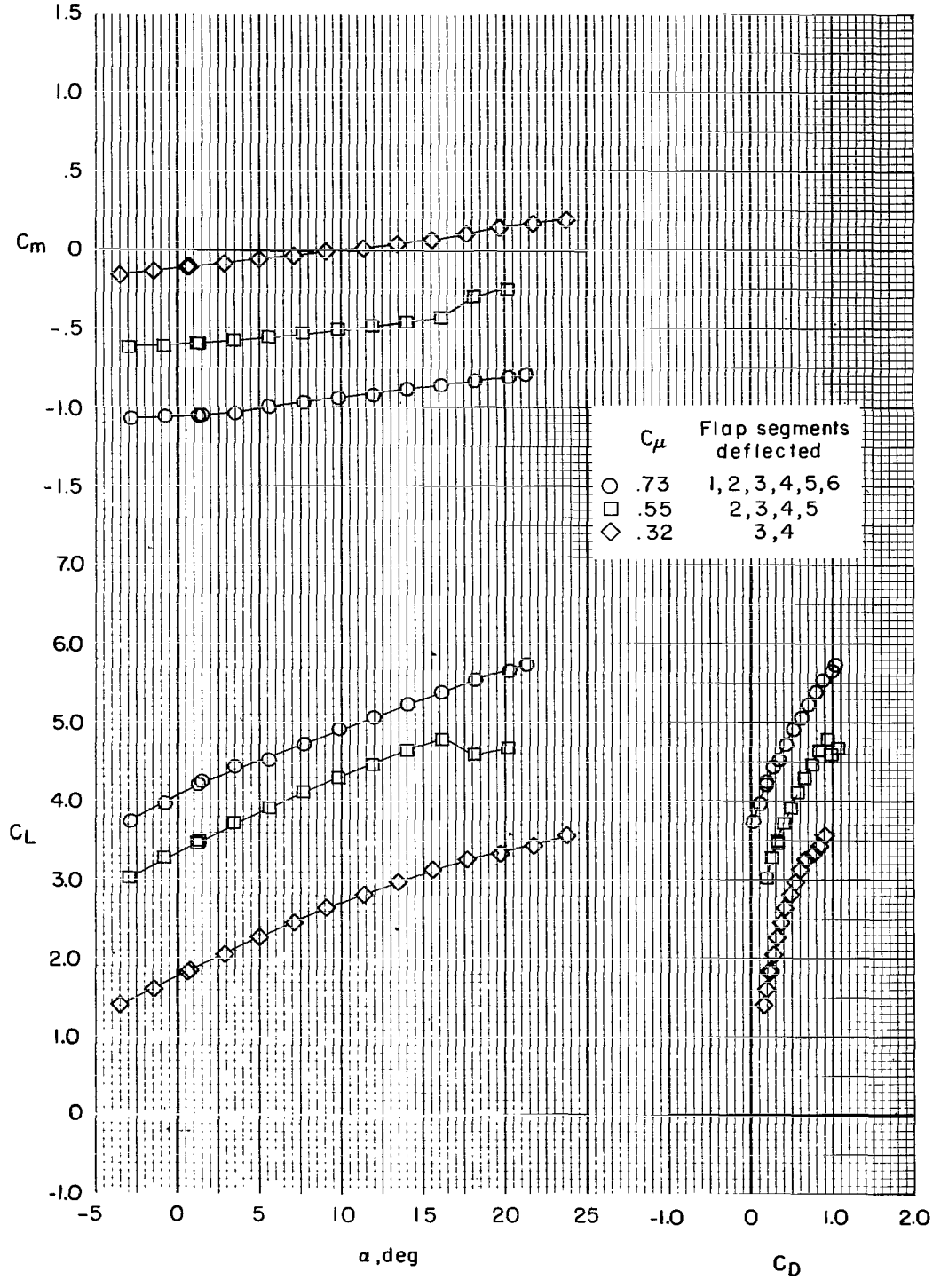

Figure 20.- Continued.

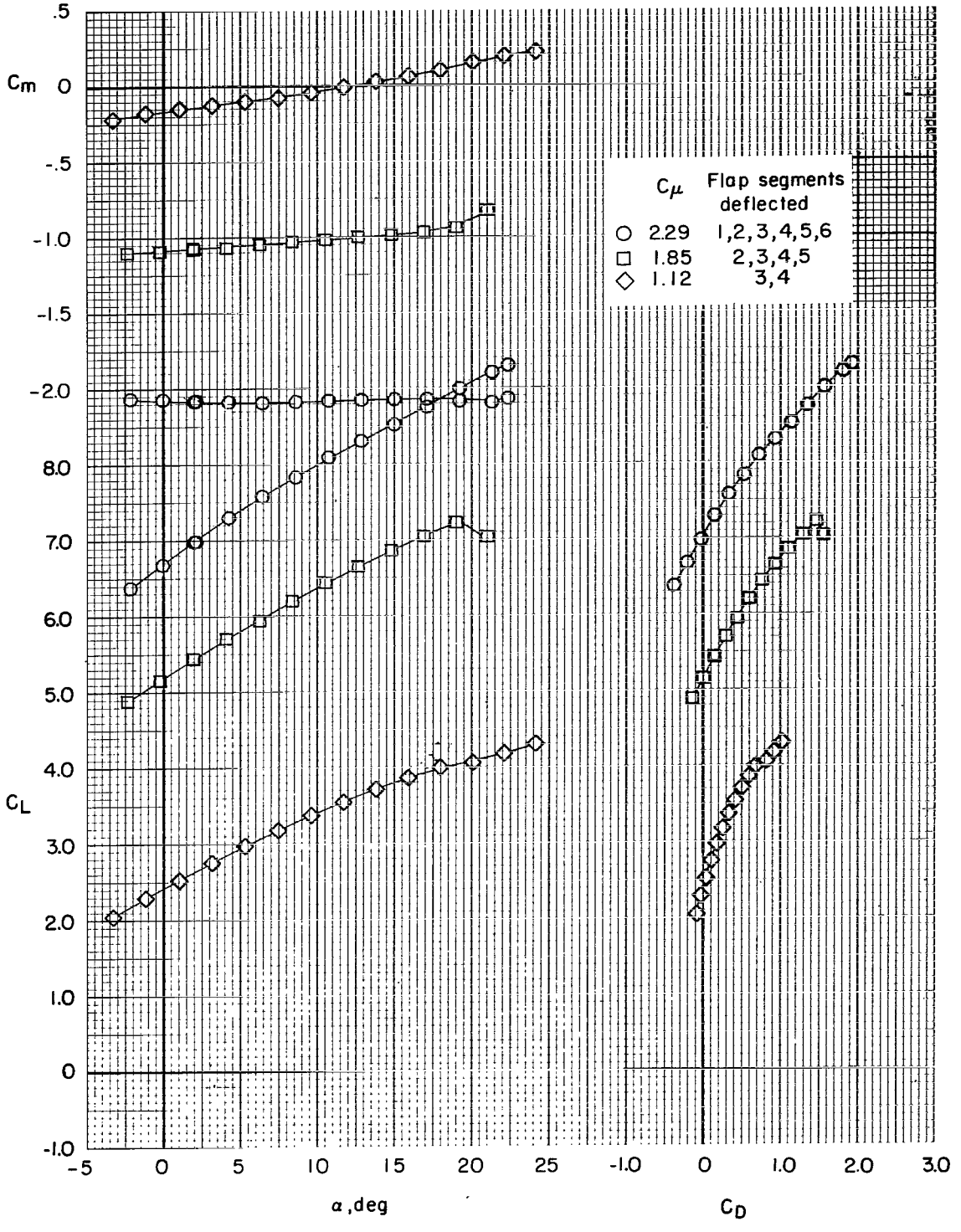

Figure 20.- Concluded.

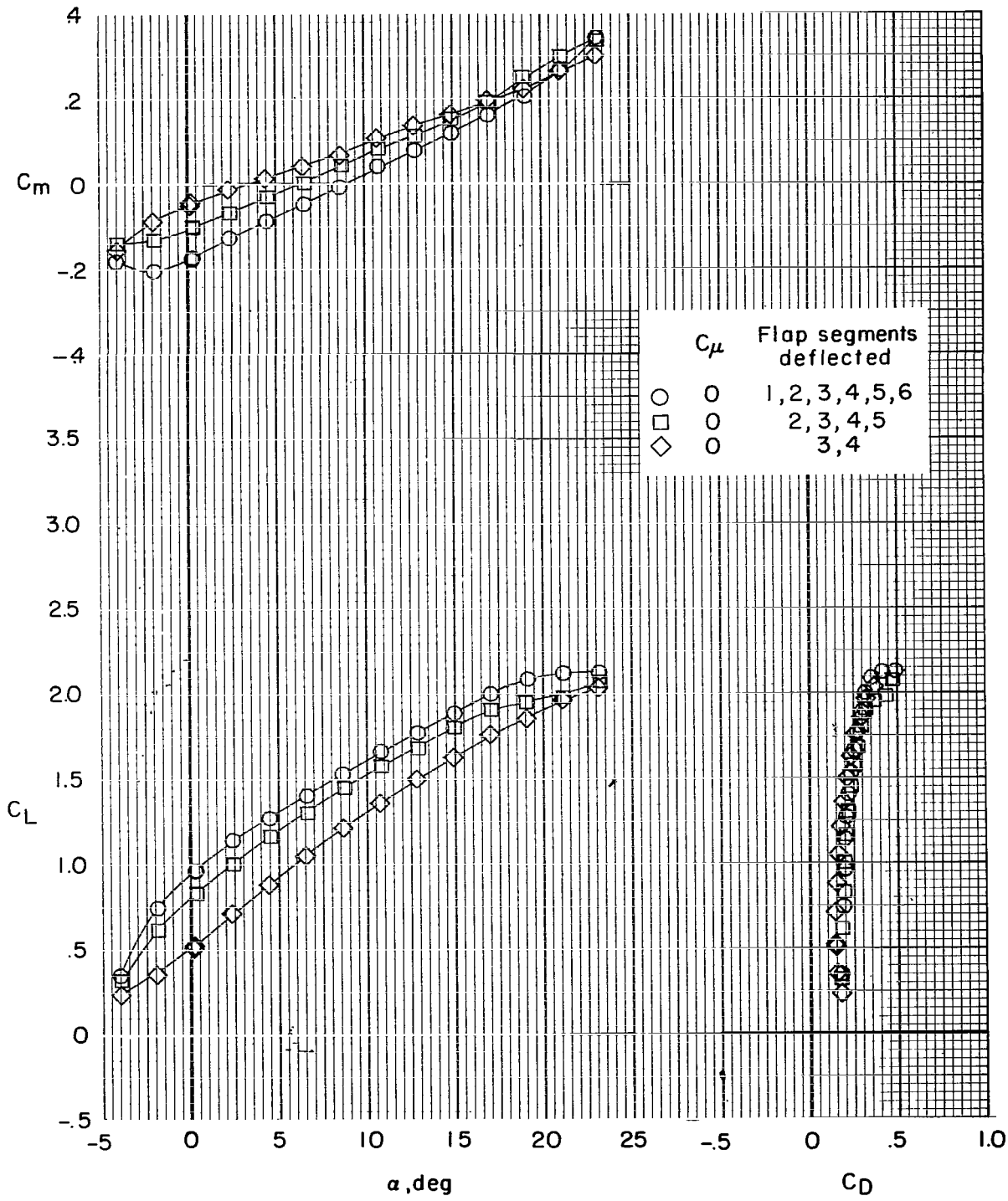

Figure 21.- Effect of partial-span flap deflection of 60° on longitudinal characteristics of model. Tail off; $\delta_{f2} = 0°$; $\delta_s = 50°$ (0.25c).

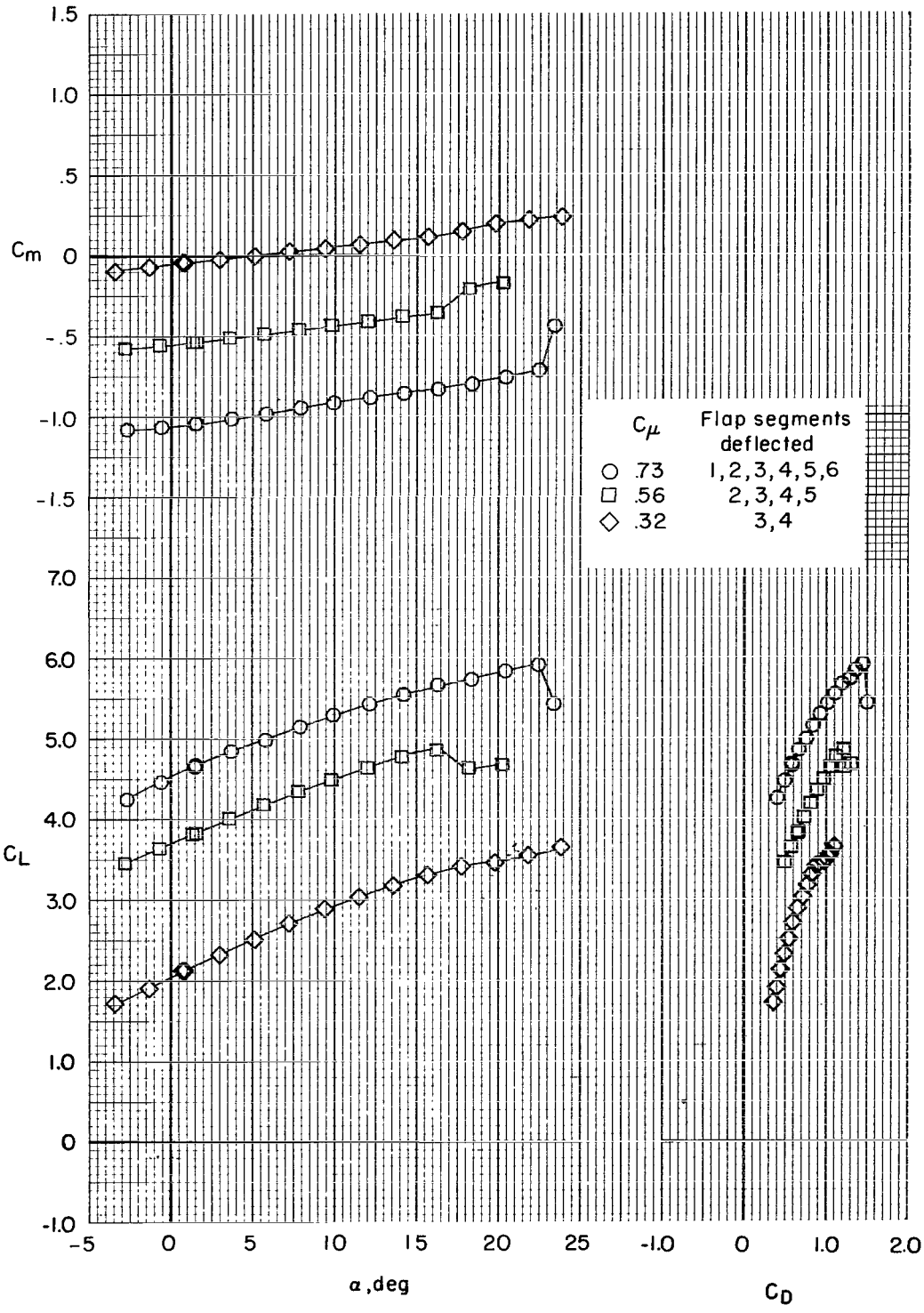

Figure 21.- Continued.

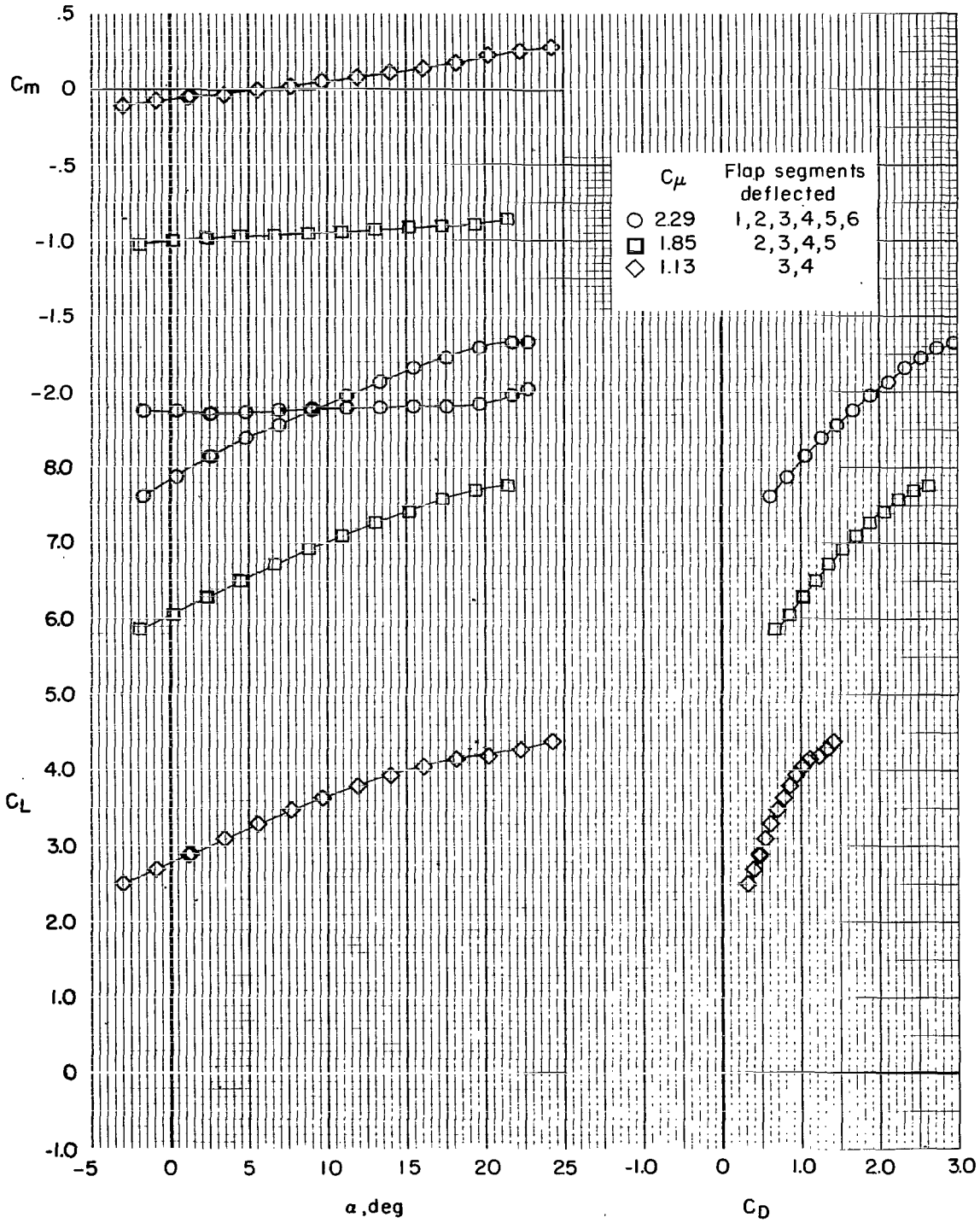

Figure 21.- Concluded.

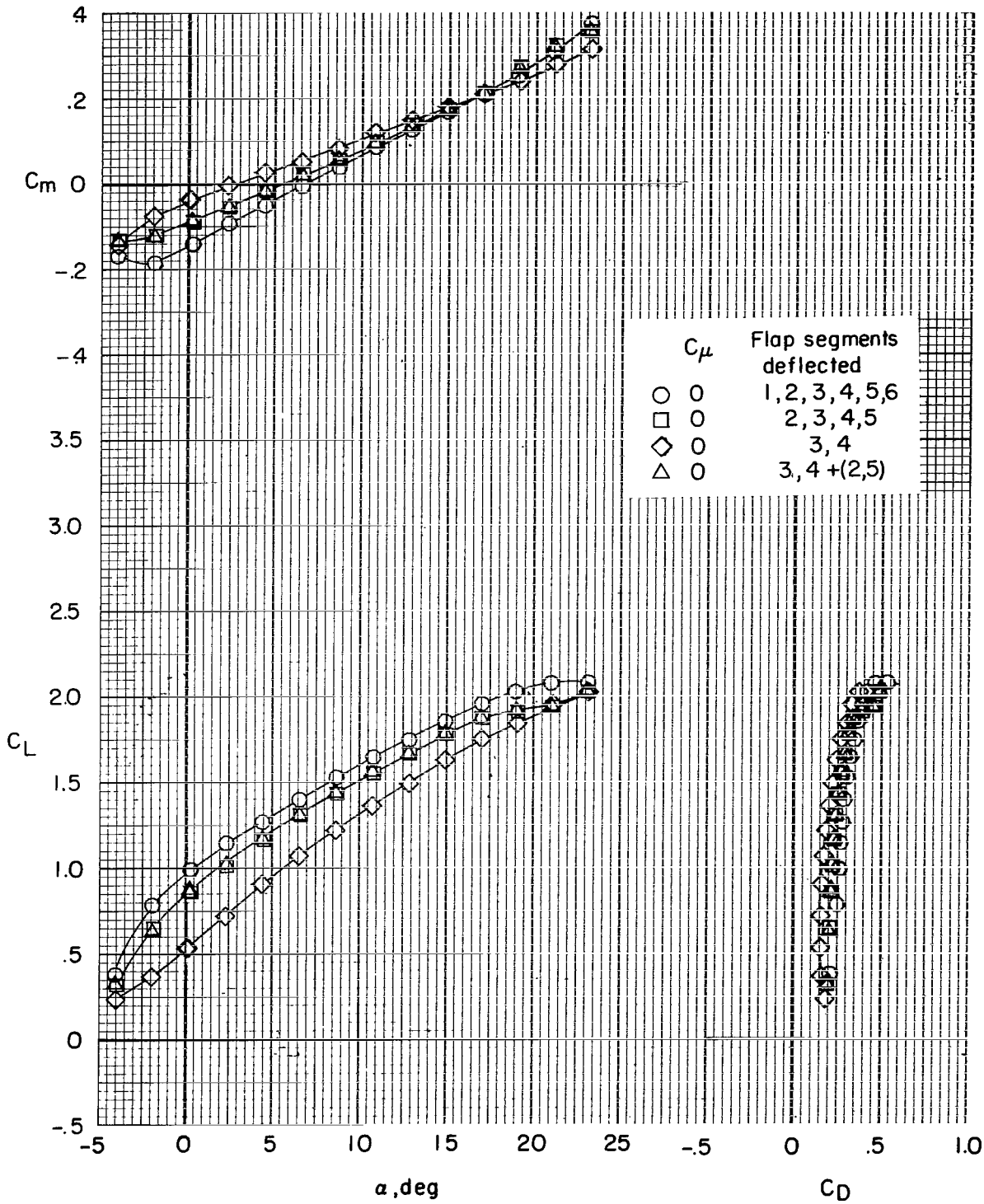

Figure 22.- Effect of partial-span flap deflection of 70° on longitudinal characteristics of model. Tail off; $\delta_{f2} = 0°$; $\delta_s = 50°$ (0.25c).

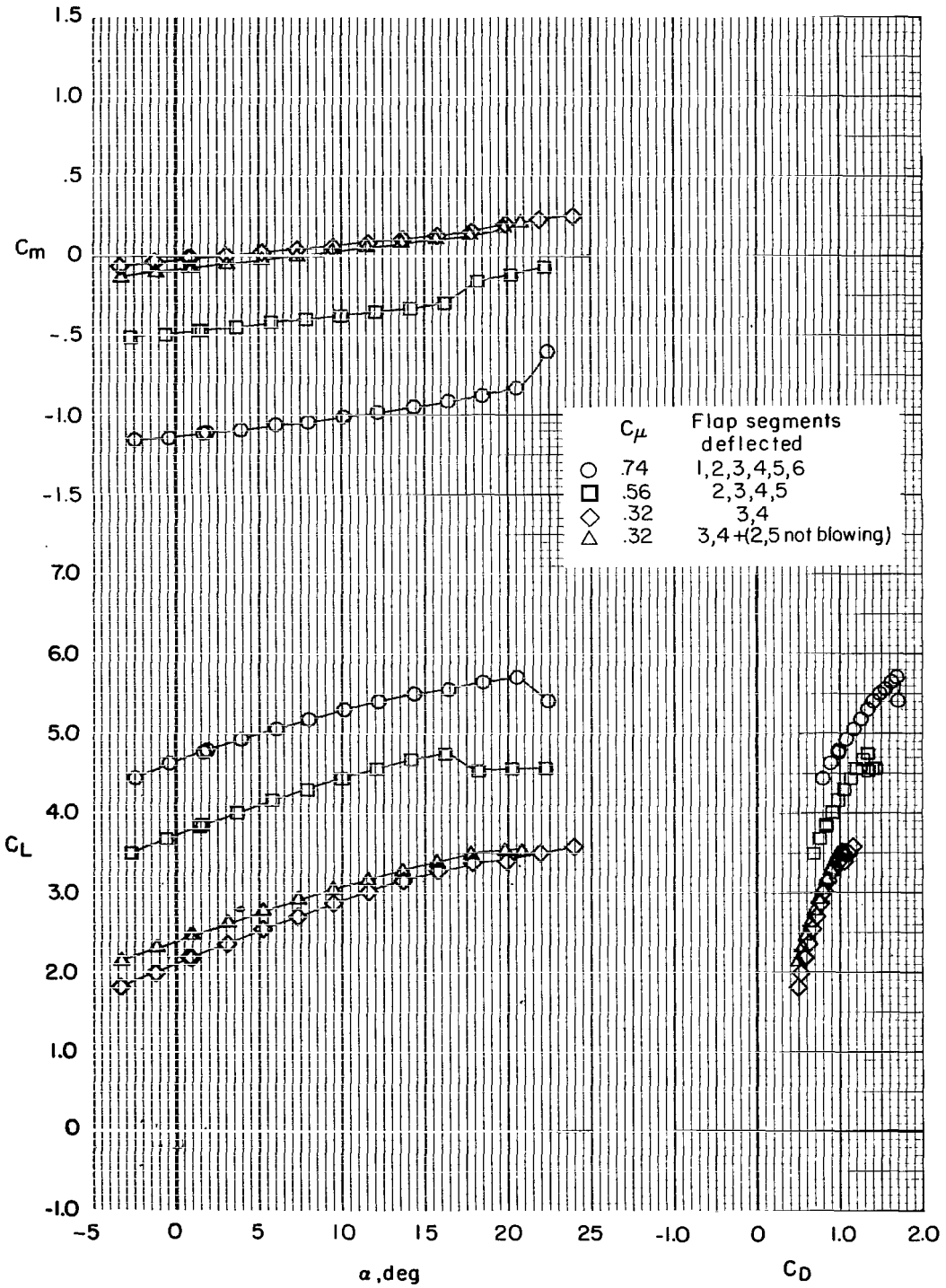

Figure 22.- Continued.

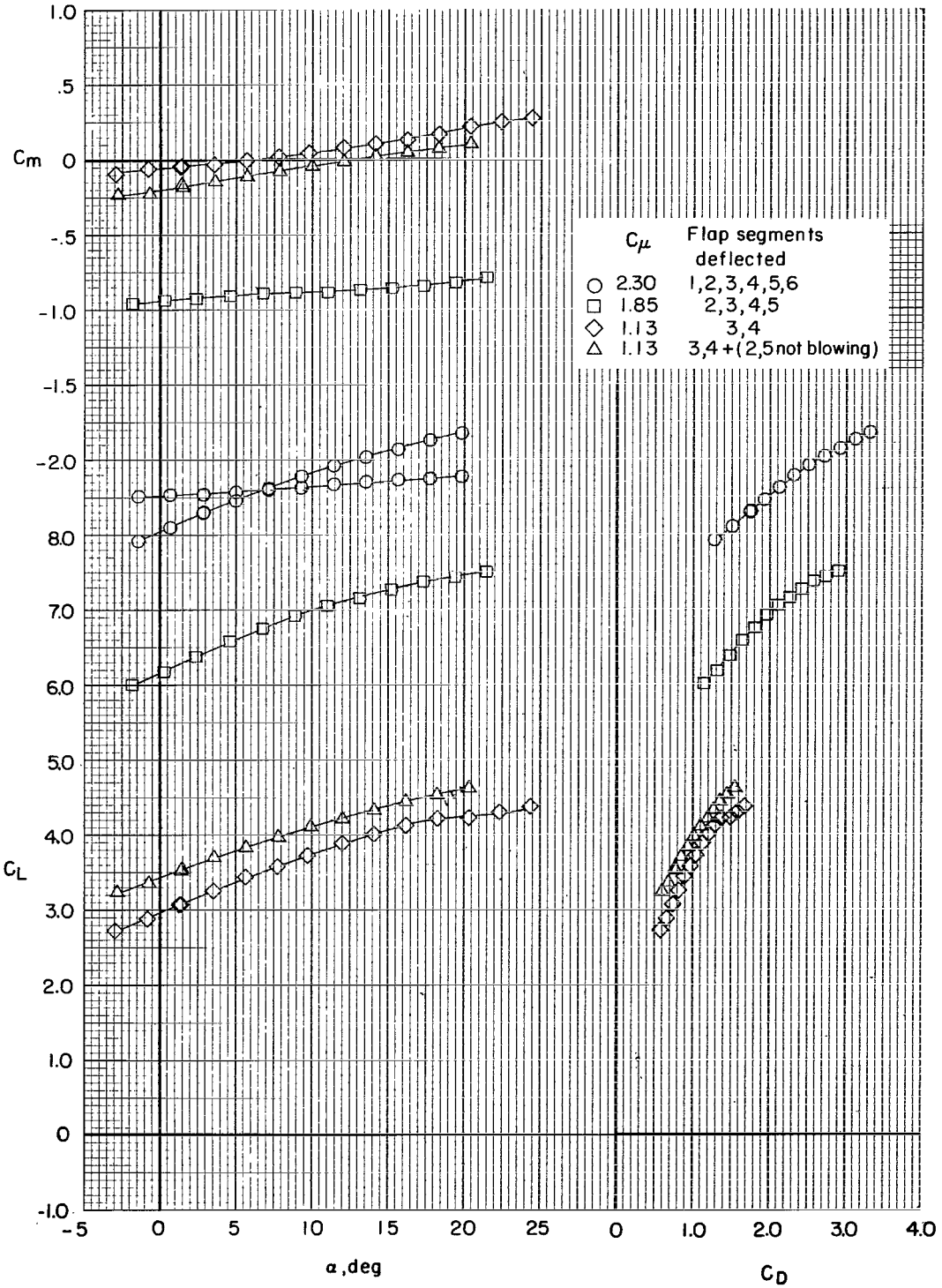

Figure 22.- Concluded.

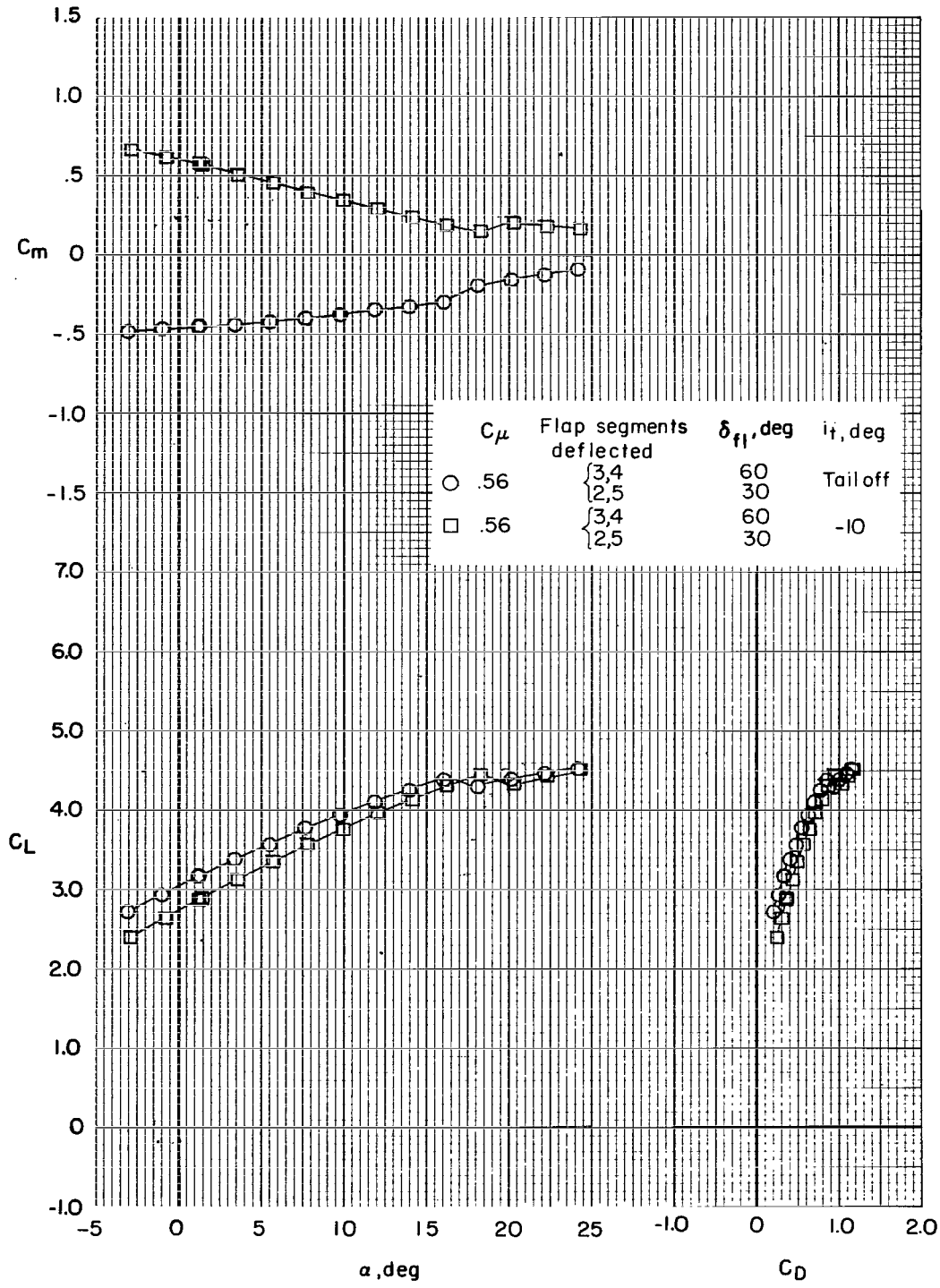

Figure 23.- Effect of partial-span flap deflections of 30° and 60° on longitudinal characteristics of model. Tail flap and slat on when tail is on; $\delta_{f2} = 0°$; $\delta_s = 50°$ (0.25c).

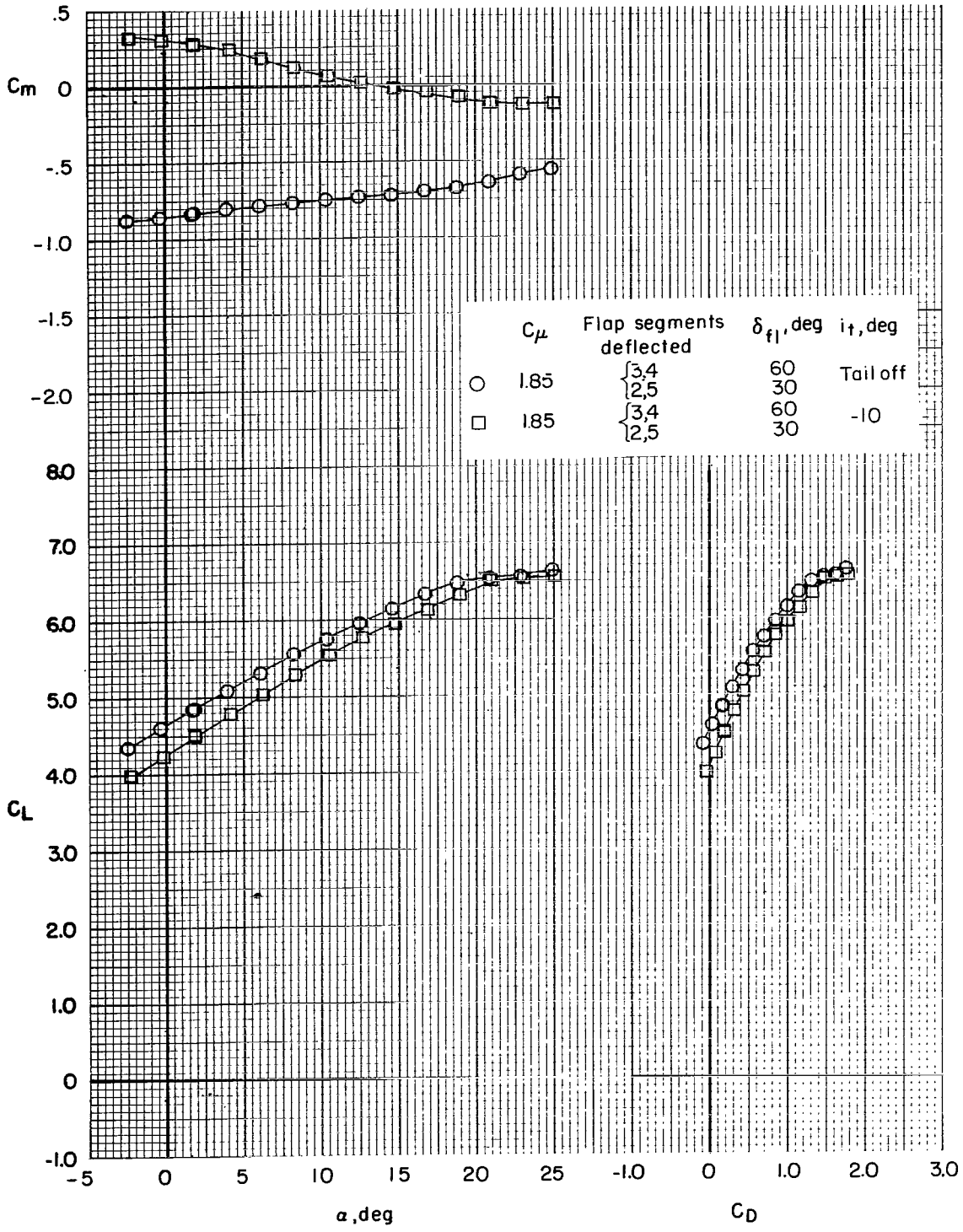

Figure 23.- Concluded.

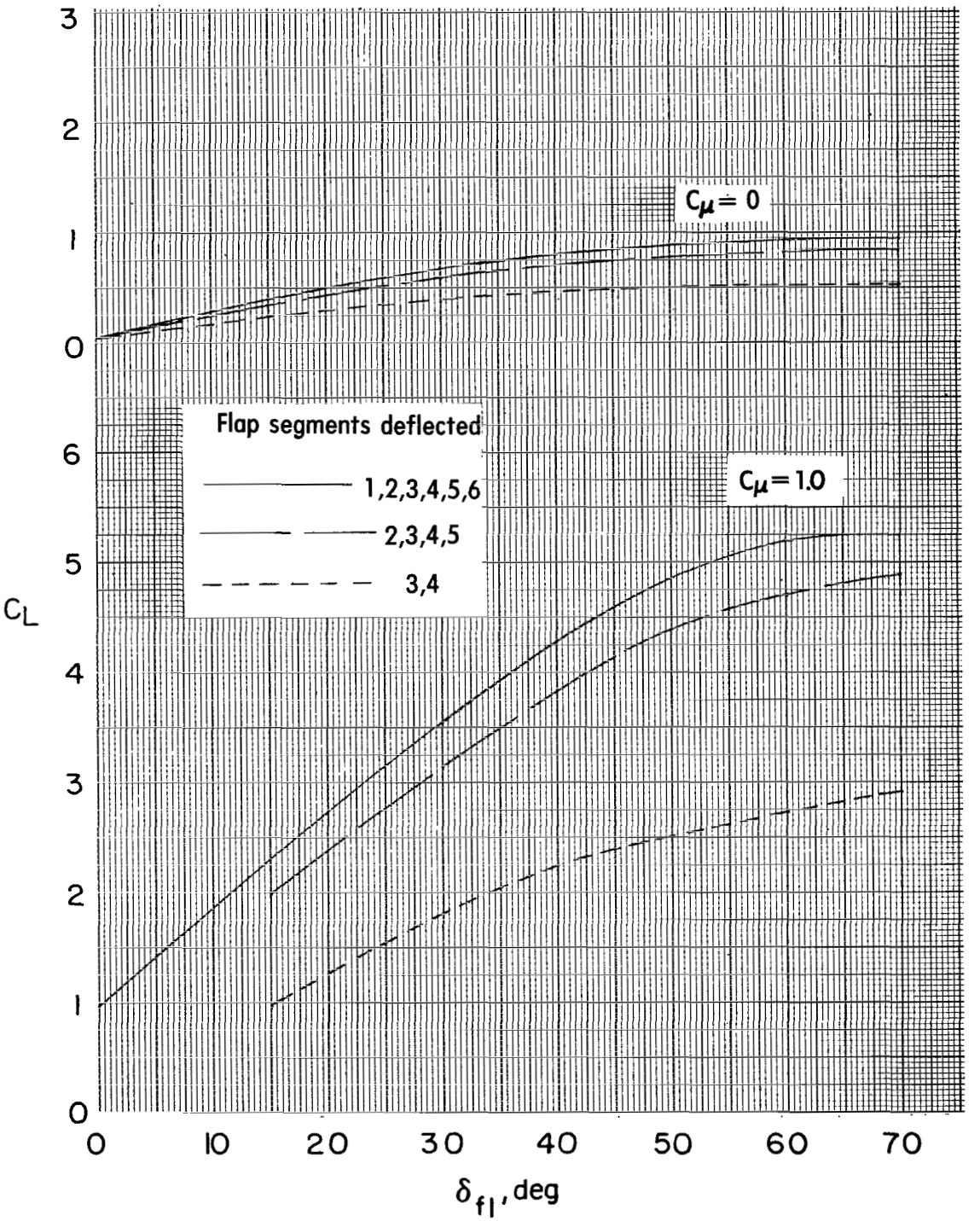

Figure 24.- Variation of lift coefficient with flap deflection for three flap segments. $\delta_{f2} = 0^\circ$; $\alpha = 0^\circ$.

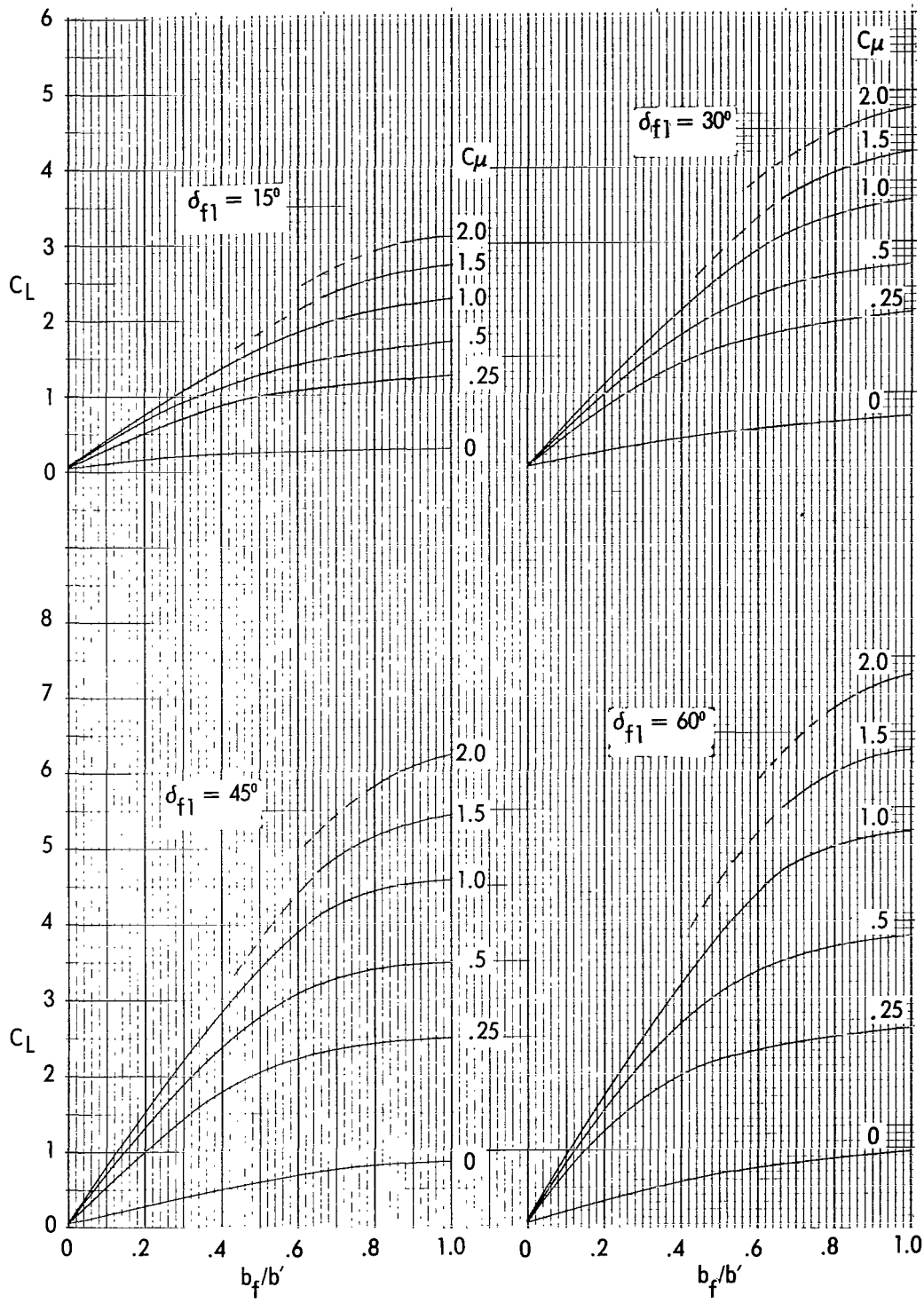

Figure 25.- Variation of lift coefficient with flap span.
$\alpha = 0^o$; $\delta_{f2} = 0^o$.

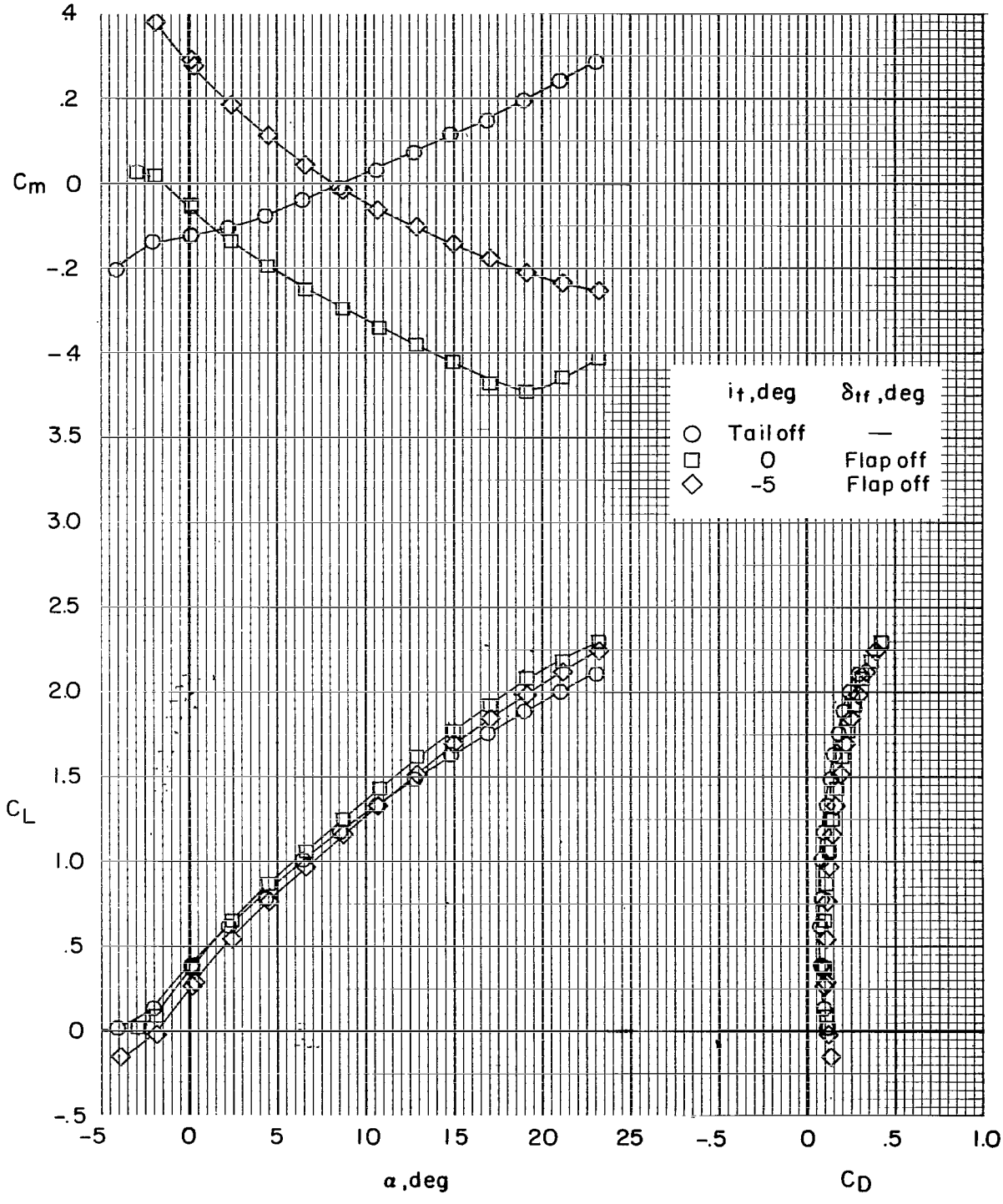

(a) $C_\mu = 0$.

Figure 26.- Effect of horizontal-tail incidence on longitudinal characteristics of model with flaps deflected 15°. $\delta_{f2} = 0°$; $\delta_s = 50°$ (0.25c); $\delta_{ts} = -40°$.

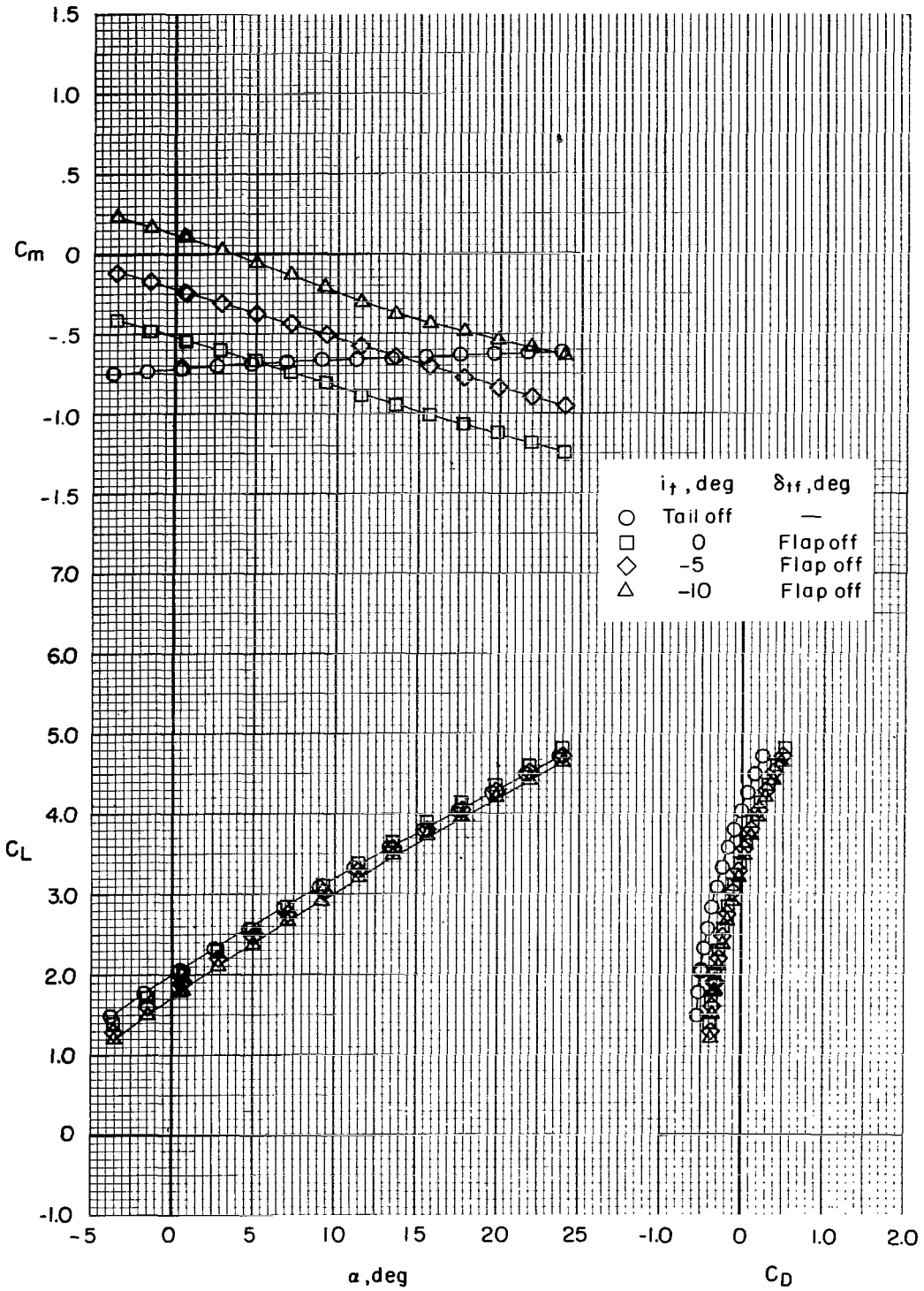

(b) $C_\mu = 0.73$.

Figure 26.- Concluded.

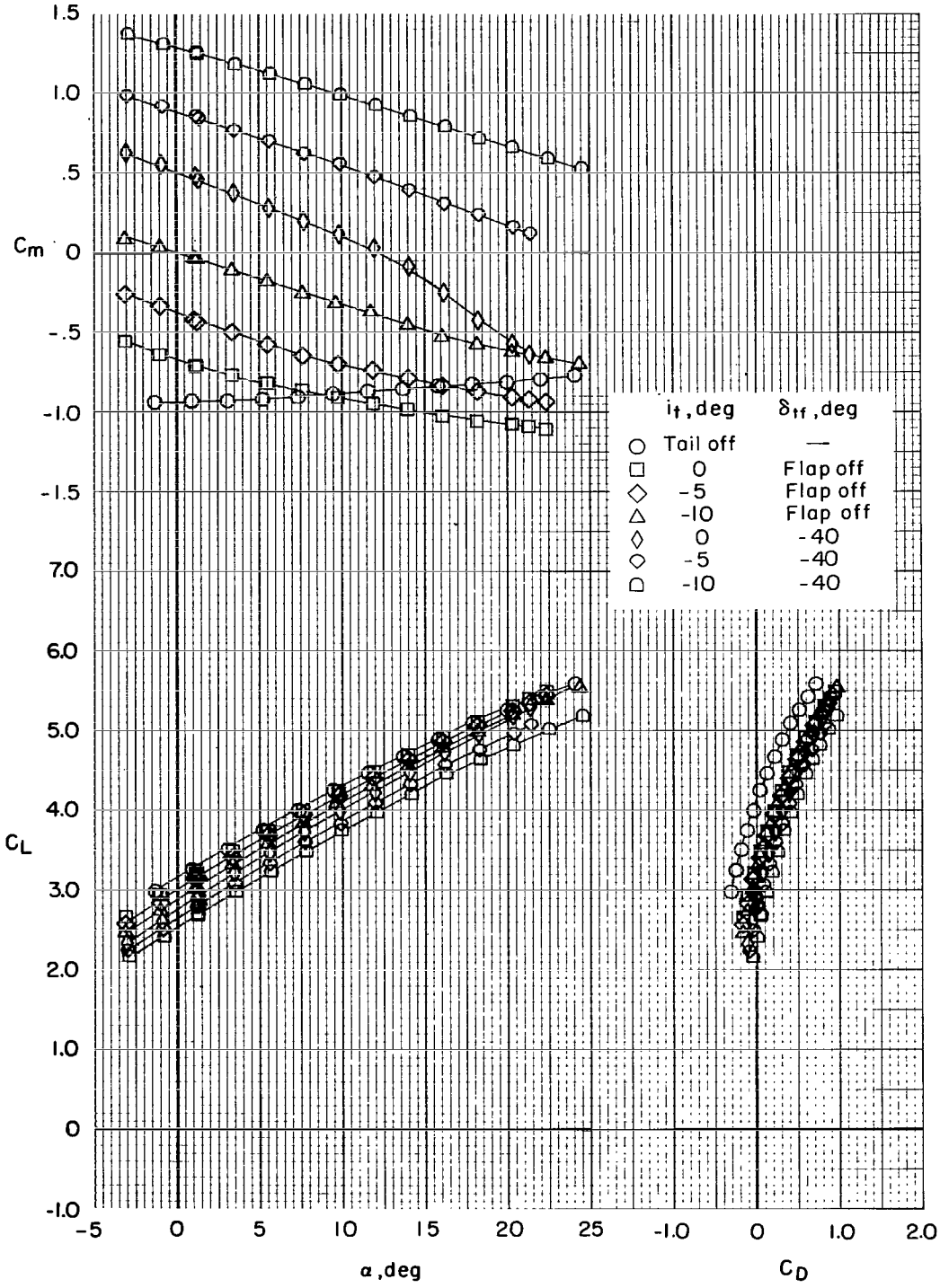

(a) $C_\mu = 0.73$.

Figure 27.- Effect of horizontal-tail incidence on longitudinal characteristics of model with flaps deflected 30°. $\delta_{f2} = 0°$; $\delta_s = 50°$ (0.25c); $\delta_{ts} = -40°$.

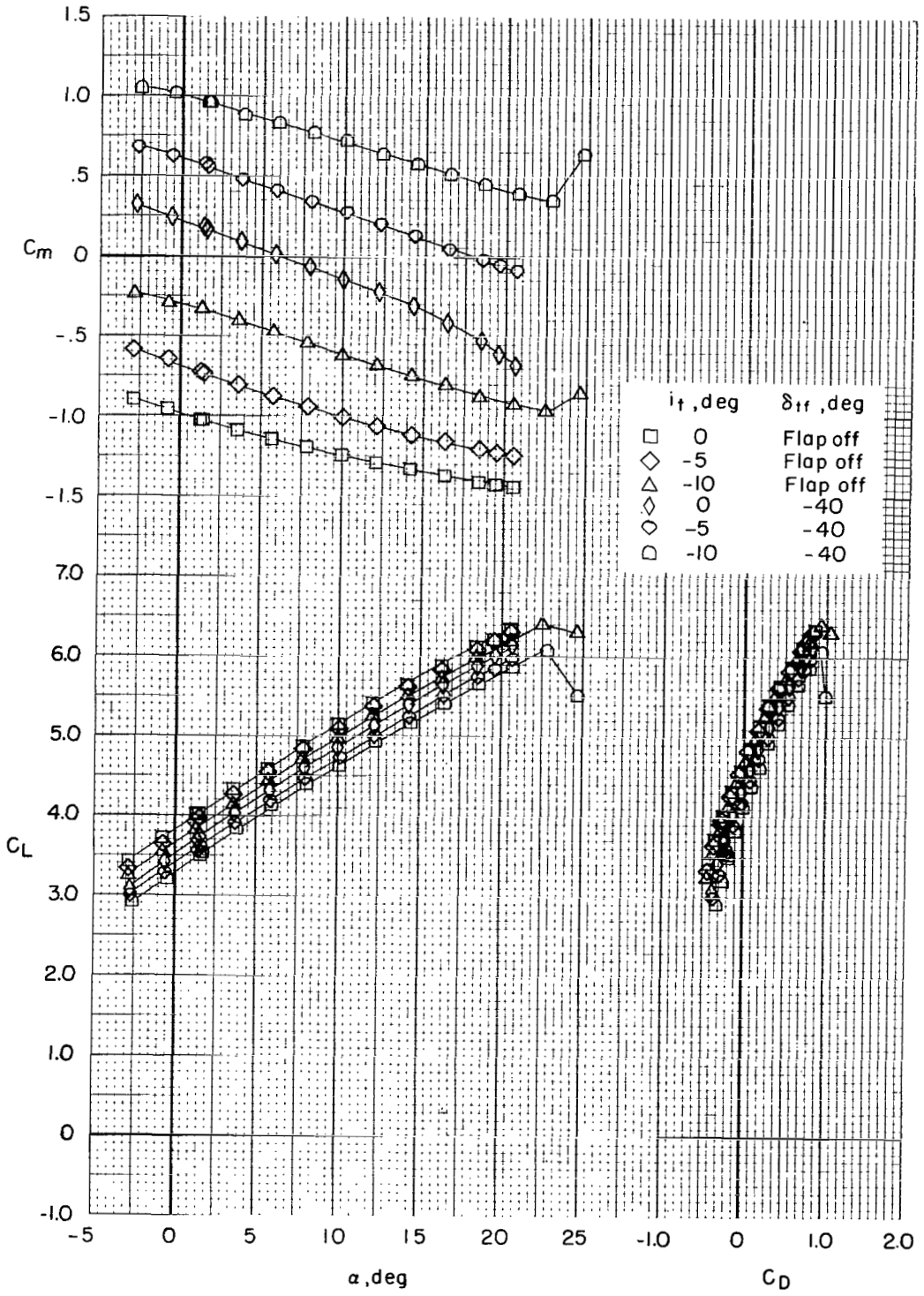

(b) C_μ = 1.27.

Figure 27.- Continued.

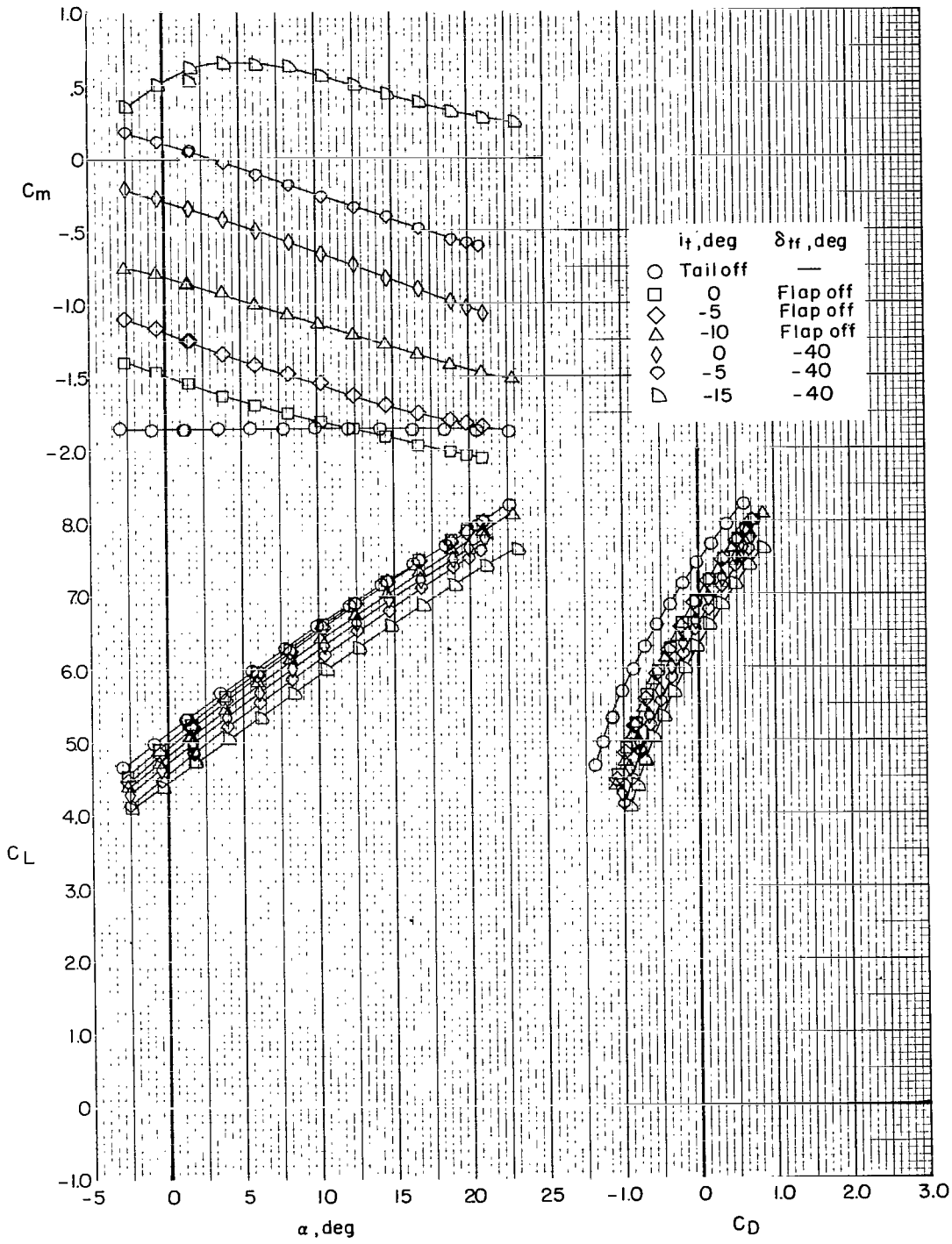

(c) C_μ = 2.29.

Figure 27.- Concluded.

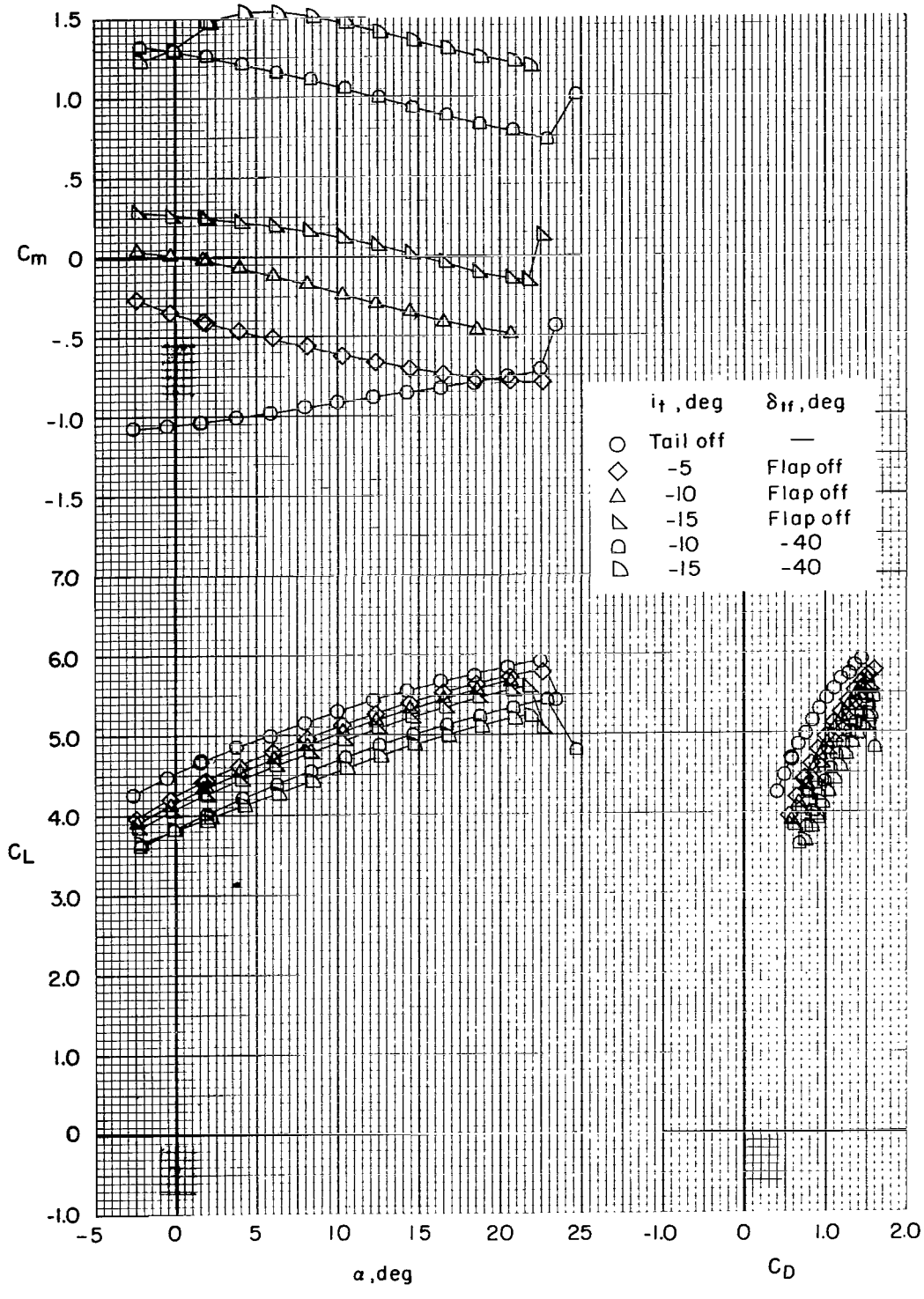

(a) $C_\mu = 0.73$.

Figure 28.- Effect of horizontal-tail incidence on longitudinal characteristics of model with flaps deflected 60°. $\delta_{f2} = 0°$; $\delta_s = 50°$ (0.25c); $\delta_{ts} = -40°$.

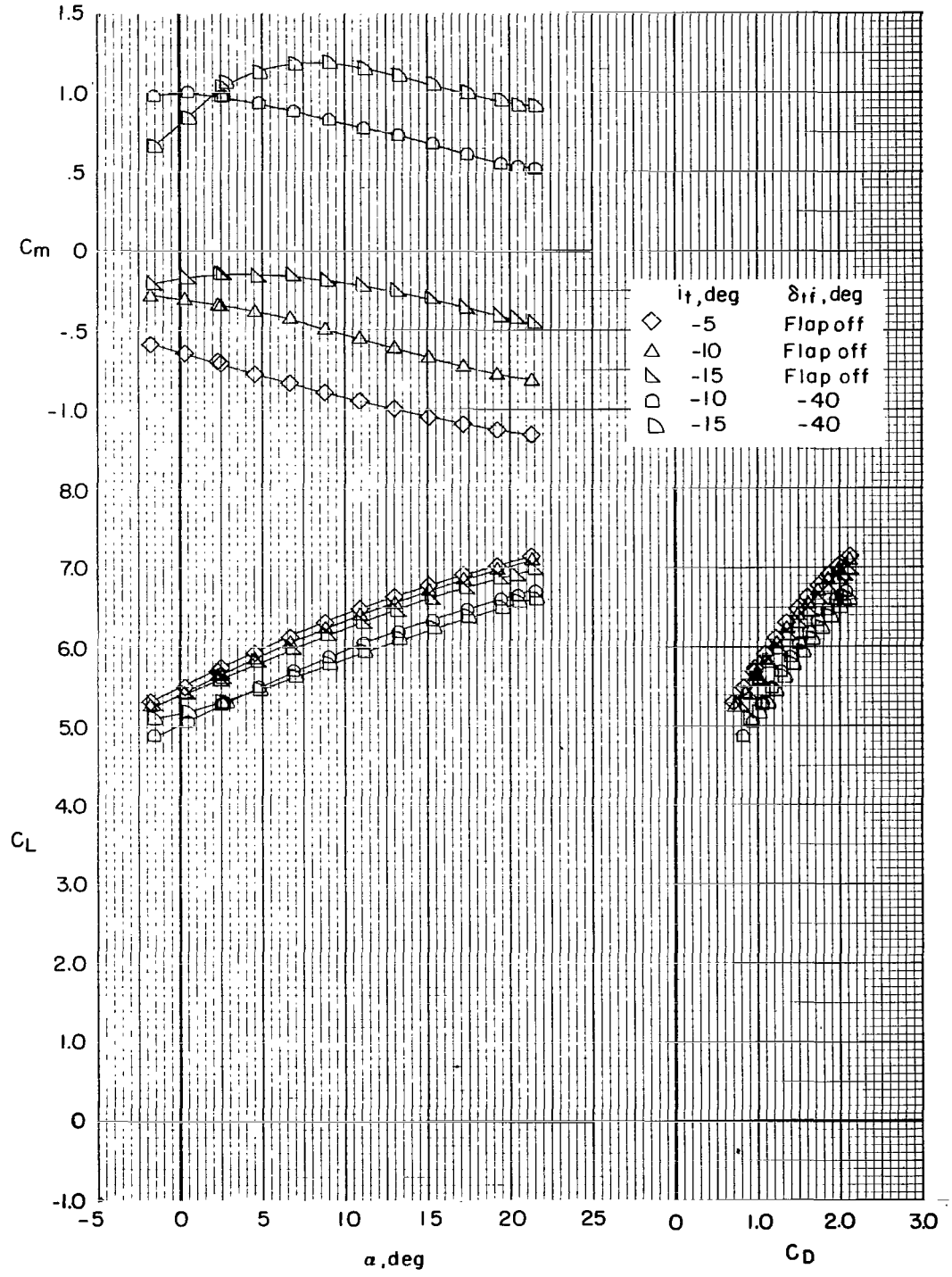

(b) C_μ = 1.27.

Figure 28.- Continued.

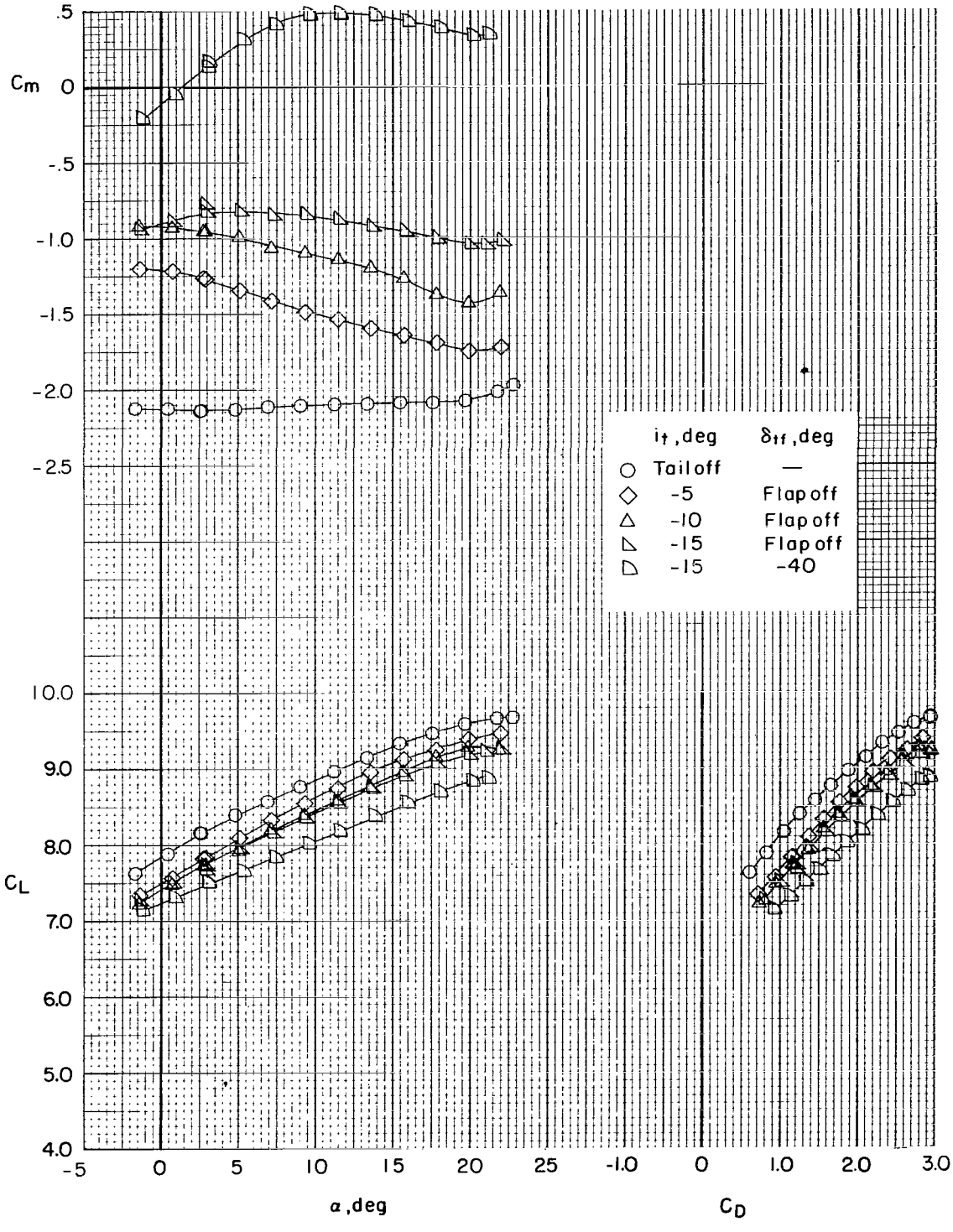

(c) C_{μ} = 2.29.

Figure 28.- Concluded.

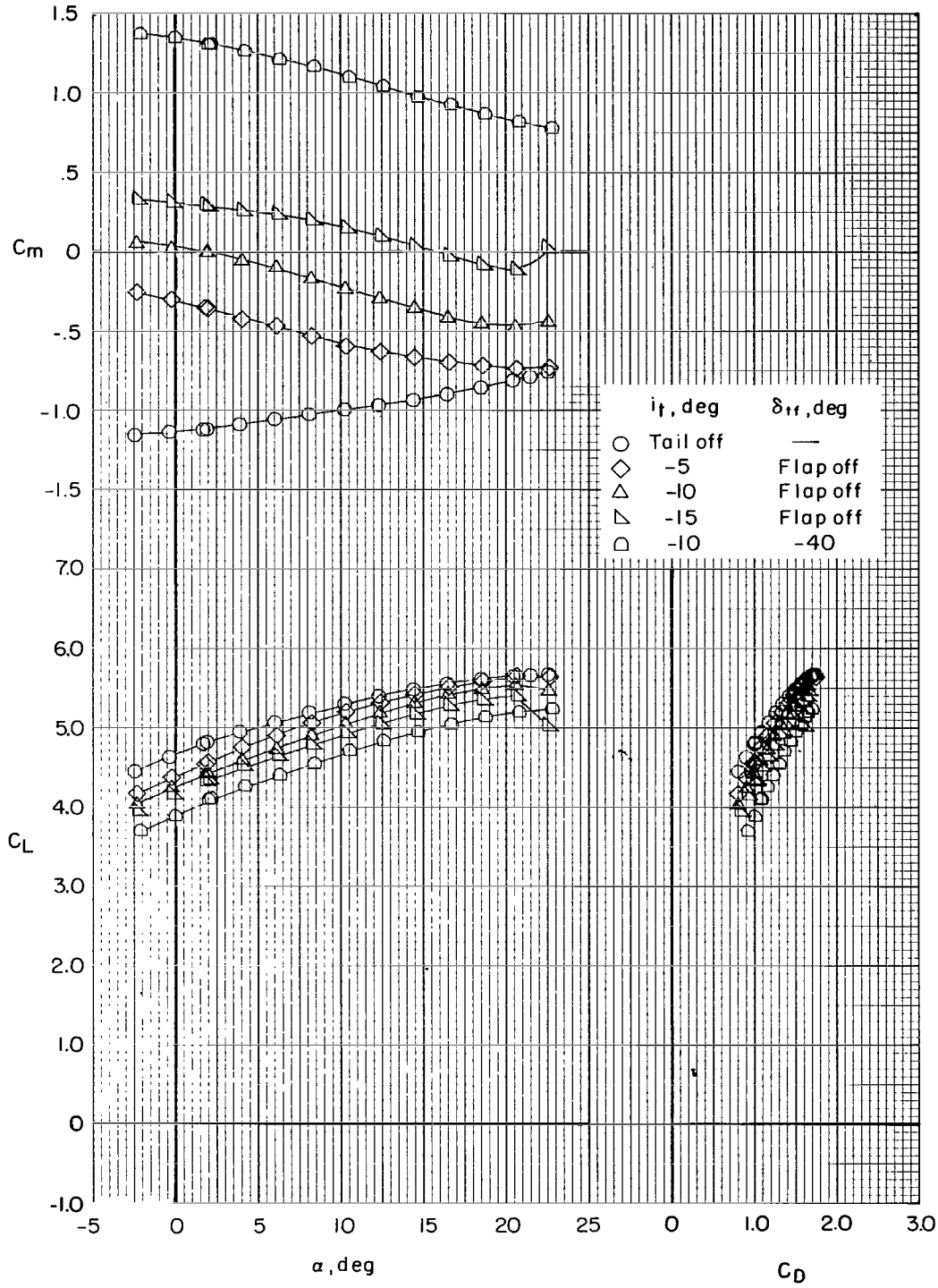

(a) C_μ = 0.73.

Figure 29.- Effect of horizontal-tail incidence on longitudinal characteristics of model with flaps deflected 70°. δ_{f2} = 0°; δ_s = 50° (0.25c); δ_{ts} = -40°.

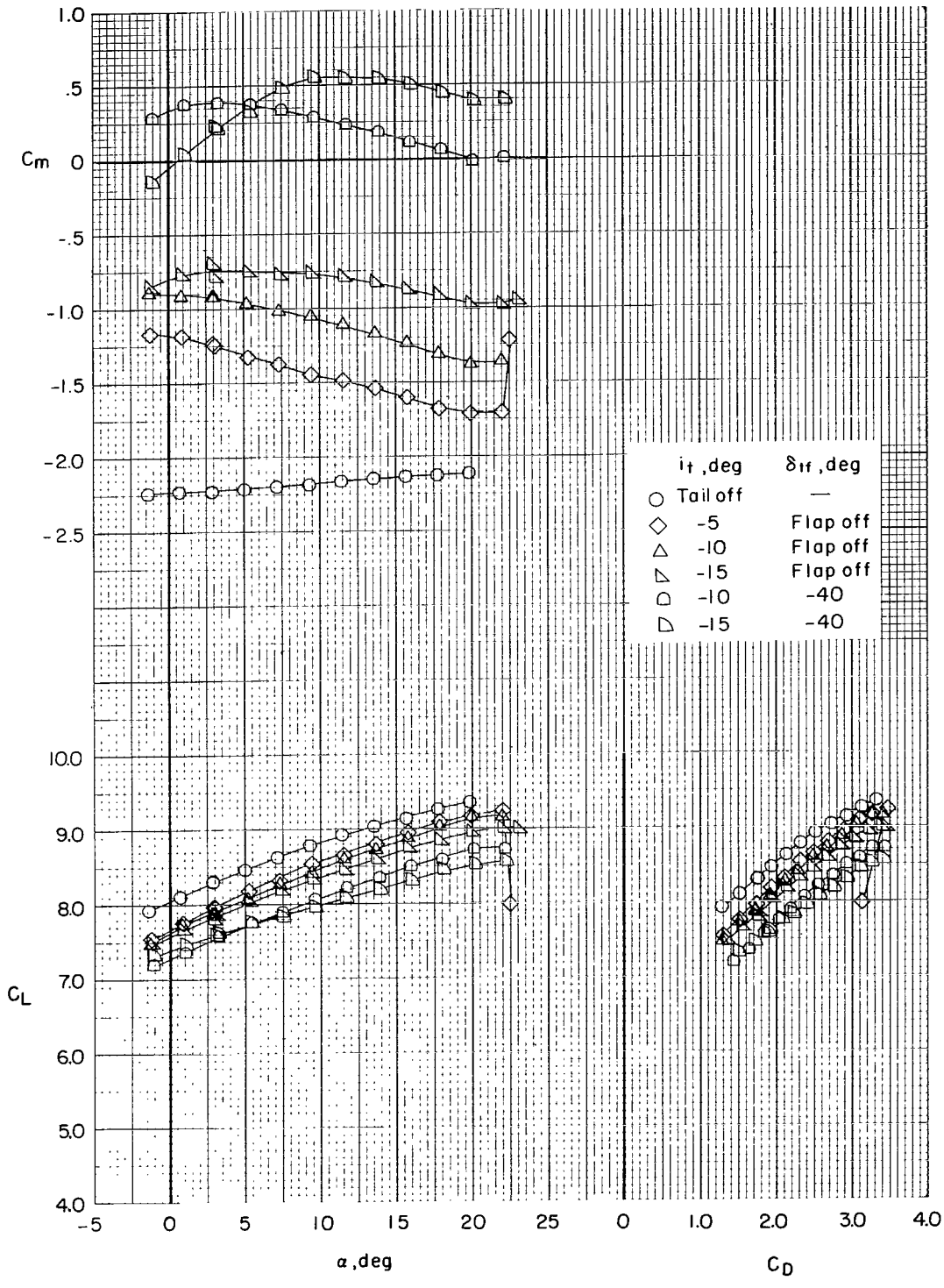

(b) C_μ = 2.29.

Figure 29.- Concluded.

NATIONAL AERONAUTICS AND SPACE ADMINISTRATION
WASHINGTON, D.C. 20546

OFFICIAL BUSINESS
PENALTY FOR PRIVATE USE $300

SPECIAL FOURTH-CLASS RATE BOOK

POSTAGE AND FEES PAID
NATIONAL AERONAUTICS AND SPACE ADMINISTRATION
451

U.S.MAIL

POSTMASTER: If Undeliverable (Section 158 Postal Manual) Do Not Return

"The aeronautical and space activities of the United States shall be conducted so as to contribute . . . to the expansion of human knowledge of phenomena in the atmosphere and space. The Administration shall provide for the widest practicable and appropriate dissemination of information concerning its activities and the results thereof."

—NATIONAL AERONAUTICS AND SPACE ACT OF 1958

NASA SCIENTIFIC AND TECHNICAL PUBLICATIONS

TECHNICAL REPORTS: Scientific and technical information considered important, complete, and a lasting contribution to existing knowledge.

TECHNICAL NOTES: Information less broad in scope but nevertheless of importance as a contribution to existing knowledge.

TECHNICAL MEMORANDUMS: Information receiving limited distribution because of preliminary data, security classification, or other reasons. Also includes conference proceedings with either limited or unlimited distribution.

CONTRACTOR REPORTS: Scientific and technical information generated under a NASA contract or grant and considered an important contribution to existing knowledge.

TECHNICAL TRANSLATIONS: Information published in a foreign language considered to merit NASA distribution in English.

SPECIAL PUBLICATIONS: Information derived from or of value to NASA activities. Publications include final reports of major projects, monographs, data compilations, handbooks, sourcebooks, and special bibliographies.

TECHNOLOGY UTILIZATION PUBLICATIONS: Information on technology used by NASA that may be of particular interest in commercial and other non-aerospace applications. Publications include Tech Briefs, Technology Utilization Reports and Technology Surveys.

Details on the availability of these publications may be obtained from:

SCIENTIFIC AND TECHNICAL INFORMATION OFFICE

NATIONAL AERONAUTICS AND SPACE ADMINISTRATION

Washington, D.C. 20546